

**Microwave enhanced advanced oxidation process (MW/H₂O₂-AOP) treatment of
sewage sludge at different pH conditions**

by

Indrè Tunilè

B.Eng., Queen's University Belfast, 2011

A THESIS SUBMITTED IN PARTIAL FULFILLMENT OF
THE REQUIREMENTS FOR THE DEGREE OF

MASTER OF APPLIED SCIENCE

in

THE FACULTY OF GRADUATE AND POSTDOCTORAL STUDIES
(Civil Engineering)

THE UNIVERSITY OF BRITISH COLUMBIA

(Vancouver)

April, 2018

© Indre Tunile, 2018

Abstract

The primary focus of this study was to investigate the effectiveness of a microwave-enhanced advanced oxidation process (MW/H₂O₂-AOP) for treating sludge from a membrane-enhanced biological phosphorus removal process in neutral, acidic (pH 4) and alkaline (pH 9) conditions. Two different MW systems were utilized; the bench-scale (2450 MHz) and pilot-scale (915 MHz) systems that operate in batch-mode and continuous-flow mode, respectively. The effects of pH on solids disintegration, nutrient release and the physical properties of sludge were examined. The MW/H₂O₂-AOP treatment was very effective; the total suspended solids reduction and chemical oxygen demand solubilization was better for alkaline sets rather than acidic. However, acidic conditions were superior in the release of orthophosphate, particle size distribution, dewatering properties and settling.

In the treatment of acidified dairy manure, with the 915 MHz pilot-scale system at temperatures of 90 and 110°C and with a hydrogen peroxide dosage of 0.6% (v/v) per percent of total solids, the MW/H₂O₂-AOP yielded a clear supernatant, rich in the nutrients required for struvite (MgNH₄PO₄·6H₂O₂) crystal formation.

A total of fifteen salt water experiments were conducted with a salt concentration ranging from 10 to 120 g/L at three different flow rates (6, 7.5 and 9 L/min). The dominant heating mechanism was dipolar polarization and ionic conduction at a high flow rate and high salt concentration, respectively. High concentrations of ions suppressed the dielectric polarization, resulting in lower temperatures. Energy consumption was similar among the sets.

Lay Summary

The biggest challenge wastewater treatment facilities face today is the amount of sludge that is being generated after water has been treated; it is very expensive to dispose of as well as hazardous to the environment. The technology that was developed by this research group, led by Dr. K. V. Lo, Professor Emeritus, uses microwave radiation as a main treatment mechanism that can reduce the volume of sludge by 80 per cent. Furthermore, treated sludge enhances the production of methane gas that can be used as energy and it is also an abundant source of scarce nutrients such as phosphorus, which can be recovered and after further processing, used as a soil fertilizer. This technology is a solution to sustainable waste management and can minimize environmental impacts on society. This study investigates various operating conditions in an effort to optimize the process for future, full-scale operation.

Preface

The work carried out in this dissertation contributes to research on microwave technology in the treatment of organic slurries led by Dr. K. Victor Lo, Professor Emeritus in the Civil Engineering Department in the University of British Columbia. Dr. Asha Srinivasan, Research Associate, and Dr. Ping H. Liao, Research Scientist, provided supervision of the work undertaken.

Chapter 1 is original, unpublished work by Indre Tunile.

Chapter 2 is based on an experimental design prepared by Dr. Srinivasan and Dr. Liao. Experiments and sample analyses were carried out by Hanji Tan, Tim Burton, Tiffany Kang and Indre Tunile under the direct supervision of Dr. Srinivasan. Data analyses and the manuscript writing was carried out by Dr. Liao, Dr. Srinivasan, Hanji Tan, Tim Burton, Tiffany Kang and Indre Tunile. A version of this chapter has been published by the Journal of Separation and Purification Technology under the title, “Microwave enhanced advanced oxidation treatment of sewage sludge from the membrane-enhanced biological phosphorus removal process.”

Chapter 3 is original, unpublished work by Indre Tunile. Experimental design was prepared by Dr. Srinivasan. Hanji Tan assisted with the experimental execution and data analyses. The manuscript is in its preparation phase for submission to publish.

Chapter 4 is based on an experimental design prepared by Dr. Srinivasan and Dr. Liao. Experiments and sample analyses were carried out by Hanji Tan, Tim Burton, Tiffany Kang and Indre Tunile under the supervision of Dr. Srinivasan. Data analyses and the manuscript writing was carried out by Dr. Liao, Dr. Srinivasan and Indre Tunile. A version

of this chapter is under review to be published in the Journal of Environmental Science and Health under the title, “Microwave enhanced advanced oxidation treatment of dairy manure.”

The author also contributed to the execution of experiments, data analysis and writing of the manuscript for the article which is under review to be published in the Journal of Environmental Engineering, entitled, “Microwave enhanced advanced oxidation treatment of municipal wastewater sludge.” The manuscript is not included in this thesis; it is beyond the scope of this thesis.

Table of Contents

Abstract.....	ii
Lay Summary.....	iii
Preface.....	iv
Table of Contents	vi
List of Tables	ix
List of Figures.....	x
List of Abbreviations	xiii
List of Symbols.....	xiv
Acknowledgements	xv
Dedication	xvi
Introduction.....	1
Chapter 1: Literature review.....	3
1.1 Thermal hydrolysis	3
1.2 Microwave treatment (MW) of sludge	5
1.3 Advanced oxidation processes (AOPs).....	7
1.4 Advantages of microwave advanced oxidation process (MW/H ₂ O ₂ -AOP)	9
1.5 The main factors affecting the MW/H ₂ O ₂ -AOP process	10
1.6 The role of pH in the treatment process.....	12
1.6.1 Acid hydrolysis	12
1.6.2 Alkali hydrolysis.....	13
1.6.3 pH effect on the MW/H ₂ O ₂ -AOP treatment	15
Research objectives.....	17
Chapter 2: Waste activated sludge (WAS) experiments at different pH conditions	19
2.1 Introduction.....	19
2.2 Materials and methods	22
2.2.1 Microwave system	22
2.2.2 Substrate.....	23
2.2.3 Experiment design	24
2.2.4 Physical and chemical sample analysis.....	25

2.2.5	Energy analysis	27
2.3	Results and discussion for the 2450 MHz batch-mode system.....	28
2.3.1	Solids disintegration	28
2.3.2	Nutrient release	32
2.3.3	Physical properties	34
2.4	Results and discussion for the 915 MHz pilot-scale continuous-flow system.....	36
2.4.1	Solids disintegration.....	36
2.4.2	Nutrient release	42
2.4.3	Physical properties	45
2.4.4	Energy analysis	47
2.5	Conclusion	48
Chapter 3: Salt water experiments.....		49
3.1	Introduction.....	49
3.1.1	Basics behind the use of salt water as a control liquid	49
3.1.2	Previous salt water experiments with 915 MHz MW system.....	51
3.2	Materials and methods	53
3.2.1	Substrate.....	53
3.2.2	Experiment design	53
3.3	Results and discussion	54
3.3.1	Comparison study	55
3.3.2	Heating rate.....	56
3.3.3	Temperature rise per pass	58
3.3.4	Power consumption.....	59
3.3.5	Energy absorption	61
3.4	Conclusion	62
Chapter 4: Dairy manure experiments.....		63
4.1	Introduction.....	63
4.2	Materials and methods	67
4.2.1	Microwave system	67
4.2.2	Substrate.....	67

4.2.3	Experiment design	68
4.2.4	Chemical and physical sample analysis.....	68
4.3	Results and discussion	69
4.3.1	Solids disintegration.....	69
4.3.2	Nutrient release	75
4.3.3	Physical properties	83
4.3.4	Energy analysis	85
4.4	Conclusion	87
Chapter 5: Conclusions		88
Chapter 6: Recommendations		89
Bibliography		90
Appendix A Waste activated sludge experiments		100
A.1	Complete data set for 2450 MHz batch-mode MW/H ₂ O ₂ -AOP treatment of WAS.....	101
A.2	Complete data set for 915 MHz pilot-scale MW/H ₂ O ₂ -AOP treatment of WAS...	105
Appendix B Salt water experiments		110
B.1	10 g/L salt concentration comparison graphs	111
B.2	Graphical presentation of temperature rise per pass in response to flow rate/salt concentration.....	113
B.3	Graphical presentation of heating rate in response to flow rate/salt concentration.....	115
B.4	Graphical presentation of power consumption in response to flow rate/salt concentration.....	116
B.5	Energy absorption in response to flow rate/salt concentration	118
B.6	Tuning rod heights	122
Appendix C Dairy manure experiments		123
C.1	Complete data set for dairy manure experiments	124

List of Tables

Table 1 Operating conditions for 2450 MHz batch-mode MW/H ₂ O ₂ -AOP treatment of WAS ..	24
Table 2 Operating conditions for 915 MHz pilot-scale MW/H ₂ O ₂ -AOP treatment of WAS.....	25
Table 3 Methods and instruments used for physical analysis.....	26
Table 4 Methods and instruments used for chemical analysis.....	26
Table 5 Summary of results for salt water runs	54
Table 6 The characteristics of raw dairy manure.....	67
Table 7 Operating conditions for 915 MHz pilot-scale MW/H ₂ O ₂ -AOP treatment of DM	68
Table 8 Solids concentrations before and after MW/H ₂ O ₂ -AOP treatment of DM.....	69
Table 9 VFA concentration before and after MW/H ₂ O ₂ -AOP treatment of DM	73
Table 10 Ortho-P release before and after MW/H ₂ O ₂ -AOP treatment of DM	76
Table 11 CST results before and after MW/H ₂ O ₂ -AOP treatment of DM	84
Table 12 Solids disintegrated from 2450 MHz batch-mode MW/H ₂ O ₂ -AOP treatment of WAS.....	101
Table 13 Nutrients released from 2450 MHz batch-mode MW/H ₂ O ₂ -AOP treatment of WAS	102
Table 14 Particle size distribution of WAS from 2450 MHz batch-mode MW/H ₂ O ₂ -AOP treatment	103
Table 15 Solids disintegrated from 915 MHz pilot-scale MW/H ₂ O ₂ -AOP treatment of WAS..	105
Table 16 Nutrients released from 915 MHz pilot-scale MW/H ₂ O ₂ -AOP treatment of WAS	106
Table 17 Particle size distribution of WAS from 915 MHz pilot-scale MW/H ₂ O ₂ -AOP treatment sets	107
Table 18 Tuning rod heights in cm for salt water runs	122
Table 19 Tuning rod heights in cm for WAS and DM	122
Table 20 Solids disintegration before and after acid and/or MW/H ₂ O ₂ -AOP treatments of DM	124
Table 21 Nutrient release before and after acid and/or MW/H ₂ O ₂ -AOP treatments of DM	125
Table 22 Total and soluble portions of metals before and after acid and/or MW/H ₂ O ₂ -AOP treatments of DM	125

List of Figures

Figure 1 Schematics for pilot-scale continuous-flow 915 MHz microwave system	23
Figure 2 TSS before and after MW/H ₂ O ₂ -AOP treatment of WAS for batch-mode studies.....	28
Figure 3 SCOD to TCOD ratio as percent before and after MW/H ₂ O ₂ -AOP treatment of WAS for batch-mode studies	29
Figure 4 VFA before and after MW/H ₂ O ₂ -AOP treatment of WAS for batch-mode studies.....	31
Figure 5 Ortho-P and soluble TP release as percent of Total P after MW/H ₂ O ₂ -AOP treatment of WAS for batch-mode studies.....	32
Figure 6 Nitrogen in the MW/H ₂ O ₂ -AOP treated solution of WAS for batch-mode studies	33
Figure 7 TSS before and after MW/H ₂ O ₂ -AOP treatment of WAS for pilot-scale studies.....	37
Figure 8 SCOD to TCOD ratio before and after MW/H ₂ O ₂ -AOP treatment of WAS for pilot-scale studies	38
Figure 9 VFA before and after MW/H ₂ O ₂ -AOP treatment of WAS for pilot-scale studies.....	40
Figure 10 Ortho-P and soluble TP release as percent of TP after MW/H ₂ O ₂ -AOP treatment of WAS for pilot-scale studies	42
Figure 11 Nitrogen solubilization after MW/H ₂ O ₂ -AOP treatment of WAS for pilot-scale studies	44
Figure 12 Energy consumed by the 915 MHz continuous-flow microwave system plotted against solids solubilization and nutrient release indices for the MW/H ₂ O ₂ -AOP treatment of WAS.....	47
Figure 13 Heating rate as a function of salt concentration and flow rate	56
Figure 15 Power consumption as a function of salt concentration and flow rate	60
Figure 16 SCOD to TCOD ratio before and after MW/H ₂ O ₂ -AOP treatment of DM.....	70
Figure 18 The effect of temperature and/or hydrogen peroxide on phosphorus release	78
Figure 20 The effect of acid and/or MW/H ₂ O ₂ -AOP treatments of DM on metals solubilization.....	81
Figure 21 Settling of acidified and MW/H ₂ O ₂ -AOP treated DM.....	83
Figure 22 Energy consumed by the 915 MHz continuous-flow microwave system plotted against solids solubilization and nutrient release indices for the MW/H ₂ O ₂ -AOP treatment of DM	85

Figure 23 Particle size distribution of WAS from 2450 MHz batch-mode MW/H ₂ O ₂ -AOP treatment at 90°C.....	104
Figure 24 Particle size distribution of WAS from 2450 MHz batch-mode MW/H ₂ O ₂ -AOP treatment at 110°C.....	104
Figure 25 Particle size distribution of WAS from 915 MHz pilot-scale MW/H ₂ O ₂ -AOP treatment at 110°C/pH4	108
Figure 26 Particle size distribution of WAS from 915 MHz pilot-scale MW/H ₂ O ₂ -AOP treatment at 90°C/pH4	108
Figure 27 Particle size distribution of WAS from 915 MHz pilot-scale MW/H ₂ O ₂ -AOP treatment at 110°C/pH9	109
Figure 28 Particle size distribution of WAS from 915 MHz pilot-scale MW/H ₂ O ₂ -AOP treatment at 90°C/pH9	109
Figure 29 Temperature rise per pass vs flow rate for 10 gNaCl/L	111
Figure 30 Heating rate vs flow rate for 10 gNaCl/L.....	111
Figure 31 Energy consumed vs flow rate for 10 gNaCl/L.....	112
Figure 32 Heating time vs flow rate for 10 gNaCl/L.....	112
Figure 33 Temperature rise per pass vs flow rate for different salt concentrations.....	113
Figure 34 Temperature rise per pass in response to flow rate	113
Figure 35 Temperature rise per pass vs salt concentration for different flow rates.....	114
Figure 36 Heating rate vs flow rate for different salt concentrations	115
Figure 37 Heating rate vs salt concentration for different flow rates	115
Figure 38 Energy consumed vs flow rate for different salt concentrations	116
Figure 39 Energy consumed vs salt concentration for different flow rates	116
Figure 40 Power consumption rate vs salt concentration for different flow rates	117
Figure 41 Power consumption rate vs flow rate for different salt concentrations.....	117
Figure 42 Energy absorbed vs treatment time for 6 L/min flow rate at different salt concentrations	118
Figure 43 Energy absorbed vs treatment time for 7.5 L/min flow rate at different salt concentrations	118

Figure 44 Energy absorbed vs treatment time for 9 L/min flow rate at different salt concentrations	119
Figure 45 Energy absorbed vs treatment time for 10 gNaCl/L at different flow rates	119
Figure 46 Energy absorbed vs treatment time for 50 gNaCl/L at different flow rates	120
Figure 47 Energy absorbed vs treatment time for 80 gNaCl/L at different flow rates	120
Figure 48 Energy absorbed vs treatment time for 100 gNaCl/L at different flow rates	121
Figure 49 Energy absorbed vs treatment time for 120 gNaCl/L at different flow rates	121

List of Abbreviations

•OH	hydroxyl radicals
AD	anaerobic digestion
ANOVA	analysis of variance
AOPs	advanced oxidation processes
BOD	biological oxygen demand
CH	conventional heating
COD	chemical oxygen demand
CST	capillary suction time
DM	dairy manure
EPS	extracellular polymeric substances
H ₂ O ₂	hydrogen peroxide
H ₂ SO ₄	sulphuric acid
HRT	hydraulic retention time
MADP	anaerobic digestion process
MEBPR	membrane-enhanced biological phosphorus removal
MW	microwave
MW/H ₂ O ₂ -AOP	microwave hydrogen peroxide - advanced oxidation process
NaOH	sodium hydroxide
O ₃	oxygen
ortho-P	orthophosphates
PSD	particle size distribution
SBR	sulphate -reducing bacteria
SCOD	soluble chemical oxygen demand
SRT	solid retention time
STP	soluble total phosphorus
STKN	soluble total Kjeldahl nitrogen
TCOD	total chemical oxygen demand
TKN	total Kjeldahl nitrogen
TP	total phosphorus
TS	total solids
TSS	total suspended solids
TWAS	thickened waste activated sludge
VFAs	volatile fatty acids
VS	volatile solids
VSS	volatile suspended solids
WAS	waste activated sludge
WWTPs	wastewater treatment plants

List of Symbols

S_L - solids solubilization index

N_e - nutrient release index

x_0 - parametric ratio of the untreated sludge

x_t - parametric ratio of the treated sludge at time t

Acknowledgements

I would like to take this opportunity to thank the people that supported, guided and encouraged me during my time in UBC.

Many thanks to my research supervisor, Dr. Victor Lo, for providing me with this opportunity.

To Dr. Asha Srinivasan and Dr. Ping Liao for their continued guidance and advice throughout the research development and analysis stages.

To Hanji Tan, Tim Burton and Tiffany Kang for their help with experiments, laboratory work, data analyses and their friendship and support throughout the research stage.

Tim Ma, for analyzing samples and providing help and advice during laboratory work carried out. Ruihuan Ning and Cristina Kei Oliveira, for teaching me how to perform sample analyses in the laboratory.

To Reza Bahreini, Sylvia Wooley Stefanie Teo, Erica Kennedy and Mike Beswick for their support, encouragement, help with coursework and friendship.

To the Natural Science and Engineering Research Council (NSERC) of Canada and The India – Canada Water for Health Collaborative Research funded by IC-IMPACTS Centres of Excellence, Canada, for providing funding opportunities, without which none of this would have been possible.

Dedication

I would like to dedicate this work to my family; without their presence, love and support, my motivation to succeed would have been diminished.

Introduction

Municipal wastewater treatment plants (WWTPs) generate vast amounts of sewage sludge and the management and disposal of sewage sludge attributes to 50% of overall cost of WWTPs. Population growth and more stringent disposal regulations to protect natural waters, soil and air calls for an efficient and environmentally sound management of the sludge practices.

Canada alone produces more than 3.0 billion liters of sewage sludge a day (Sierra Legal Defence Fund report, 2004). According to the United Nations Environment Programme (UNEP), in the US and Europe, the most popular sludge management methods from most to least are landfilling, agriculture and incineration.

Unfortunately, landfilling is a short-term solution that poses the risks of polluting groundwater and surface water. Also, such a disposal method does not take advantage of the nutrient value and soil building properties of bio-solids. Incineration on the other hand, produces hazardous waste and is energy intensive and expensive. The use of sewage sludge in agriculture is limited due to toxic pollutants. Common pollutants found in sewage sludge are total suspended solids (TSS), biological oxygen demand (BOD), faecal coliform and bacteria. Other toxic pollutants found in municipal sewage are heavy metals and persistent organic pollutants such as polychlorinated biphenyls (PCBs) and polycyclic aromatic hydrocarbons (PAHs); substances known to cause mutations and cancer (Sierra Legal Defence Fund report, 2004).

Sewage sludge is currently gaining recognition as valuable resource that can generate energy, produce bio-solids and act as a source of valuable non-renewable nutrients such as phosphorus. However, sludge minimization is of primary interest to WWTPs (UNEP).

In conventional WWTPs after preliminary screening, settleable organic and inorganic solids are removed by sedimentation. The resultant effluent is then further treated using aerobic biological treatment processes that utilizes oxygen to remove biodegradable, dissolved and colloidal organic matter. The byproduct of this process is the production of waste activated sludge (WAS) that requires treatment to reduce its water and organic content to obtain a stabilized product suitable for end-use or safe disposal. The common methods employed to reduce the excess sludge is anaerobic digestion (AD) and dewatering.

WAS has a complex floc structure that is comprised of various groups of microorganisms; organic and inorganic matter agglomerated together in a polymeric network formed by microbial extracellular polymeric substances (EPS) and cations (Frolund et al., 1996). EPS makes up nearly 80% of WAS, greatly influencing the dewaterability properties (Neyens et al., 2004). Thermal hydrolysis was found to be very effective in destroying EPS and cells releasing organic matter into solution for biological degradation or the recovery of useful components like nitrogen and phosphorus (Neyens and Baeyens, 2003).

Chapter 1: Literature review

1.1 Thermal hydrolysis

A thermal hydrolysis process involves heating of sludge commonly provided by a live steam injection under pressure followed by rapid decompression. Temperatures between 60 and 275°C are usually utilized in the process with treatment times in the range of 10-180 min. (Barber, 2016). Thermal hydrolysis was found to be more effective in the treatment of WAS rather than primary sludge as it contains less amount of lipids and high concentrations of carbohydrates and proteins (Wilson and Novak, 2009). Thermal hydrolysis had little to no influence on lipids solubilization (Noike, 1992; Bougrier et al., 2008; Lu et al., 2014).

Sludge treatment by thermal hydrolysis was initially developed to improve dewaterability properties (Lumb, 1940). The technology was studied in full scale operation for 10 years proving its effectiveness, where moisture content of the sludge cake was reduced to 48% compared to 70% without thermal pretreatment (Lumb, 1951). Although the process was effective in improving dewaterability, it also solubilized sludge solids, resulting in effluent high in chemical oxygen demand (COD) that was unfit for discharge to water bodies or recycling to the treatment plant (Erickson and Knapp, 1970; Boyle and Gruenwald, 1975). Everett (1972) observed that COD solubilization increased with an increase in treatment temperature (up to 170°C) and holding time (up to 60 minutes). However, cell destruction ceased after heating to 200°C for 1 hour, where all the chemicals dissolved or saturation point was reached. Despite reaching the optimum operating conditions for cell destruction, chemical reactions were still occurring. For example, organic nitrogen was converted to ammonia and the concentration increased with an increased holding time (Brooks, 1970).

Despite the drawbacks of the process, the COD loading could be substantially decreased by introducing a secondary treatment process such as anaerobic digestion.

Anaerobic digestion is the process of stabilizing high strength organic wastes by microbes in the absence of oxygen. The process reduces the amount of sludge solids while generating biogas. The disadvantage of a sole AD process is its incapability to produce sludge that is free from viral and bacterial pathogens for it to be used as fertilizer (Haug, 1977). Therefore, utilizing thermal hydrolysis before AD is beneficial for sterilization of sludge as well as enhancing biodegradability properties and in turn reducing hydraulic retention time (HRT) and increasing biogas production (Haug, 1977; Lu et al., 2014; Hiraoka et al., 1985). Other reported benefits are odor control and inactivation of bacteria (Haug et al., 1978; Neyens and Baeyens, 2003). Haug et al. (1978) reported the optimum operating temperature of 175°C for gas production beyond which gas production decreased. Similarly, the effect of temperature above 175°C negatively impacted biodegradability of WAS where nitrogenous organic material present in WAS became less biodegradable, resulting in the formation of toxic/refractory compounds (Stuckey and McCarty, 1978; Bougrier et al., 2008). The addition of chemicals such as sodium hydroxide allowed the treatment temperature to be reduced to 130°C to achieve the same results as a treatment at 180°C thus eliminating the formation of refractory compounds (Tanaka et al., 1997).

1.2 Microwave treatment (MW) of sludge

Microwave (MW) irradiation in the application of sewage sludge treatment is a relatively new concept with the majority of research still performed in lab-scale environments. Treatment by MW irradiation is superior to conventional heating (CH) in that it provides rapid and selective heating, higher energy efficiency, a capacity to enhance yield and quality of products whilst diminishing hazardous product formation and emission (Tyagi and Lo, 2013). In a conventional heating process, the material is heated from outside to inside and the rate of heating depends on the material thermal properties and temperature differential (Mehdizadeh et al., 2013).

The microwave energy in itself is not thermal energy; heat is generated when microwave and dielectric materials interact (Decareau and Peterson, 1986). During MW irradiation, energy is transferred to material by interaction of the electromagnetic fields at the molecular level, and the dielectric properties ultimately determine the effect of the magnetic field on the material (Thostenson and Chou, 1999). Electromagnetic energy is converted to heat when the applied electromagnetic field interacts with the dielectric properties of material. The dielectric properties are dependent on the mobility of the dipoles (water molecules) within the material, and therefore the dielectric properties are functions of temperature, frequency, and degrees of reaction. As a result, the ability of the material to absorb energy changes during processing.

Water is a dielectric material and hence it is a good absorber of MW irradiation; high amounts of water in sewage sludge alters its properties when it is exposed to MW irradiation (Wojciechowska, 2005). During MW irradiation the main compounds found in sludge are hydrolyzed as follows: lipids are converted to palmitic acid, stearic acid and oleic acid;

proteins are hydrolyzed into saturated and unsaturated acids; ammonia to carbon dioxide; and carbohydrates are hydrolyzed to lower molecular-weight polysaccharides and simple sugars.

Soluble COD is a good indicator of the extent of the disruption of the complex WAS floc structure, releasing extracellular and intracellular biopolymers such as protein and sugar into a soluble phase (Eskicioglu et al., 2006). It was also found, that DNA and bacterial cellular membranes are damaged by MW irradiation independent of thermal heating (Hong et al. 2006). Eskicioglu et al. (2007) investigated the athermal effect of MW irradiation at temperatures of 50-96°C and compared with CH treated samples. In terms of COD and biopolymer solubilisation, both pretreatment methods yielded similar results, however, MW pretreated samples performed better in the mesophilic anaerobic biodegradation process (MADP) resulting in 13% higher biogas production that was attributed to the MW athermal effect. Similarly, lower MW treatment temperatures of 60-65°C resulted in a higher biogas production and reduced capillary suction time (CST) of MADP samples by 6.3 and 10.7%, respectively, compared to CH pretreated digested sludge (Pino-Jelicic et al., 2006). MW treated WAS also yielded considerable amounts of soluble COD and achieved higher fecal coliform reduction.

Mehdizadeh et al. (2013) extended the research to investigate the effects of MW irradiation and CH above boiling point temperatures (80-160°C). Authors concluded that temperature was the most significant factor effecting solids solubilization irrespective of treatment methods. Both particulate COD and biopolymer solubilization in biological sludge was similar among both pretreatment methods and the different temperatures studied.

Chang et al. (2011) showed that energy consumption by MW irradiation was 5 times lower than that of CH. MW treatment took only 2 min to reach a temperature of 85°C, whereas 12 min were required to reach 80°C for CH.

1.3 Advanced oxidation processes (AOPs)

Advanced oxidation processes (AOPs) have been defined as the aqueous phase chemical oxidation of target organic or inorganic pollutants through a process involving hydroxyl-free radicals (Rosenfeldt et al., 2006). AOPs involve the two stages of oxidation; the formation of strong oxidants such as hydroxyl radicals and the reaction of these oxidants with pollutants in water.

The use of oxidizing agents in wastewater treatment is of interest to researchers since the generation of hydroxyl radicals increases the reaction rates and mineralization of organics. Hydrogen peroxide and ozone are strong chemical oxidants; they both produce water and carbon dioxide as end products. Through catalysis of UV, MW-radiation and/or Fe^{2+} ions (Fenton reagent), hydrogen peroxide (H_2O_2) and ozone (O_3) can be converted into highly reactive hydroxyl radicals ($\bullet\text{OH}$) (oxidation potential 2.33 V) that have a higher oxidation potential than H_2O_2 (1.8 V) or O_3 (2.1 V) itself. Ozone can also act as catalysis as it is able to dissociate hydrogen peroxide to form hydroxyl radicals.

When H_2O_2 is added to the solution with O_3 , the decomposition of O_3 to hydroxyl radicals is accelerated, shifting the process entirely to AOP (Acero and Von Gunten, 2001; Griffini and Iozzelli, 1996). This is recommended for waters in which ozone is stable and resulting pollutant degradation is slow. During oxidative treatment by ozone, activated sludge is mineralized to water and carbon dioxide, as well as solubilized to biodegradable

organics that can be biologically treated (Liu, 2003). The use of ozone in the sludge reduction process was reported to produce refractory organic carbon, which is unfavorable. The use of H_2O_2 was also superior compared to the use of the Fenton catalysis method in oxidizing phenol (Sanz et al., 2002). When H_2O_2 absorbs UV light, it breaks down into hydroxyl radicals, degrading the contaminant via $\bullet\text{OH}$ radical oxidation (Bolton and Cater, 1994). MW radiation is non-ionizing unlike UV-radiation and it is less energetic; it is found at lower frequencies and has a longer wavelength.

Oxidative treatments combined with biological degradation have been shown to be very effective methods in reducing EPS in the treatment of WAS (Paul et al., 2006b). More than 40% reduction in EPS was achieved by utilizing thermal treatment (95°C) in combination with O_3 or H_2O_2 . Similarly, MW irradiation as a heat source with H_2O_2 increased polymeric network disintegration (Eskicioglu et al, 2008). Although MW/ H_2O_2 pretreated samples yielded lower methane production, the dewaterability of digested sludge improved.

Yin et al. (2007) conducted a comparative study of MW (100°C), H_2O_2 , O_3 and a combination of all in the treatment of WAS. Hydrogen peroxide yielded higher solids solubilization and ammonia release with and without MW treatment compared to O_3 treated samples; however, the decomposition rate was accelerated with MW irradiation. An addition of O_3 to MW/ H_2O_2 improved the results slightly. Lo et al. (2015) extended the research into oxidant effects to include different temperature regimes and to assess process efficiency with regards to changes in physical properties of WAS. In addition to the 2450 MHz batch digester, 915 MHz pilot-scale system was utilized. It was concluded that the sequence of

introducing oxidants into the treatment process was very important. The best result was achieved by ozone followed by hydrogen peroxide and MW.

The dipolar polarization mechanism is responsible for enhancing the degradation rate of various pollutants in the system combining MW and oxidants (Eskichioglu et al., 2006). Their mechanism increases temperature within a short period of time that provokes the increased decomposition of H_2O_2 into $\bullet\text{OH}$. However, H_2O_2 at high concentrations can decrease degradation rate, therefore, it is important to determine an optimum dosage (Remya and Lin, 2011). When utilizing the 915 MHz pilot-scale system, a dosage of 0.6% (v/v) per percent of total solids was found to be the optimum level in the treatment of WAS at 90 and 110°C (Lo et al., 2017). Also, at low temperature ($< 40^\circ\text{C}$), H_2O_2 reacts quickly with organic matter and decomposes into water and molecular oxygen. Catalase, a terminal respiratory enzyme present in all aerobic cells, is active over a wide range of pH (3-9) but is temperature-dependent (Gabbita and Huang, 1984). Its function is to protect cells from damage caused by reactive oxygen species (Guwy et al 1998; Guwy et al 1999). The activity of catalase was completely deactivated at a temperate of 60°C (Lo et al., 2014).

1.4 Advantages of microwave advanced oxidation process (MW/ H_2O_2 -AOP)

MW in combination with H_2O_2 , outperformed MW only in solubilization of organic matter (Wong et al., 2006b; Yin et al., 2007; Yin et al., 2008; Eskisioglu et al., 2008; Lo et al., 2010). The addition of hydrogen peroxide facilitates the production of highly reactive $\bullet\text{OH}$ radicals; thus, the treatment can be operated at lower temperatures and/or shorter time. At treatment temperature above 80°C, all of the COD was solubilized after the MW/ H_2O_2 -

AOP, compared to only 50% COD solubilization with MW only at 120°C (Wong et al., 2006a).

Yu et al. (2010a) demonstrated that a H₂O₂ dosage of 0.08% or higher at MW treatment temperature of 70°C, inhibited reproduction of fecal coliforms in the treated solids, resulting in A class bio-solids. Without addition of hydrogen peroxide, MW treatment temperatures of 100°C and above were required to inhibit microbial activity (Liao et al., 2005a).

Higher ammonia concentrations were achieved in the MW treatment with H₂O₂ (Wong et al., 2006a, b; Yin et al., 2007). Treatments at 60-120°C resulted in ammonia concentration in the range of 1.2-3.5 mg/L for MW alone treated sets and 29.5-108 mg/L for MW with addition of H₂O₂ (Wong et al., 2006b). Low yield of ammonia in MW treated samples without H₂O₂, was found to be a limiting nutrient in the struvite crystallization process.

The efficiency of the MW/H₂O₂-AOP can be further enhanced by identifying key process-parameters that affect solids disintegration and nutrient release from WAS.

1.5 The main factors affecting the MW/H₂O₂-AOP process

Hydrogen peroxide plays an important role in solids disintegration in the MW/H₂O₂-AOP process. In general, solids disintegration is enhanced with a higher H₂O₂ dosage (Wang et al., 2009; Lo et al., 2017). The effect of dosage is especially evident among different temperature regimes. Low H₂O₂ concentration was ineffective at treatment temperatures below 70°C, beyond which SCOD started to increase with a higher H₂O₂ dosage (Yu et al.,

2010a). Low temperatures require high H₂O₂ dosages in order to solubilize organic matter (Wong et al., 2006a). The production of volatile fatty acids (VFAs) exhibited the same trend as SCOD (Liao et al., 2007, Lo et al., 2014). The optimum dosage of hydrogen peroxide for solids solubilization was determined to be 0.6 %H₂O₂/%TS at treatment temperatures of 90 and 110°C (Lo et al., 2017). Nutrient release was less impacted by the H₂O₂ dosage especially phosphorus release, however, in the formation of ammonia, the effects of H₂O₂ were more pronounced particularly at a high operating temperature (Wong et al., 2006b; Kenge et al., 2009b; Yin et al., 2007; Yin et al., 2008; Lo et al., 2014).

Temperature significantly affects the release of nutrients, especially phosphorus. MW treatment with and without H₂O₂ solubilized 76 and 84% of total phosphorus at 170°C and 5 minutes heating time (Liao et al 2005a; Liao et al 2005b). The release of phosphorus into solution can be facilitated at temperatures of 60-90°C, however, most of it is in the form of polyphosphate; therefore, higher temperatures are required to degrade polyphosphate to orthophosphate (ortho-P), constituent in struvite crystal formation (Chan et al., 2007; Kuroda et al., 2002; Yu et al., 2010b; Lo et al., 2014). The conversion of polyphosphates formed during MW treatment into ortho-P can also be facilitated by acid hydrolysis (Harold 1960).

Heating period is a significant factor affecting SCOD although it is not as significant as temperature and H₂O₂ dosage (Wong et al., 2006b; Chan et al., 2010; Yu et al., 2010c; Lo et al., 2014). Longer heating times also favor the formation of ammonia in alkaline conditions (Chan et al., 2010).

Irradiation intensity was found to affect COD solubilization and dewaterability properties and to a lesser extent, ammonia and ortho-P release (Chan et al., 2010).

PH was found to have an effect on SCOD and VFA concentrations in the solution. It was reported that a low pH helped to retain carbon in the solution at a high treatment temperature (Liao et al., 2007). In addition, low pH greatly improved dewaterability and settling properties of WAS (Yu et al., 2010c).

1.6 The role of pH in the treatment process

Understanding the interactions between different chemicals is crucial in the process of WAS treatment. New components formed during treatment can either enhance or suppress the effectiveness of treatment by MW irradiation.

1.6.1 Acid hydrolysis

Acid hydrolysis is very effective in the treatment of materials high in lignocellulosic matter that is widely utilized in the production of ethanol (Wyman, 1994). During acid hydrolysis, the cellulose and hemicellulose polymers are broken down into lignocellulosic biomass to form individual sugar molecules which can be converted to ethanol by fermentation. Acid can also penetrate lignin without pretreatment which then condensates and precipitates out of solution (Lenihan et al., 2009; Ariunbaatar et al., 2014).

The acid hydrolysis process involves heating the substrate to temperatures of 100-150°C with either sulphuric acid (H_2SO_4) or hydrochloric acid (HCl) at concentrations of 1-10% (Wingren et al., 2008). Sulphuric acid was found to be more effective in causing cell lysis (Rocher et al., 1999). Dilute acid and/or low temperatures (<160°C) can only break down hemicellulose and the yield of glucose from cellulose is low (Romero et al., 2010; Wyman, 1994). To facilitate hydrolysis of crystalline cellulose, high temperatures (200-

240°C) are required, however, these conditions degrade xylose and glucose to furfural and hydroxymethyl-furfural (HMF), an inhibitory byproduct, which in turn degrade to tars and other undesirable products (Wyman, 1994). Sulphuric acid, the most commonly used in hydrolysis at high concentrations, was reported to hydrolyze cellulose and hemicellulose at moderate temperatures with little sugar degradation.

In the treatment of WAS, acid-hydrolysis disintegrates floc structure by changing the microorganisms surface properties, thus releasing EPS and intracellular material (Chen et al., 2001). The presence of net-negative surface charge on sludge surface creates electrostatic repulsion that prevents agglomeration of sludge particles; however, the effect is minimized in the pH range of 2.6 to 3.6, near the isoelectric point (Neyens et al., 2003b). The concentration of supracolloidal ($>1\mu\text{m}$) solids released from cells is also reduced with decreasing pH and the reduced charge of solids allows aggregation that decreases the total surface area of particles and their specific resistance (Karr and Keinath, 1978). The decrease of EPS and colloidal solids result in greatly improved settleability and dewaterability.

The optimum treatment condition for acid-induced thermal hydrolysis was at pH 3, a treatment temperature of 120°C and a heating time of 60 minutes (Neyens et al., 2003b)

1.6.2 Alkali hydrolysis

Alkaline treatment of WAS is an effective pretreatment method. High pH conditions cause cell disruption due to the cell losing their viability, at which point it cannot maintain an appropriate turgor pressure (Neyens et al., 2003a). The cell membrane is then solubilized by means of saponification, releasing intracellular material out of the cell. As a result, anaerobic microbes can easily access the substrates, thus making this pretreatment method ideal for an

anaerobic digestion process. Sodium hydroxide (NaOH) was reported to be the most effective alkaline reagent in causing cell lysis (Rocher et al., 1999) Lin et al. (1997) demonstrated that WAS, pretreated with NaOH, was superior to that of untreated WAS in terms of COD, volatile solids (VS) removal and gas production in the AD process. WAS, with 2% TS subjected to 20 meq/L NaOH, resulted in 14% higher COD reduction, 163% higher gas production and greatly improved dewaterability of digested sludge. Furthermore, alkali treatment reduced sludge particle size and increased electrostatic repulsion by increasing the net negative charge of bacterial surface, which causes the desorption of some parts of EPS (Xiao and Liu, 2006; Neyens and Baeyens, 2003).

The effectiveness of alkaline treatment is further enhanced when combined with thermal hydrolysis. Tanaka et al. (1997) investigated alkaline (pH 12), thermal and alkaline thermal treatment of WAS. The best results were obtained when the two processes were combined together yielding 45% in volatile suspended solids (VSS) solubilization, 120% higher gas production with a treatment temperature of 130°C for 5 minutes. Alkaline (ambient temperature) and thermal treatment (180°C) resulted in only 50 and 80% increases in biogas production, respectively. Lower treatment temperature (90°C) and much longer HRT (10 hours) also achieved a high degree reduction of VSS (85%) and COD solubilization (80%) (Vlyssides, 2004). The process was also efficient in terms of reducing the residual sludge amounts, removing pathogens and improving dewaterability (Neyens et al., 2003a). The combined treatment is able to reduce the size of the solids and increase reaction rate.

WAS adjusted to pH 10-12.5, resulted in a 50-70% VSS reduction while 80% of total chemical oxygen demand (TCOD) was solubilized at a MW treatment temperature of 120-170°C with a treatment time of 5 minutes (Qiao et al., 2008). Settleability also improved

greatly after subjecting alkaline WAS to MW treatment for the duration of 1 minute. The same study examined MW and alkali pretreated digested sludge characteristics and found that dewaterability improved by 22% and methane production was increased by 18.9%. Similarly, Dogan and Sanin (2009) reported that MW alkaline pretreated sludge, subjected to MADP for a period of 15 days, resulted in an increased daily biogas production.

The effectiveness of pretreatment methods employing MW irradiation with an addition of NaOH on thickened activated sludge (TWAS) in the process of AD was investigated by Chi et al. (2011). MW treatment at 170°C and a 1 min holding time, yielded the reduction of VS and TCOD by 28 and 18%, respectively, and had a potential to increase the biodegradability of TWAS despite the resulting effluent having increased SCOD and decreased dewaterability.

1.6.3 pH effect on the MW/H₂O₂-AOP treatment

It is important to understand the effect of pH in the MW/H₂O₂-AOP treatment since the stability of H₂O₂ is influenced to a great extent by pH. Hydrogen peroxide decomposes easily under alkaline conditions and is stable in acidic conditions (Wang et al., 2015). Organic matter can be solubilized without MW irradiation at different pH conditions over a long period of time. Unlike a low pH, an extremely high pH increases net negative charge of bacterial surface that impacts dewaterability properties.

In the case of MW/H₂O₂-AOP treatment, Wong et al. (2007) reported that acid treatment was advantageous in solids solubilization and nutrient release, but it was not a significant factor in the overall treatment process. Authors investigated treatment temperatures in the range of 60-200°C, a hydrogen peroxide dosage of 0-2 ml added to a 30

ml sample, and sulphuric acid volume of 0.25-0.5 ml. Despite these finding, Kenge et al. (2009a) investigated the treatment of WAS at pH 4 and 7.8 and found that the addition of acid was superior in the treatment of WAS. At a treatment temperature of 160°C, soluble COD, ortho-P and ammonia increased by 190, 527 and 56%, respectively, whereas a pH of 7.8 resulted in an 80% increase in soluble COD and had a negative effect on ortho-P and ammonia release. Acid treatment (pH 2.2-4.9) resulted in increased particle size, therefore drastically improving dewaterability (Chan et al., 2010).

Alkaline conditions (pH 10-11) yielded better solids solubilization and nutrient release, however, dewaterability was compromised due to high volume of small particles after MW/H₂O₂-AOP treatment. The optimum conditions for solids disintegration was reported with a TSS of 20 g/L, H₂O₂ of 2 (w/w) and a pH of 10 (Wang et al., 2015). The authors assessed the degree of interactions between TSS (2-20 g/L), pH (4-10) and H₂O₂ dosage (0-2 w/w) and concluded that interaction of these variables were not significant.

Research objectives

The primary research objective was to examine the effects of pH (4-9) on the MW/H₂O₂-AOP treatment of WAS under batch-mode (2450 MHz) and continuous-flow (915 MHz) operations. As a result, the treatment efficiency with respect to changes in chemical and physical properties was evaluated by investigating the following:

- The effect of MW treatment temperature (90-110°C).
- The effect of hydrogen peroxide dosage (0-0.8% per percent TS).
- The degree of treatment effectiveness for batch-mode and continuous-flow mode.
- The resultant effluent suitability for resource recovery and/or AD process and/or sludge residual reduction.

The secondary objective was to identify and eliminate, where possible, the 915 MHz pilot-scale system's performance-suppressing factors. As a result, the post modification system's characterization was conducted and the following was evaluated:

- The degree of enhancement with respect to temperature rise, energy consumption and treatment time to that of previous studies.
- The effect of various salt concentrations and flow rates on temperature rise.
- Energy consumption rate and efficiency.

Finally, the effectiveness of the 915 MHz pilot-scale system in the treatment of acidified DM was assessed by evaluating the results from this and previous studies, and by investigating the following:

- The effect of treatment temperature (90-130°C) and hydrogen peroxide (0.15-0.6% per percent TS) on the physical and chemical characteristics of treated dairy manure.
- The optimum operating conditions for the consequent nutrient recovery process.

Chapter 2: Waste activated sludge (WAS) experiments at different pH conditions

2.1 Introduction

Thermal hydrolysis using a conventional heating process has been used for destroying cell walls and degrading intracellular and extracellular substrates of waste activated sludge (WAS) (Sakai et al., 1997; Neyens et al., 2002; Menedez et al., 2002; Neyens and Baeyens, 2003; Neyens et al., 2003a, b; Appels et al., 2010; Abelleiraa et al., 2012). A combination of thermal heating and chemicals, such as ozone, hydrogen peroxide, acids or alkali resulted in higher rate of degradation than the individual thermal or chemical treatment processes (Neyens et al., 2003b); it was effective in reducing amounts of sludge solids, improving dewaterability of sludge and releasing nutrients (phosphorus and nitrogen).

Both microwave treatment (MW) and microwave-advanced oxidation process (MW/H₂O₂-AOP) were very effective in treating sewage sludge (Liao et al., 2005a; Wojciechowska, 2005; Hong et al., 2004; Eskicioglu et al., 2007; Hsieh et al., 2007; Carrere et al., 2010; Wong et al., 2007; Qiao et al., 2008; Dogan and Sanin 2009; Chi et al., 2010; Chang et al., 2011; Tyagi and Lo, 2012; Lo et al., 2014; Lo et al., 2015; Lo et al., 2016). The advantages of microwave heating over conventional heating is rapid and uniform heat transfer, shorter reaction times, and better energy efficiency. Temperature, heating time, and power intensity were the significant factors affecting the MW process efficiency. Besides the above-mentioned factors, hydrogen peroxide dosage was also a significant factor for the MW/H₂O₂-AOP (Wong et al., 2006a; Chan et al., 2010). In a batch operation mode, each factor can be selected independently. However, temperature, heating time and power

intensity are intertwined in a continuous-flow system: the heating rate of the substrate is controlled by its flow rate; a higher flow rate results in a lower heating rate of the substrate and a shorter process retention time. A higher flow rate also reduces the amount of microwave radiation transmitted to the substrate (Yu et al., 2010c). The advantage of a continuous-flow system over a batch mode operation is that H_2O_2 and sludge can be simultaneously introduced into the system at any given time in the process. Hydrogen peroxide added at higher MW temperatures ($> 80^\circ\text{C}$) increases the decomposition of H_2O_2 into hydroxyl radicals, that will increase both oxidation and the particulate disintegration of WAS (Eskicioglu et al., 2008; Yu et al. 2010c; Wang and Wang, 2016). As a result, less H_2O_2 was required when it was added at higher temperatures. At low temperatures, H_2O_2 can be consumed first by highly active catalase before it can react with sludge particulates when it is introduced at low temperatures below 60°C (Guwy et al., 1998; Guwy et al., 1999). In a closed-vessel batch microwave system, H_2O_2 was added to the substrate prior to the microwave treatment. To curtail catalase activity, addition of H_2O_2 can be carried out after preheating the substrate to the desired temperature. It thus required the substrate loading to and removing from a batch microwave system twice (Wang et al, 2015).

Albeit extensive studies investigating sludge treatment by the MW/ H_2O_2 -AOP, there are only few studies at the effect of pH on the process (Chan et al., 2007; Chan et al., 2010; Wang et al., 2015). Furthermore, the pH applied in these studies was usually very low or extremely high (< 4 or > 11). It was reported that extremely high pH greatly enhanced solids solubilization resulting in improved biodegradability and thus biogas production. Acidic conditions greatly favored the settling and dewaterability properties of WAS. Therefore, the MW/ H_2O_2 -AOP treatment efficiency could be greatly enhanced when the process combined

with significant pH changes. This study was thus undertaken to examine the effects of pH (4-9) on the MW/H₂O₂-AOP treatment of sludge under batch-mode and continuous-flow operation. This is part of our continued efforts to explore the MW/H₂O₂-AOP for sludge treatment for producing an effluent that can be used for subsequent struvite (MgNH₄PO₄·6H₂O) crystallization and anaerobic digestion.

2.2 Materials and methods

2.2.1 Microwave system

A 2450 MHz microwave digestion system (Ethos TC Digestion Lab station 5000, Milestone Inc., USA) is operated in batch mode with two magnetrons with a maximum power supply of 1 kW that is designed to operate at the temperature and pressure of up to 220°C and 30 bar, respectively. It consists of 12 vessels that sit on a rotating microwave diffuser with maximum speed 200 rpm that aids in electromagnetic radiation (EMR) distribution. The total volume is approximately 1.2 L. The temperature of a sample is recorded via a temperature probe placed in one of the vessels. The mixing is performed by magnetic stir bars placed in the sample. The temperature, heating time and power intensity is controlled by an independent system controller and can be selected independently.

A 915 MHz microwave digestion system, shown in Figure 1 on the following page, was custom-designed to operate as a continuous-flow system with a temperature and pressure capacity of up to 120°C and 200 kPa, respectively. The system consists of a generator (Sairem) with a power output of 5 kW, an applicator (1 m long, hollow aluminum conduit) and a substrate feeding system. The feeding system included feeding and hydrogen peroxide pumps, a holding tank (46 L), a H₂O₂ tank and a reservoir tank.

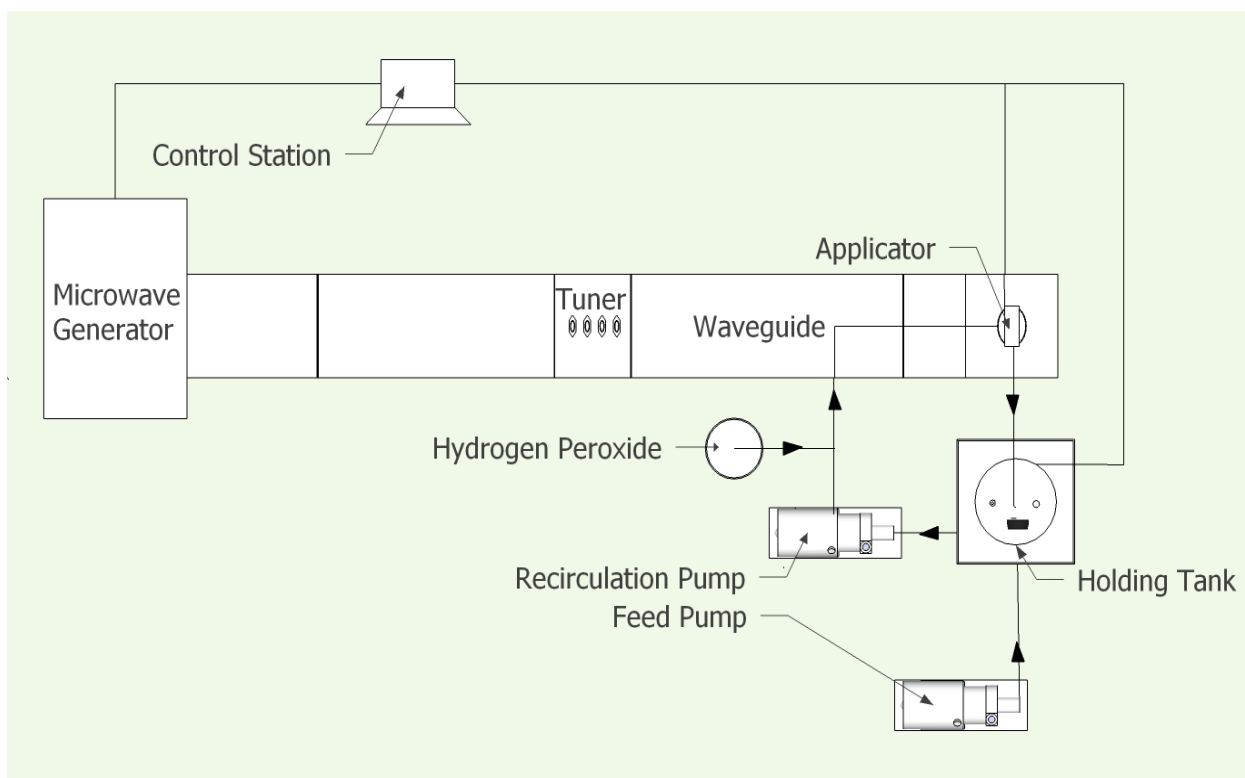


Figure 1 Schematics for pilot-scale continuous-flow 915 MHz microwave system

2.2.2 Substrate

Aerobic secondary sewage sludge used in this study was collected from the recently decommissioned pilot plant located at the University of British Columbia (UBC) south campus. The pilot-scale wastewater treatment plant utilizes the membrane-enhanced biological phosphorus removal (MEBPR) process. It consists of three stages which utilizes anaerobic, anoxic and aerobic zones to remove carbonaceous materials and nitrogenous compounds, as well as phosphorus from the wastewater. A recycle line allows flow from the aerobic zone back to the anoxic zone for increased denitrification efficiency and enhanced phosphorus up-take by bacteria. Sludge retention time (SRT) was maintained at

approximately 40 days. The MEBPR process was operated at a hydraulic retention time of 10 hours.

2.2.3 Experiment design

For batch mode operation, eight sets of microwave treatments, summarised in Table 1, were conducted at 90 and 110°C with a ramp rate of 20°C/min and held for 5 minutes. Based on the results from previous studies, hydrogen peroxide dosage of 0.6 %H₂O₂/%TS was used. Four experimental sets were used at each temperature: microwave heating without hydrogen peroxide (MW), MW with hydrogen peroxide (MW/H₂O₂), MW with hydrogen peroxide at pH 4 (MW/H₂O₂/pH 4) and MW with hydrogen peroxide (MW/H₂O₂/pH 9). Sludge was adjusted to the predetermined pH using either sodium hydroxide or sulfuric acid. Due to a closed-vessel microwave unit, hydrogen peroxide was added in at the beginning of the process when required.

Table 1 Operating conditions for 2450 MHz batch-mode MW/H₂O₂-AOP treatment of WAS

Set No.	pH	Sludge Volume (mL)	H ₂ O ₂ %/%TS	Temperature (°C)	Ramp Time (min)	Holding Time (min)	Total Time (min)
1	4	30	0.6	110	4.5	5	9.5
2	9	30	0.6	110	4.5	5	9.5
3	6.2	30	0.6	110	4.5	5	9.5
4	6.2	30	0.0	110	4.5	5	9.5
5	4	30	0.6	90	3.5	5	8.5
6	9	30	0.6	90	3.5	5	8.5
7	6.7	30	0.6	90	3.5	5	8.5
8	6.7	30	0.0	90	3.5	5	8.5

Four sets of MW/H₂O₂/pH 4 and MW/H₂O₂/pH 9, summarised in Table 2, were operated at 90 and 110°C in the 915 MHz pilot-scale microwave system. Hydrogen peroxide (0.6 or 0.8 %H₂O₂/ %TS) was introduced into the system at 60°C for all treatment sets. This was to enhance the synergistic effect of heating and H₂O₂, and to deactivate catalase activity. The authors have previously studied the MW and the MW/H₂O₂ treatment of the same substrate (MacSween, 2015; Lo et al., 2017; Lo et al., 2016). Multiple linear regression statistical analysis to study the effect of dosage, temperature and pH on solids disintegration and nutrient release was performed using Microsoft Excel.

Table 2 Operating conditions for 915 MHz pilot-scale MW/H₂O₂-AOP treatment of WAS

Set No.	pH	Sludge Volume (L)	H₂O₂ %/% TS	Temperature (°C)
1	4	20	0.8	110
2	9	20	0.6	110
3	4	20	0.6	90
4	9	20	0.6	90

2.2.4 Physical and chemical sample analysis

Physical and chemical sample analysis was carried out in accordance with the procedures outlined in Standard Methods (APHA, 2012). Table 3 and 4 on the following page provides methods and instruments used in physical and chemical analysis, respectively. Soluble fractions of the samples, raw and treated, were obtained by centrifuging at 3500 rpm for 15 minutes followed by vacuum filtration utilizing fiberglass filter paper with a pore size of 0.45 µm. For accuracy and precision, all the tests were carried out in triplicate.

Table 3 Methods and instruments used for physical analysis

Parameter	Method	Instrument
Total/Volatile Solids (TS/VS)	2540 B/E	Muffle Furnace
Total/Volatile Suspended Solids (TSS/VSS)	2540 D/E	
Capillary Suction Time (CST)	2710 G	Komline-Sanderson capillary suction timer Whatman, 17CHR chromatography paper
Particle Size Distribution (PSD)	2560 D	Mastersizer 2000 (Hydro2000S, Malvern Instruments) light scattering particle counter

Table 4 Methods and instruments used for chemical analysis

Parameter	Method	Instrument
Volatile Fatty Acids (VFA)	2720 C	Hewlett Packard, HP5580 Series 2 Gas Chromatograph Mass Spectrometer
Chemical Oxygen Demand (TCOD/SCOD)	5220-COD D	Hach, DR 2800 Spectrophotometer
Total Phosphorus (TP/STP)	4500-P F	Lachat Instruments, Quickchem 8000 Flow Injection Analysis System
Orthophosphate (ortho-P)	4500-P G	
Ammonia (NH ₃)	4500-NH ₃ H	
Total Kjeldahl Nitrogen (TKN/STKN)	4500-N D	PerkinElmer, Optima 7300 DV Atomic Emission Spectrometer
Calcium (Ca), Magnesium (Mg)	3120 B	

2.2.5 Energy analysis

During the entire operation, the energy demand in kWh by the 915 MHz microwave generator to provide the desired temperature was recorded directly using a power meter (Acuvim-L, Optimum Energy Product Ltd., Canada). To correlate the energy consumption data with the performance, the treatment performance was provided in terms of nutrient solubilization and solids solubilization (Lo et al., 2017). The degree of solids solubilization was evaluated by the solids solubilization index, S_L , and release of nutrients was evaluated by the nutrient release index, N_e , as shown in Equation (1):

$$S_L \text{ or } N_e = \frac{x_t - x_o}{x_o} \quad (1)$$

Where S_L is the solids solubilization index, N_e is the nutrient release index, and x_o is the parametric ratio of the untreated sludge. (x_o was denoted by the SCOD/TCOD ratio for S_L and ortho-P/TP ratio for N_e .) x_t is the corresponding parametric ratio of the treated sludge at time t ; the SCOD/TCOD ratio at time t was used for S_L and ortho-P/TP ratio at time t was used for N_e .

2.3 Results and discussion for the 2450 MHz batch-mode system

2.3.1 Solids disintegration

Total suspended solids (TSS)

All sets had a decrease in TSS (Figure 2): alkaline treatments (MW/H₂O₂/pH 9) had the highest reduction of TSS about 27 and 22% at 110 and 90°C, respectively. About 15, 18 and 10% reduction of TSS were obtained for acidic, MW/H₂O₂, and MW treatments at both temperatures. The results demonstrated that alkaline treatment was the most effective treatment for suspended solids reduction. The MW/H₂O₂ treatment resulted in a higher TSS reduction than the MW treatment only.

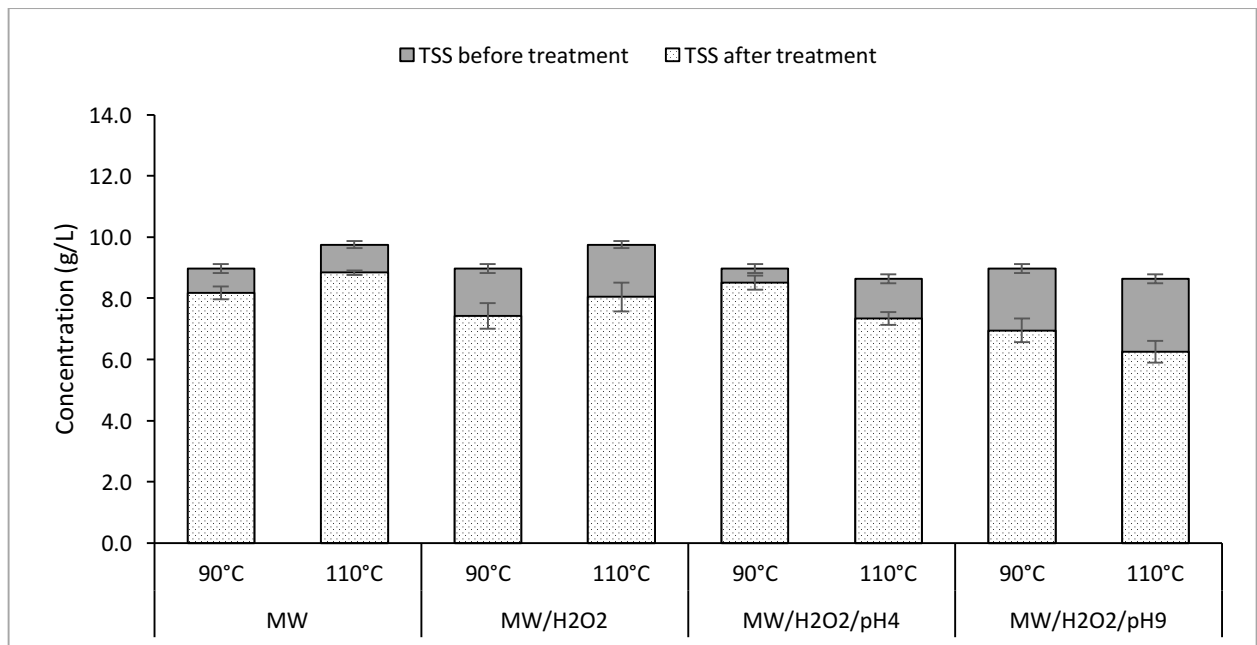


Figure 2 TSS before and after MW/H₂O₂-AOP treatment of WAS for batch-mode studies

Chemical Oxygen Demand (COD)

A similar trend was observed in SCOD release (Figure 3). The highest SCOD/TCOD ratio was 26 and 20% for alkaline treatment (MW/H₂O₂/pH 9) at 110 and 90°C, respectively; pH and temperature were the significant factors affecting SCOD release. The reasons for the high yield of SCOD in the alkaline treatment were: 1) addition of alkali promotes structural damage within the sludge. This is due to alkali reactions with the fatty acids of cell membranes, resulting in changing membrane's permeability. As a result, it favors the release of intracellular polymeric substances into the solution; 2) alkali also promotes decomposition of H₂O₂ into •OH·, H₂O₂ itself can increase the permeability and fluidity of cell membranes, thus a combination of alkali and H₂O₂ results in a synergistic effect to enhance sludge disintegration (Erdinçler and Vesilind, 2000; Neyens et al., 2003a).

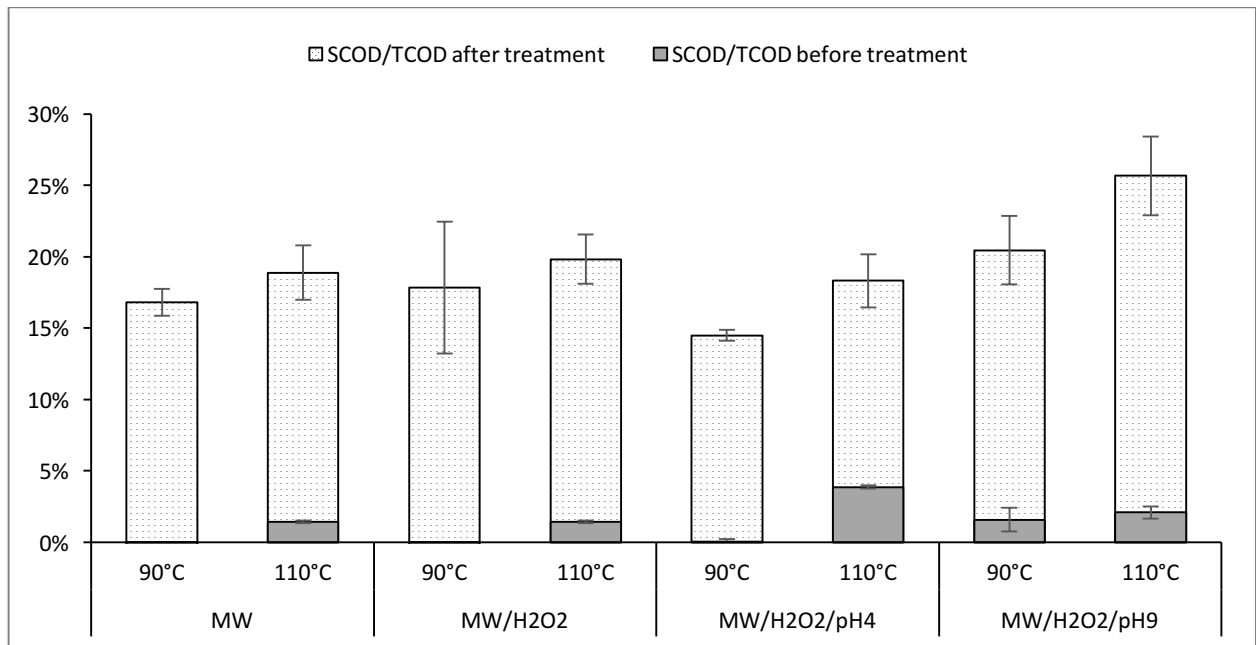


Figure 3 SCOD to TCOD ratio as percent before and after MW/H₂O₂-AOP treatment of WAS for batch-mode studies

The SCOD/TCOD ratios for the sets of MW/H₂O₂/pH 4, MW/H₂O₂, and MW were 18, 20 and 19% at 110°C, while they were 14, 18 and 17% at 90°C, respectively. The results were not statistically different among MW/H₂O₂/pH 4, MW/H₂O₂ and MW sets at each temperature. Under current operating conditions, H₂O₂ was introduced in the beginning of the experiment at ambient temperature (about 22°C). It was expected that a large quantity of H₂O₂ would be consumed by catalase, regardless of pH applied in the MW treatments. The assertion was supported by the following analyses: a higher TSS reduction and SCOD occurred in a continuous-flow system with the same H₂O₂ dosage, because of introducing H₂O₂ into the MW system at 60°C (reported in the next section). Higher yields were also obtained using a similar H₂O₂ dosage strategy in batch mode studies (Wang et al., 2009; Nkansah-Boadu et al., 2015a; Wang et al., 2015). Catalase, an enzyme present in aerobic sludge, was very active at low temperatures (4-25°C) and gradually became less active above 40°C. It also displayed a wide range of tolerance to pH (4-9); the maximum catalase activity occurred at pH 7 (Guwy et al. 1998; Guwy et al. 1999). The low yields of TSS reduction and SCOD also indicated that it did not have sufficient amounts of H₂O₂ to complete the reaction in these sets after most of the H₂O₂ was consumed by catalase. It was evident that a slightly higher yield was obtained at a higher temperature. This was attributed to the temperature effect, but not H₂O₂; higher temperature favors decomposition of substrate. The effect of H₂O₂ and pH on the TSS and SCOD yield was minimal in these sets (MW/H₂O₂/pH 4, MW/H₂O₂, and MW). As noted, there was not sufficient H₂O₂ applied in the process, but H₂O₂ is stable under acidic conditions and cannot be easily decomposed into •OH.

Volatile Fatty Acids (VFA)

VFA concentrations in terms of acetic equivalent, as expected, were much higher at 110 than 90°C as illustrated in Figure 4. It was in a range of 99 to 127 mg/L at 110°C and 11 to 25 mg/L at 90°C. The formation of VFA and other forms of intermediate oxidation products during advanced oxidation treatment causes a drop in the effluent pH levels (Lo et al., 2014). As shown in Table 12, Appendix A1, pH decreased in most of the treated sets, however, there was no clear trend.

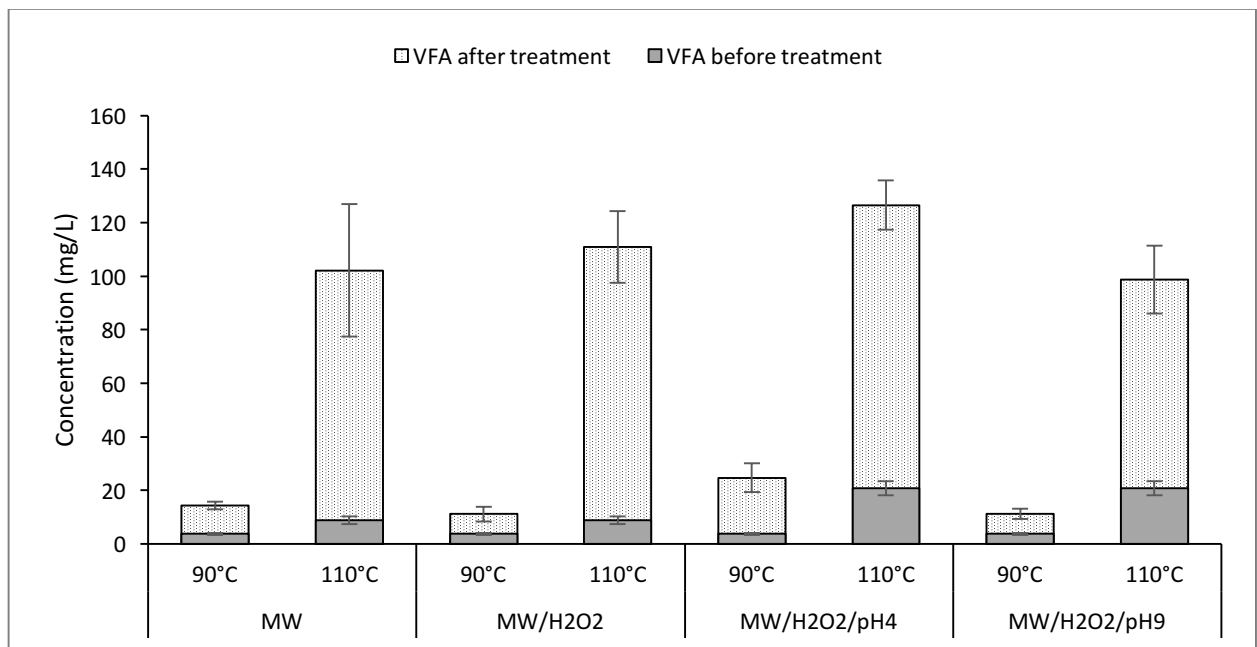


Figure 4 VFA before and after MW/H₂O₂-AOP treatment of WAS for batch-mode studies

2.3.2 Nutrient release

Phosphorus release

The process released orthophosphate and increased soluble TP and soluble TKN in the solution (Figure 5). All sets had significant release of phosphorus, mostly in the form of soluble TP. After treatment, soluble P to TP ratio increased to 44-77% at 110°C, and 14-60.5% at 90°C. Ortho-P to TP ratio increased from approximately 1% in untreated samples to approximately 20% in treated samples at 110°C. Ortho-P concentration was almost two times higher at 110°C than at 90°C sets. Ortho-P release was not significantly different between acidic and alkaline conditions. Hydrogen peroxide dosage did not play a major role for release of ortho-P or soluble TP. Temperature was the most significant factor affecting phosphorus release. This was consistent with the findings from the earlier studies that temperature was the most significant factor affecting ortho-P release compared to hydrogen peroxide dosage (Wong et al. 2007; Kenge et al. 2009b).

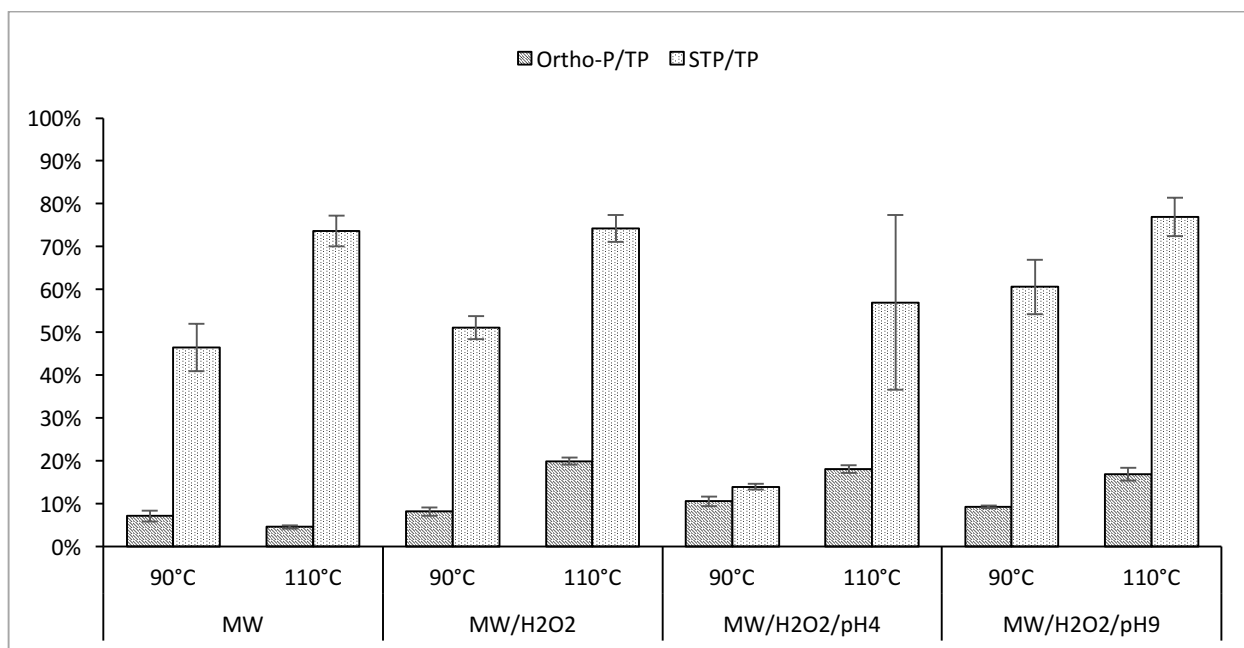


Figure 5 Ortho-P and soluble TP release as percent of Total P after MW/H₂O₂-AOP treatment of WAS for batch-mode studies

Nitrogen solubilization

The TKN, soluble TKN, and ammonia concentrations in the treated solutions varied. Soluble TKN increased substantially for all sets, while ammonia only increased slightly (Figure 6). No general trend for soluble TKN was observed in this study. Soluble TKN increase was due to the production of intermediate compounds such as protein, amino acids and other nitrogen components (Yi et al., 2014), however, they weren't further oxidized to form ammonia (Wong et al., 2006a; Yi et al., 2014).

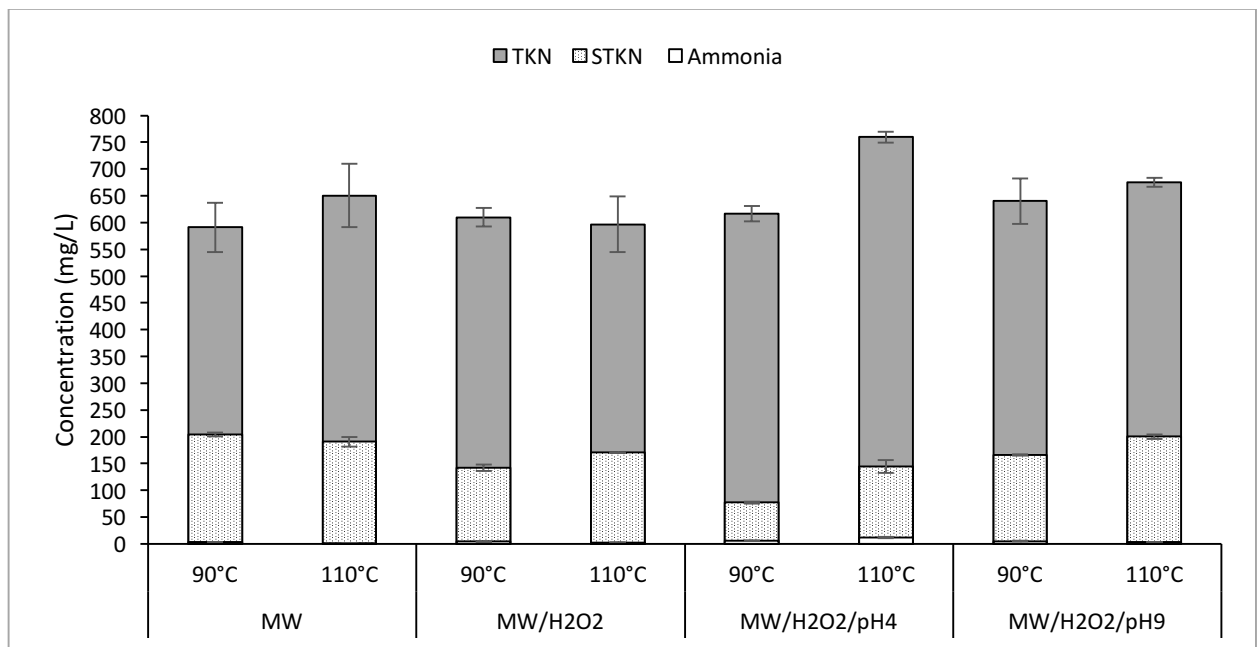


Figure 6 Nitrogen in the MW/H₂O₂-AOP treated solution of WAS for batch-mode studies

Metals solubilization

Metal ions, such as Ca and Mg were released from sludge during the MW process (Table 13, Appendix A1). A much higher concentration of both were obtained at 110 than 90°C. It clearly indicated that high degrees of sludge disintegration occurred at 110°C. PH adjustment did not influence Ca and Mg release. Mg is a constituent of struvite; however, the

presence of Ca ions can affect struvite formation either by competing for phosphorus ions or by interfering with struvite crystallization. Therefore excess Ca in the solution required removal prior to the crystallization (Zhang et al., 2014).

2.3.3 Physical properties

Settling

The MEBPR sludge used in this study had very poor settling. Poor settling may be due to poor floc microstructure resulting in the compact core of sludge flocs being too small. There was no sludge settling at all for all the MW treatment or the MW/H₂O₂-AOP at 90°C. Settling improved for all sets at 110°C.

Capillary Suction Timer (CST)

The CSTs increased for all of the treatment sets, except MW/H₂O₂/pH 4 at 110°C. It was assumed that the release of EPS from sludge was responsible for the deterioration of CST in the treated sludge.

Particle Size Distribution (PSD)

The particle size distribution profiles for the sets at 90°C were similar to the raw sludge (Figure 23, Appendix A1). At 110°C, for MW/H₂O₂/pH 9, MW/H₂O₂/pH 4 and MW/H₂O₂ treatment sets, the peak volume percent D90 increased and shifted towards large particle sizes (Figure 24, Appendix A1). Larger particle size formation was due to either the chemical reactions with hydrogen peroxide or the coagulation of smaller particles upon detachment of extracellular polymeric substances (EPS) from sludge. The break off of EPS

from the sludge surface would make coagulation easier (Neyens and Baeyens, 2003). The peak volume percent D10 decreased and slightly shifted towards smaller particle sizes for the MW treatment, indicating that particle breakdown was achieved by thermal treatment.

2.4 Results and discussion for the 915 MHz pilot-scale continuous-flow system

Alkaline or acidic treatment of sludge without heating is very effective to solubilize extracellular polymeric substances (EPS). EPS maintain not only the structural integrity of microbial cell, but also act as an ion-exchange resin, thus controlling the movement of ions from solution into the cell (Houghton, et al., 2001; Neyens, et al., 2004). The main components of EPS are polysaccharide, protein and DNA, which entrap water and cause a high viscosity. Polysaccharides, protein and phosphorus were released immediately by addition of alkali or acid, as indicated in increased concentrations of ortho-P, soluble TP, and SCOD (Table 15 and 16, Appendix A2). The release of phosphorus was most likely caused by the breakup of EPS (Neyens et al., 2004; Xiao et al., 2012).

2.4.1 Solids disintegration

Total suspended solids (TSS)

The decrease of TSS by the MW/H₂O₂/pH 4 (79% reduction), MW/H₂O₂/pH 9 (72% reduction), MW/H₂O₂ (77% reduction) and MW treatments (25% reduction) was very substantial in the continuous-flow system (Figure 7 on the following page), compared to the batch operation.

The TSS reductions were not significantly different at 90 and 110°C for the respective MW/H₂O₂ and MW sets. However, sets with hydrogen peroxide yielded 50% higher reduction in TSS concentration.

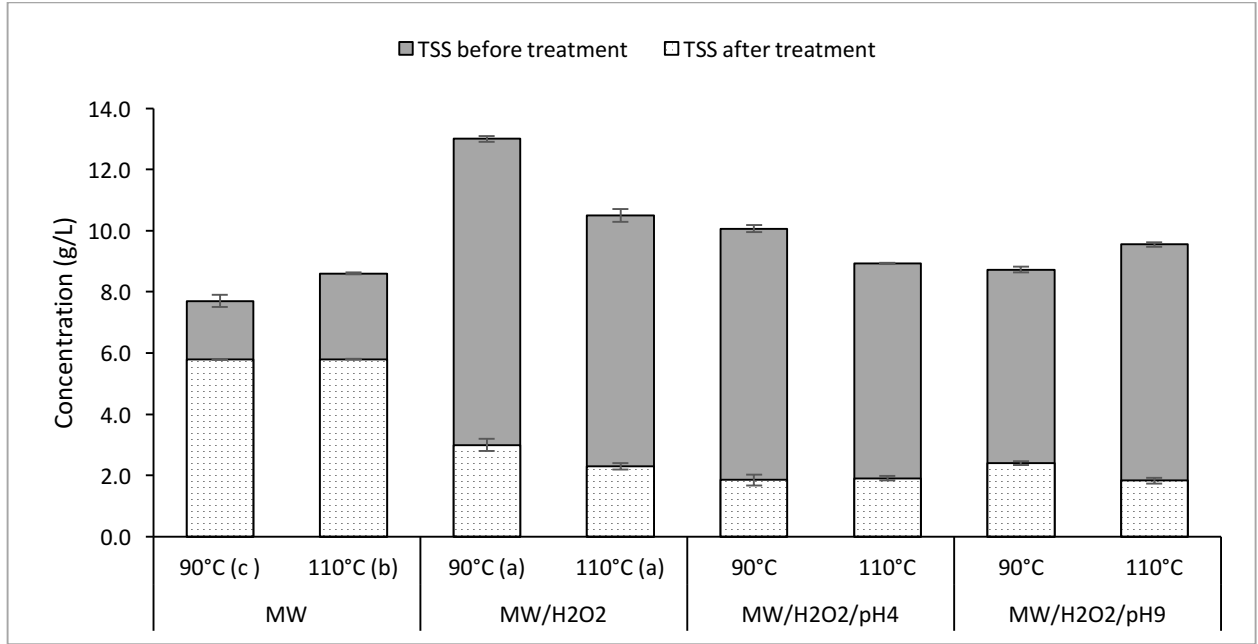


Figure 7 TSS before and after MW/H₂O₂-AOP treatment of WAS for pilot-scale studies

Linear regression equations used to predict solids disintegration based on TSS (g/L) to TS (g/L) ratio for the eight treatment sets within the range of factors studied: hydrogen peroxide dosage (0-0.6 %H₂O₂/%TS), temperature (90-110°C) and pH (4-9) are given in Equations 2. The null hypothesis is that the means of the measured response are the same for the different treatment sets.

$$\frac{TSS}{TS} = 0.76 - (0.78 * dosage) - (0.001 * temperature) + (0.01 * pH) \quad (2)$$

A correlation coefficient (R) of 0.99 was obtained for the TSS/TS ratio indicating a good fit. At 95% confidence interval, the null hypothesis was rejected for the hydrogen peroxide dosage (p-level was less than 0.002). The analysis indicated that TSS reduction was statistically different with changes in H₂O₂ dosage levels.

Chemical Oxygen Demand (COD)

Very high SCOD concentrations ranging from 51 to 76% of TCOD was also obtained, while only 18 to 26% of SCOD/TCOD resulted from the batch operation system. A higher SCOD concentration was obtained at 110 than 90°C (Figure 8). A higher SCOD concentration occurred in an alkaline addition than in an acidic addition.

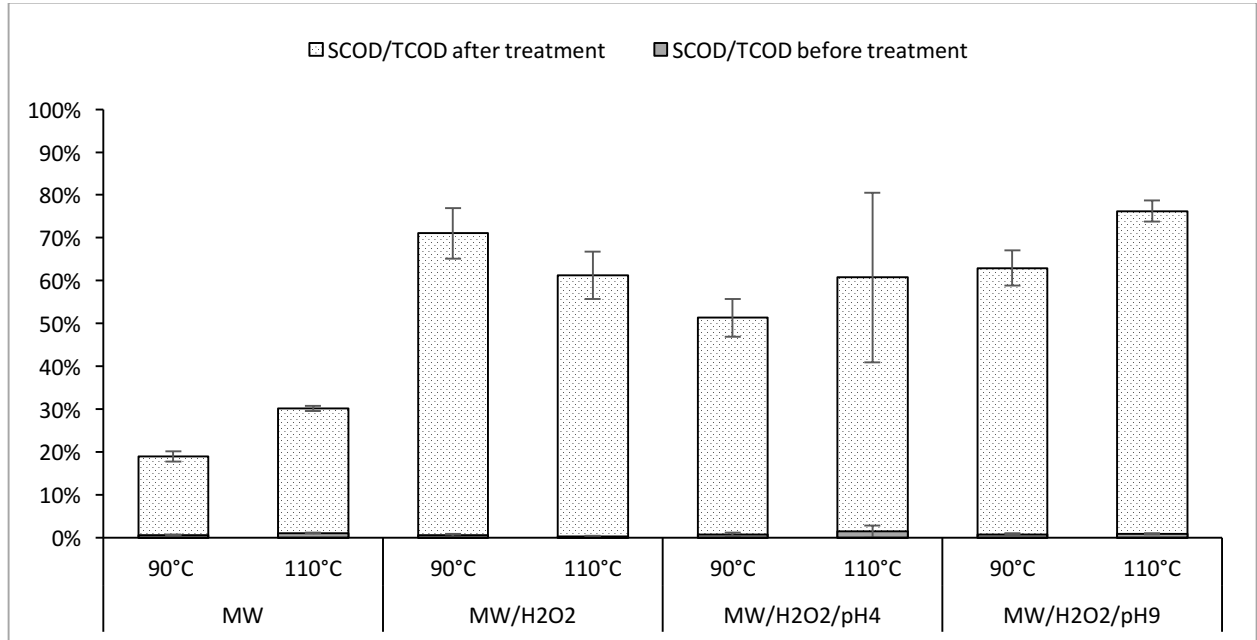


Figure 8 SCOD to TCOD ratio before and after MW/H₂O₂-AOP treatment of WAS for pilot-scale studies

The results point out that it is very important to deactivate catalase in aerobic sludge to improve the treatment efficiency of the MW/H₂O₂-AOP. A higher treatment efficiency was obtained in a continuous-flow system than a batch mode operation. In order to reach similar results, a higher H₂O₂ dosage was required in a batch operation than a continuous-flow system. Alternately, the strategy would be to use a two-step heating process in a batch operation system as used by Wang et al. (2015).

The SCOD release was not significantly different at 90 and 110°C for the respective MW/H₂O₂ and MW set. Linear regression equations to predict solids disintegration based on SCOD (mg/L) to TCOD (mg/L) ratios for the eight treatment sets within the range of factors studied yielded the following equation:

$$\frac{SCOD}{TCOD} = -0.25 + (0.67 * dosage) + (0.003 * temperature) + (0.03 * pH) \quad (3)$$

A correlation coefficient (R) of 0.97 was obtained for the SCOD/TCOD ratio, indicating a good fit. At 95% confidence interval, the null hypothesis was rejected for the hydrogen peroxide dosage (p-level < 0.002). The analysis indicated SCOD release was statistically different with changes in H₂O₂ dosage levels, and H₂O₂ dosage was a significant factor affecting solids disintegration. Based on the results from energy analysis (Section 2.4.4), the solids solubilization index for the MW/H₂O₂ was substantially higher than MW set for both temperatures, for a lesser amount of energy consumed; at 110°C the MW/H₂O₂ process consumed 0.59 kWh/L while the MW process consumed 0.79 kWh/L. This clearly indicated that H₂O₂ was the significant factor affecting solids solubilization and energy consumption confirming the previous findings (Lo et al., 2016; Lo et al., 2017).

Volatile Fatty Acids (VFA)

The final pH of treated sludge was found to be much lower than the initial pH (Table 15, Appendix A2). A drastic decrease in pH occurred in the alkaline treatments, which may be due to sludge microbe remaining active at pH 9. The microbial activity was reduced, but not ceased at pH 12.5 (Dogan and Sanin, 2009). With a combination of alkali, H₂O₂ and microwave treatment, a significant amount of intermediate oxidation products such as carboxylic acids and VFA was produced, resulting in a low pH. The resulting pH was lower for the continuous-flow system than for the batch operating system. Very high VFA concentrations were also produced in the alkaline treatment. A much higher VFA was produced at 110 than at 90°C (Figure 9). Also, a high VFA concentration was observed in the set with H₂O₂. A higher VFA produced in a continuous-flow system indicated that catalase consumed a large quantity of H₂O₂ in a batch system, resulting in less amounts available to react with particulates.

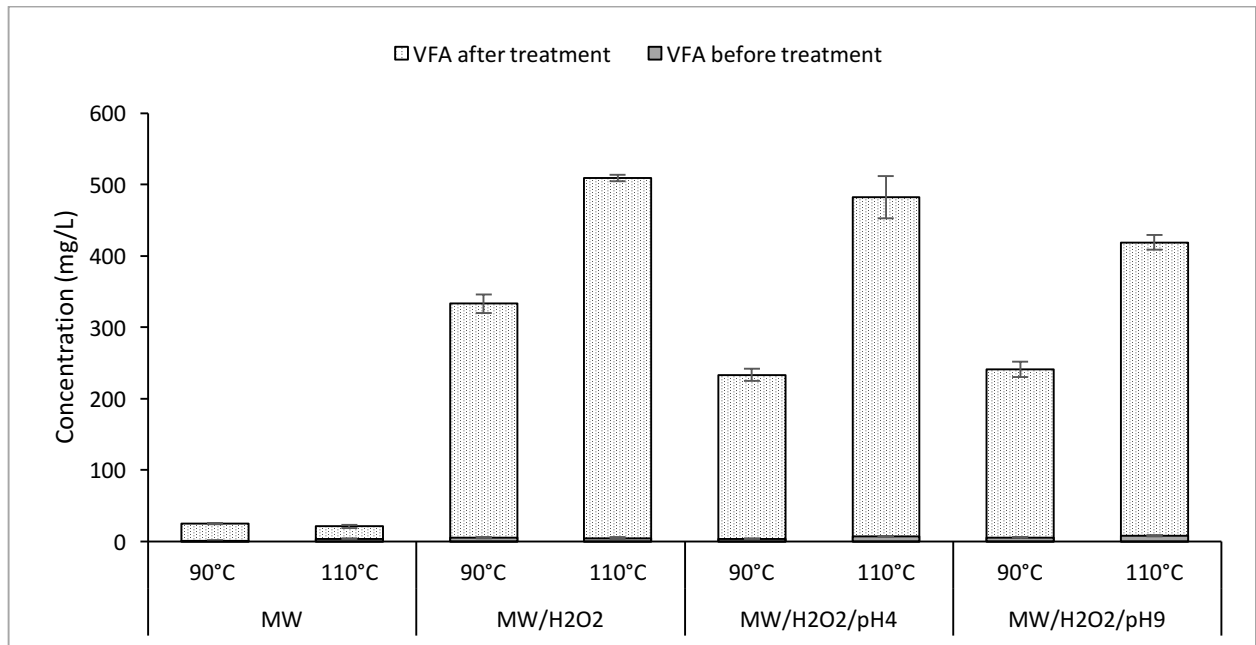


Figure 9 VFA before and after MW/H₂O₂-AOP treatment of WAS for pilot-scale studies

Linear regression equation to predict VFA (mg/L) to TS (g/L) ratio for the eight treatment sets (Table 15, Appendix A2) within the range of factors studied obtained the following equation:

$$\frac{VFA}{TS} = -91 + (57.5 * dosage) + (0.92 * temperature) + (0.33 * pH) \quad (4)$$

A correlation coefficient (R) of 0.95 was obtained and null hypothesis was rejected for both dosage and temperature (p-level was less than 0.03), indicating that both were significant factors affecting VFA release. The results were consistent with earlier studies that temperature and H₂O₂ were the significant factors affecting VFA (Liao et al., 2007; Wong et al., 2007).

2.4.2 Nutrient release

Phosphorus release

The ortho-P and soluble TP were released substantially in the continuous-flow system (Figure 10). The soluble TP concentration was slightly higher in the continuous-flow system than its counterpart in the batch system. A higher soluble TP was obtained in an alkaline treatment than in an acidic treatment. However, it was reversed for ortho-P, that an acidic treatment yielded a higher concentration. Also, ortho-P concentrations were much higher in a continuous-flow system than in a batch system.

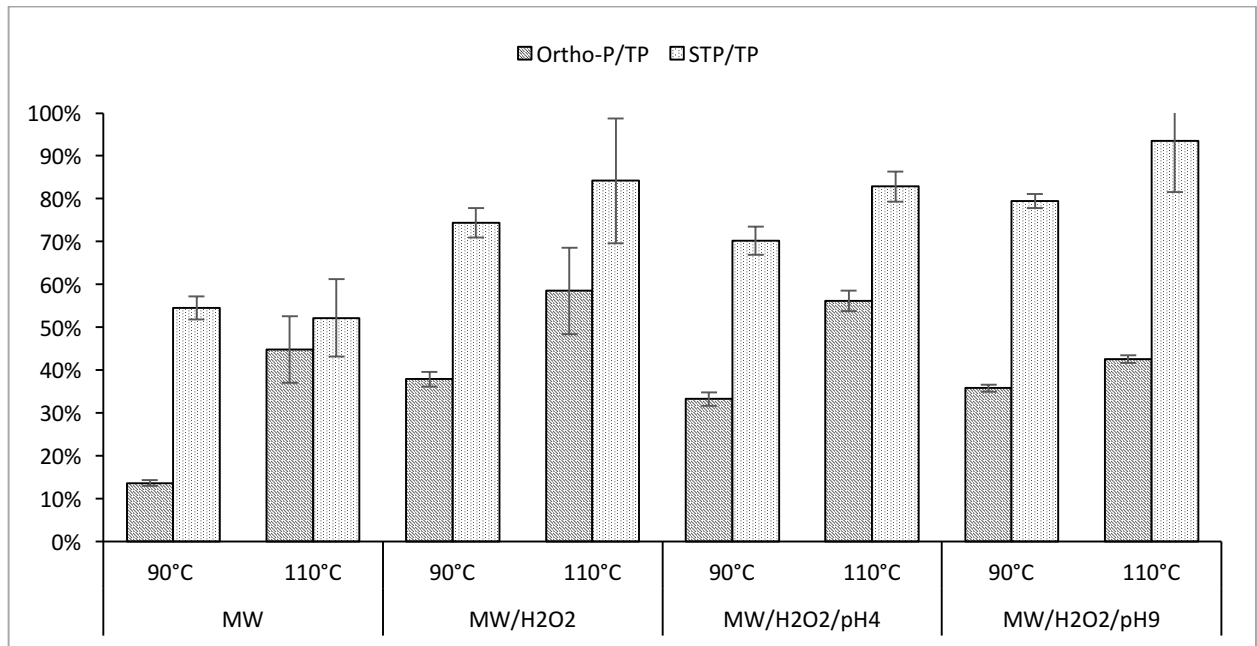


Figure 10 Ortho-P and soluble TP release as percent of TP after MW/H₂O₂-AOP treatment of WAS for pilot-scale studies

As evident from Figure 12, Section 2.4.4, the nutrient release index was higher for MW/H₂O₂/pH 4 than at pH 9 for the same amount of energy consumption. A higher soluble TP and ortho-P occurred at 110 than at 90°C. The ratios of soluble TP to TP for the MW/H₂O₂/110°C, MW/110°C, MW/H₂O₂/90°C, and MW/90°C were 84, 52, 73 and 55%,

respectively. For the ratios of ortho-P to TP in the same order, they were 59, 45, 38 and 13%, respectively. The results clearly indicated that temperature, pH and H₂O₂ were the significant factors affecting phosphorus release (Wong et al. 2007).

Linear regression equation to predict ortho-P (mg/L) to TP (mg/L) ratio for the eight treatment sets within the range of factors studied obtained the following equation:

$$\frac{Ortho-P}{TP} = -0.66 + (0.24 * dosage) + (0.01 * temperature) - (0.009 * pH) \quad (5)$$

A correlation coefficient (R) of 0.92 was obtained and temperature was found to be the significant factors affecting ortho-P release (p-level was less than 0.02). Based on the energy analysis, the nutrient release index for the MW/H₂O₂ and MW sets were not substantially different than the pH adjusted sets at the same temperature; however, the energy consumed by the two pH adjusted sets (approximately 0.41 kWh/L at 110°C) were significantly lower than the MW/H₂O₂ and MW sets (0.51 and 0.79 kWh/L, respectively) indicating that similar levels of ortho-P could be released at a lower kWh/L of energy required by the continuous-flow system.

Nitrogen solubilization

EPS was decomposed under the thermal-chemical treatment. As a result, most of the protein and amino acids could be liberated from particulates into soluble TKN. However, they were not converted into ammonia (Paul et al., 2006a). The multiple linear regression analysis on ammonia release resulted in a poor fit (R = 0.76) and none of the three factors

were found to be statistically significant. Thermal-chemical methods are not very effective for ammonia release from sludge (Kuroda et al., 2002; Liao et al., 2007). Treatment temperature of 110°C produced more ammonia than 90°C (Figure 11). Sets with adjusted pH resulted in considerably higher ammonia concentration than those without pH adjustment. Large amounts of soluble TKN were produced in all treatments. With higher H₂O₂ dosage used in the MW/H₂O₂/pH 4 set, about 88% of TKN was solubilized. Very high soluble TKN was obtained in the MW/H₂O₂ sets, regardless of pH adjustment. Less soluble TKN was produced in the MW sets. A higher soluble TKN was obtained in the continuous-flow system than in the batch system. This was due to higher amounts of H₂O₂ available for reacting with particulates. H₂O₂ dosage was one of the most significant factors affecting nitrogen release (Wong et al., 2007).

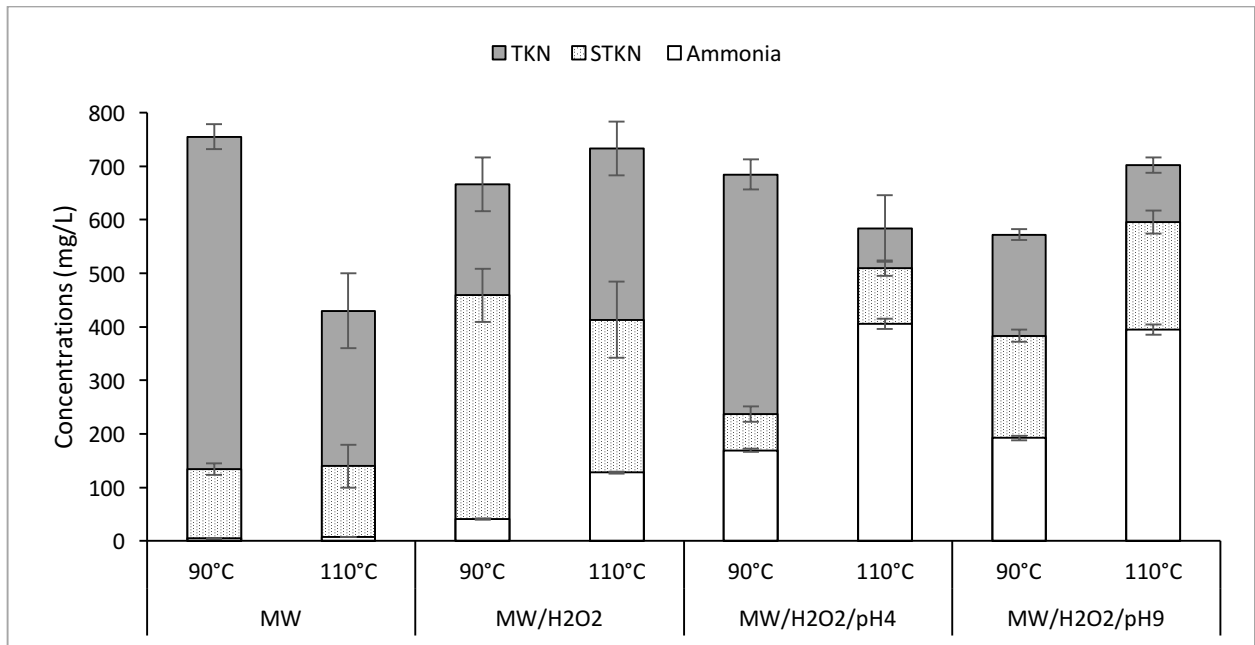


Figure 11 Nitrogen solubilization after MW/H₂O₂-AOP treatment of WAS for pilot-scale studies

Metals

Substantial amounts of soluble metals (Mg and Ca) were released in the continuous-flow system; acid and alkaline condition at 110°C released 88 and 90% of total Mg into the treated solution, respectively (Table 16, Appendix A2). All sets carried out at 110°C, irrespective of pH adjustment, resulted in substantial ortho-P and Mg release. The resulting solutions, along with a substantial reduction of TSS and good settling, were suitable for a subsequent struvite crystallization process.

2.4.3 Physical properties

Capillary Suction Timer (CST)

Dewaterability improved significantly as indicated by shorter CST values for all treated sets except the MW/H₂O₂/pH 9 at 90°C, for which the particle size decreased (Table 17, Appendix A2). An increase of electrostatic repulsion between small particles caused deterioration of dewatering properties. For all other sets, pH was near isoelectric point of sludge. Liao et al. (2002) reported that a minimum dissociation constant occurred in the pH range of 2.6 – 3.6, which is the pH range of the isoelectric point. The repulsive electrostatic interactions were minimized near the isoelectric point, so the fine flocs could approach each other closely. As a result, sludge is more stable. This would also improve dewaterability of sludge (Neyens and Baeyens, 2003).

Among the eight pilot-scale microwave treatment sets, CST generally decreased after MW/H₂O₂ treatment irrespective of pH and temperature, while CST increased for microwave alone treatment sets (Table 17, Appendix A2).

The ratio of CST from treated and initial sludge statistically compared for all eight treatment sets resulted in the following multiple linear regression:

$$\frac{CST_{treated}}{CST_{initial}} = 7.6 - (15.2 * dosage) + (0.01 * temperature) + (0.11 * pH) \quad (6)$$

A correlation coefficient (R) of 0.99 was obtained and dosage was a significant factors affecting CST (p-level was less than 0.0002).

Particle Size Distribution (PSD)

For MW/H₂O₂/pH 4 and MW/H₂O₂/pH 9 at 110°C, the peak volume percent decreased and shifted towards smaller particle size, as shown in the particle size distribution (Table 17, Appendix A2), which indicated the breakdown of large particles in the substrate. However, some also agglomerated to form larger particles. For MW/H₂O₂/pH 4/90°C, the peak volume percentage decreased and shifted towards a larger particles size. The particle size decreased towards smaller particles in the alkaline treatment at 90°C.

Settling

Settling properties of all four treated sets were significantly improved resulting in over 91% of solids being settled. As indicated by the solids solubilization, particle size, distribution and dewatering properties, settling of MW/H₂O₂/pH 4 was better than MW/H₂O₂/pH 9 sets.

2.4.4 Energy analysis

Based on the results from energy analysis, the solids solubilization index for the MW/H₂O₂ was substantially higher than MW set for both temperatures for a lesser amount of energy consumed; at 110°C the MW/H₂O₂ process consumed 0.59 kWh/L while the MW process consumed 0.79 kWh/L (Figure 12). This clearly indicated that H₂O₂ was the significant factor affecting solids solubilization and energy consumption which confirms the previous findings (Lo et al., 2016; Lo et al., 2017).

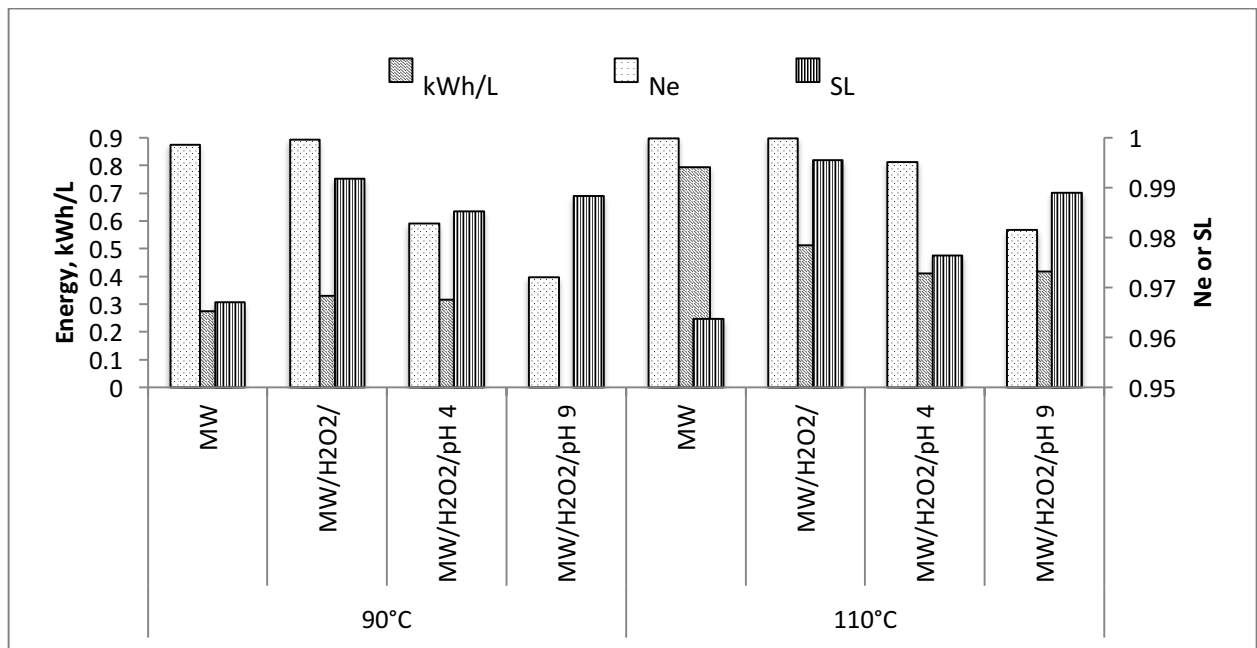


Figure 12 Energy consumed by the 915 MHz continuous-flow microwave system plotted against solids solubilization (SL) and nutrient release (Ne) indices for the MW/H₂O₂-AOP treatment of WAS

2.5 Conclusion

MW/H₂O₂-AOP, irrespective of pH adjustment, resulted in effective treatment of WAS. A substantial increase in treatment performance was exhibited by the continuous-flow treatments compared to the batch-mode operation.

TSS reduction and SCOD release were better at pH 9 sets than at pH 4 sets at both treatment temperatures. Therefore, alkaline conditions would be more favourable for consequent anaerobic digestion process. VFA formation was primarily influenced by MW temperature in combination with H₂O₂, yielding higher concentrations at 110°C irrespective of the pH levels applied.

The release of orthophosphate, dewatering properties and the settling of MW/H₂O₂-AOP at pH 4 were better than at pH 9 sets. Thus, acidic conditions would be more favourable in the process of struvite crystal formation, that necessitates a clear supernatant with high concentrations in nutrients, such ammonia and ortho-P.

The particle size decreased under alkaline conditions unlike acidic conditions, where small particles agglomerated, resulting in increased size that greatly improved dewaterability properties. Poor dewaterability at high pH levels is attributed to an increase in electrostatic repulsion between small particles that inhibited the agglomeration process.

In terms of sludge residual reduction, MW/H₂O₂ achieved a high degree of solids reduction irrespective of treatment temperature; pH adjustment was not necessary. CST was also greatly reduced indicating good dewaterability properties of treated WAS.

A lesser energy was consumed with pH adjusted sludge than the sets without adjustment; energy consumption varied between 0.32 and 0.41 kWh/L of sludge treated.

Chapter 3: Salt water experiments

3.1 Introduction

The 915 MHz pilot-scale continuous-flow system was custom-designed to treat various wastes for the research purposes. In an attempt to characterize the newly assembled system, water containing varying concentrations of sodium chloride (NaCl) was used as a control liquid. The system's response to the changing properties of control liquid is of crucial importance when evaluating the degree of sensitivity of the 915 MHz unit. The effect of control factors such as flow rate, applied power and tuning were investigated in order to optimize operating conditions, in turn making the system more efficient.

3.1.1 Basics behind the use of salt water as a control liquid

Water is capable of breaking ionic bonds, yielding solutions that contain ions. When sodium chloride (common table salt) is dissolved in water, sodium ions (Na^+) and chloride ions (Cl^-) are formed. These positively and negatively charged ions are capable of passing electricity from one to the next; the process is known as conductivity (EPA, 2012a). When these ions are subjected to MW radiation they oscillate back and forth colliding with other molecules, such process generates heat.

A material's ability to be heated by microwaves is determined by two properties; dielectric constant and dielectric loss factor. Water has a large dielectric constant, which is a measure of a material's ability to store electrical energy in the presence of an electric field. Dielectric constant is linked to a water molecule's dipole moment and the degree of resistance by water molecules to rotate and absorb electromagnetic wave energy (Hales et al., 2015). Dielectric constant decreases with an increase in frequency but at a given frequency,

increasing salt concentration and temperature reduces dielectric constant (Gadani et al., 2012). How efficiently the absorbed radiation is converted into heat is measured by a loss factor. Dielectric loss factor decreases in pure water as temperature increases, but in saline water, dielectric loss factor increases with increasing salt concentration and temperature (Gadani et al., 2012). Temperature increases the mobility of ions due to reductions in fluid viscosity that leads to an increase in fluid conductivity on which loss factor is dependent (Hales et al., 2015).

Flow rate can also impact dielectric properties of water. Yu et al. (2010c), reported that a high flow rate reduces the amount of microwave radiation transmitted to the substrate. In addition, a high flow rate reduces conductivity irrespective of temperature (Fondriest Environmental, Inc., 2014).

Conductivity is directly related to total dissolved solids (TDS) (EPA, 2012b). TDS represents all ion particles in the solution. TDS concentration in the solution can be obtained from conductivity measurements by applying a conversion factor that depends on the type of TDS in the solution or source of waste (Fondriest Environmental, Inc., 2014). Therefore, in wastewater, ionic properties may vary, as some might contain dissolved organic matter in addition to the salt ions.

In general, when a dielectric material is subjected to MW radiation, the resulting energy is transformed into heat either by dipolar rotation (water molecules trying to align themselves with the changing electric field; this friction among the molecules produces heat), ionic conductance or the combination of both called interfacial polarization (Anwar et al., 2015). The dipolar polarization mechanism is responsible for enhancing the degradation rate of various pollutants in the system combining heat and oxidants (Eskichioglu et al., 2006).

Dielectric heating principles and MW heating mechanisms are described in detail elsewhere (Bailey, 2015; MacSween, 2015; Ning, 2016).

3.1.2 Previous salt water experiments with 915 MHz MW system

Bailey (2015) was the first to operate the new technology after it was assembled. At the time, the system was operated as an open system with an exit temperature of 90°C. He conducted several salt water experiments to determine the influential factors effecting system's performance in terms of treatment and energy efficiency. The goal was achieved by operating the system with water containing various sodium chloride dosages (1-20 g/L) at different flow rates (1.75-7.5 L/min). Higher salt concentration resulted in an increased heating rate, therefore reducing heating time and energy consumption. In terms of different flow rates, it was found that an increase in flow rate reduced temperature rise per pass, consequently increasing heating time and energy used.

The follow up research was conducted by MacSween (2015), who upgraded the system so that it can be operated at temperatures above 100°C. A closed circulation vessel was installed along with new tubing that was able to withstand high temperatures and pressures. The system's performance was reassessed with salt water (1 gNaCl/L) at two different flow rates, 6 and 8.4 L/min. The issues such as higher differences in temperature between the tank and applicator as well as fluctuations in heating rate that were attributed to the incomplete mixing of the bulk liquid in the holding tank were discovered at low flow rate.

In an attempt to further optimize the operating conditions, an independent feed line with its own pump was added; these changes eliminated the need to use a high temperature

tolerance recirculation line to transport the substrate from the feed tank to the holding tank. Ning (2016) conducted nine salt-water runs after modifications took place (1, 10 and 20 gNaCl/L with each concentration tested at 6, 7.5 and 9 L/min flow rate) and reported that flow rate had a great impact on temperature rise per pass but very little effect on heating rate. No clear trend was observed with respect to different salt concentrations. Despite this, ionic concentration was found to influence reflected power consequently effecting energy consumption.

Fluid dynamics issues, observed in the past experiments, was eliminated by leveling the recirculation line connecting the holding tank to the two-stage cavity pump. The pump was operating at the desired flow rate after modifications were applied. In response to these changes, further experiments were carried out. The system dynamics were tested at high ionic concentrations and the optimum operating conditions at each concentration and/or flow rate tested were established, and general trends were identified.

3.2 Materials and methods

3.2.1 Substrate

Common table salt (NaCl) was dissolved in 20 L of water. The concentrations of salt used were 10, 50, 80, 100 and 120 g/L.

3.2.2 Experiment design

A total of fifteen salt water runs were conducted. The holding tank was filled with water with the corresponding salt concentration. The temperature of the solution was kept at room temperature (20°C). Each salt concentration was tested at 6, 7.5 and 9 L/min flow rates. The substrate was heated to 110°C. Forward power after reaching 4.5 kW within the first few minutes of the experiment was held constant throughout the test and tuning was performed where required. The following parameters with respect to time were recorded for each run: forward power, reflected power, tank and applicator temperature and power consumed.

3.3 Results and discussion

A summary of results is provided in Table 5, graphical presentation of which can be found in Appendix B. Information on tuning rod heights for some of the runs is provided in Appendix B6.

Table 5 Summary of results for salt water runs

Salt Concentration (g/L)	Flow Rate (L/min)	Heating Time (min)	Heating Rate (°C/min)	Averaged Temperature Rise per Pass (°C/pass)	Total Power Consumed (kWh)
10	6	54	1.64	0.164	5.94
10	7.5	46	1.59	0.127	4.85
10	9	58	1.55	0.103	6.32
50	6	62	1.43	0.143	6.76
50	7.5	50	1.52	0.122	5.4
50	9	64	1.36	0.090	7.17
80	6	66	1.43	0.143	7.19
80	7.5	61	1.36	0.109	6.85
80	9	60	1.35	0.090	6.7
100	6	60	1.24	0.124	3.66*
100	7.5	50	1.47	0.117	5.48
100	9	54	1.30	0.087	5.75
120	6	63	1.39	0.139	6.94
120	7.5	53	1.30	0.104	5.71
120	9	53	1.31	0.087	5.93

*Computer crashed at treatment time of 36 min, total run time 60min

3.3.1 Comparison study

The results of 10 gNaCl/L at all three flow rates (6, 7.5 and 9 L/min) were compared with Ning (2016), to establish if improved hydraulics affected the performance of the system and to what extent. Comparison graphs are provided in Appendix B1.

Results indicate that improved hydraulics resulted in 39, 54 and 40% less time taken to reach 110°C at 6, 7.5 and 9 L/min flow rates, respectively. Heating rate in terms of temperature rise per pass and per minute was increased by at least 53% at all three flow rate regimes. Energy consumed before changes were made was twice as much as energy consumed after the issue of 'no flow' was eradicated.

3.3.2 Heating rate

Heating rate is a function of heating time and initial and final temperature of the liquid. Figure 13 illustrates the intertwined relationship between heating rate, flow rate and salt concentration.

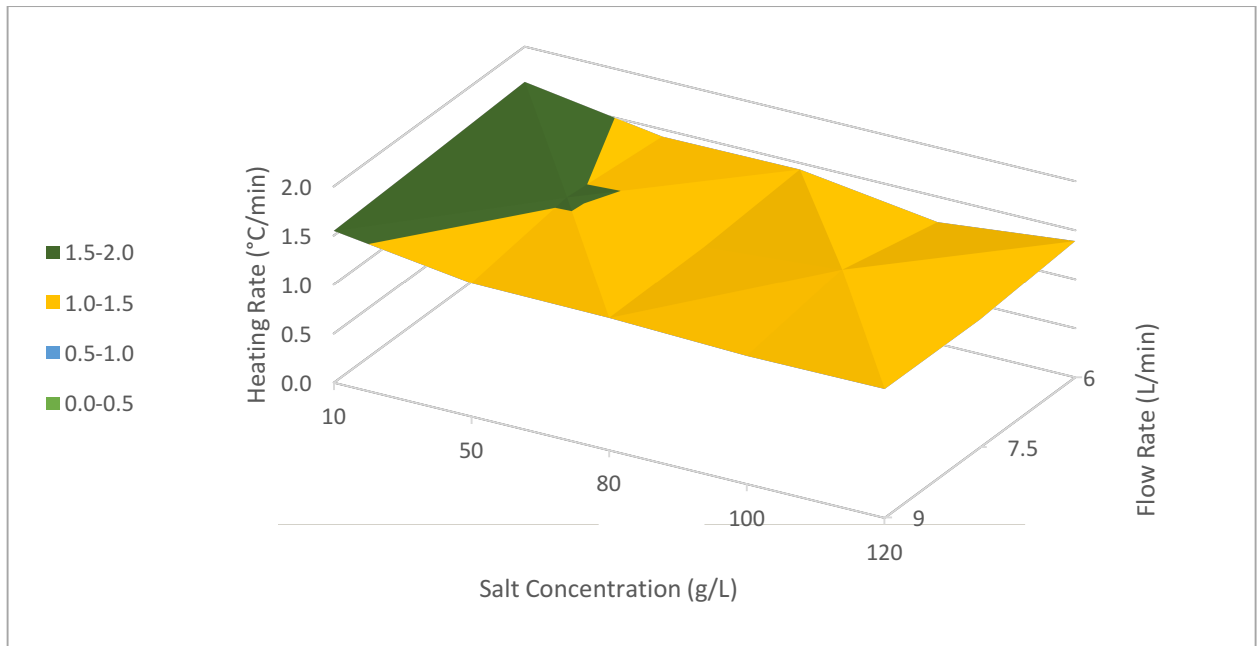


Figure 13 Heating rate as a function of salt concentration and flow rate

The flow rate of 7.5 L/min resulted in the highest average heating rate of 1.45°C/min, followed by 6 L/min (1.43°C/min) and 9 L/min (1.37°C/min). The effect of temperature rise with respect to time is more pronounced at low salt concentration irrespective of flow rate. A linear decline in the average temperature rise per minute was observed with an increasing salt concentration. Water containing 80 gNaCl/L had the lowest variance of 6% among the flow rates tested. Results of other four salt concentrations displayed high fluctuations with respect to different flow rates. Ning (2016), reported that flow had minimal impact on heating rate; salt concentration, however, effected heating rate by influencing the reflected power and therefore no clear trend was observed.

A one-way ANOVA was performed to compare the effect of multiple levels of salt concentration and flow rate on temperature rise per minute. The null hypothesis is that the means of the measured response are the same for the different treatment sets. A linear regression equation to predict temperature rise per minute within the range of flow rates (6-9 L/min) and salt concentrations (10-120 gNaCl/L) studied was obtained as follows:

$$\text{Temperature Rise/min} = 1.72206 - 0.00239 * \text{Salt Concentration} - 0.01797 * \text{Flow Rate} \quad (7)$$

A correlation coefficient (R) of 0.84 was obtained and a null hypothesis was rejected for salt concentration (p-level <0.0003) indicating that temperature rise per pass was statistically different with changes in salt concentration. A null hypothesis was accepted for the three flow rates studied indicating that temperature rise per minute was statistically similar between the sets regardless of salt concentration used. Salt concentration was a significant factor affecting temperature rise per minute.

3.3.3 Temperature rise per pass

Temperature rise per pass is similar to the temperature rise per minute in that both terms are heating time dependent. The only difference is that temperature rise per pass is also a function of flow rate. The response of temperature rise per pass with respect to flow rate and salt concentration is illustrated in Figure 14. Temperature rise per pass decreased with increase in flow rate irrespective of different salt concentrations tested. The results were consistent with previous studies that established the linear relationship with R^2 of 83 (Ning, 2016). Fondriest Environmental, Inc., (2014) reported that high flow rate reduces conductivity irrespective of temperature. As a result, the heat is primarily produced by water molecules thus less heat is generated.

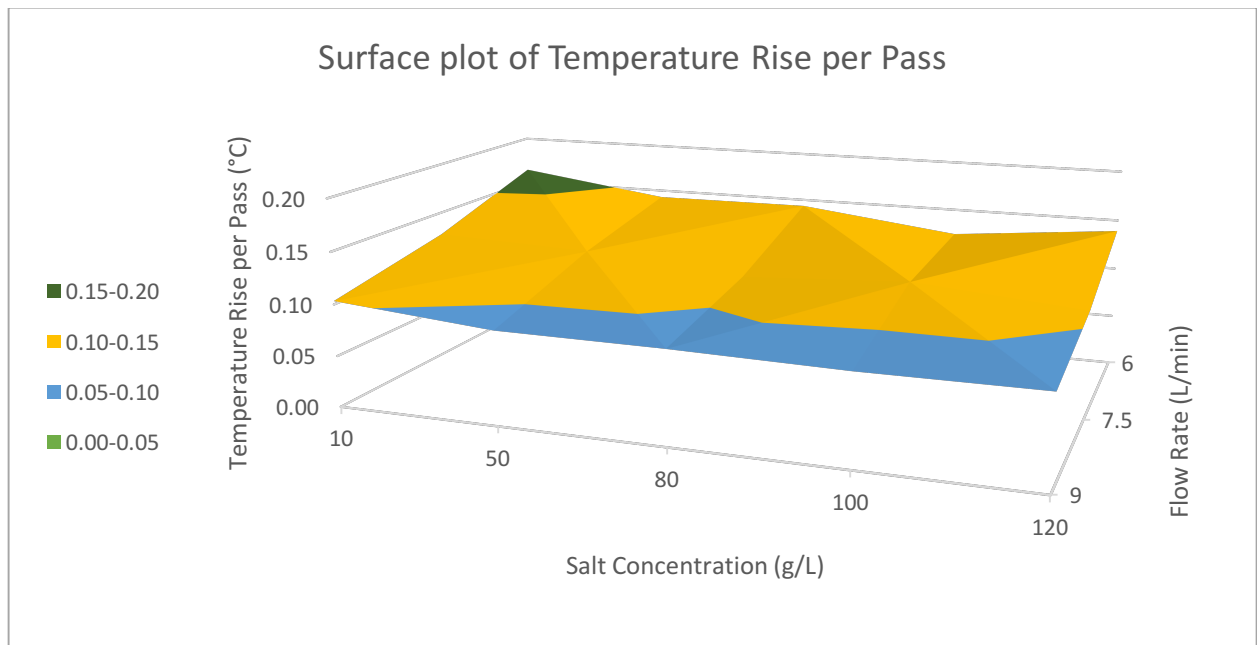


Figure 14 Temperature rise per pass as a function of salt concentration and flow rate

The same effect was displayed with an increasing salt concentration. However, this observation is contradictory to the results reported by Bailey (2015). In his study, he found that temperature rise per pass increased with an increase in ionic concentration. This could be

due to the low concentrations tested (1-20 gNaCl/L) compared to this study. The lowest temperature rise per pass was at 100 and 120 gNaCl/L at 9 L/min flow rate with the highest temperature rise per pass being at the other end of the spectrum.

A linear regression equation to predict temperature rise per pass for fifteen treatment sets within the range of factors studied obtained the following equation:

$$\text{Temperature Rise/Pass} = 0.25884 - 0.0002 * \text{Salt Concentration} - 0.01704 * \text{Flow Rate} \quad (8)$$

A correlation coefficient (R) of 0.97 was generated indicating a good fit. At 95% confidence interval, the null hypothesis was rejected for factors, salt concentration and flow rate (p-value <0.0004). This suggests that temperature rise per pass was statistically different with changes in salt concentration and flow rate.

The effect of ion concentration on temperature rise per minute and temperature rise per pass is in agreement with the finding of Anwar et al. (2015). Thermal effect was reduced at high ionic concentration due to ion's ability to surround itself by water molecules suppressing dielectric polarization of these molecules.

3.3.4 Power consumption

Energy consumption is a function of treatment time which is influenced by the initial temperature of the solution. The treatment time was shorter for the sets with high initial temperature. The sets that were operated following the set that was heated to 110°C had a shorter heating time. The heat of the holding tank transferred immediately to the solution after it was filled. Therefore, treatment sets with initial temperature below 30°C had a

treatment time in the range of 54 to 66 minutes. Sets with initial temperatures above 30°C resulted in less than 54 minutes treatment time except for set of 100 gNaCl/L at 6L/min flow rate. The treatment time for all the sets did not exceed 66 minutes. The average treatment time in order from shortest to longest was 7.5, 9 and 6 L/min flow rate and 10, 100, 120, 50 and 80 gNaCl/L.

The effect of flow rate and salt concentration on power consumption is illustrated in Figure 15.

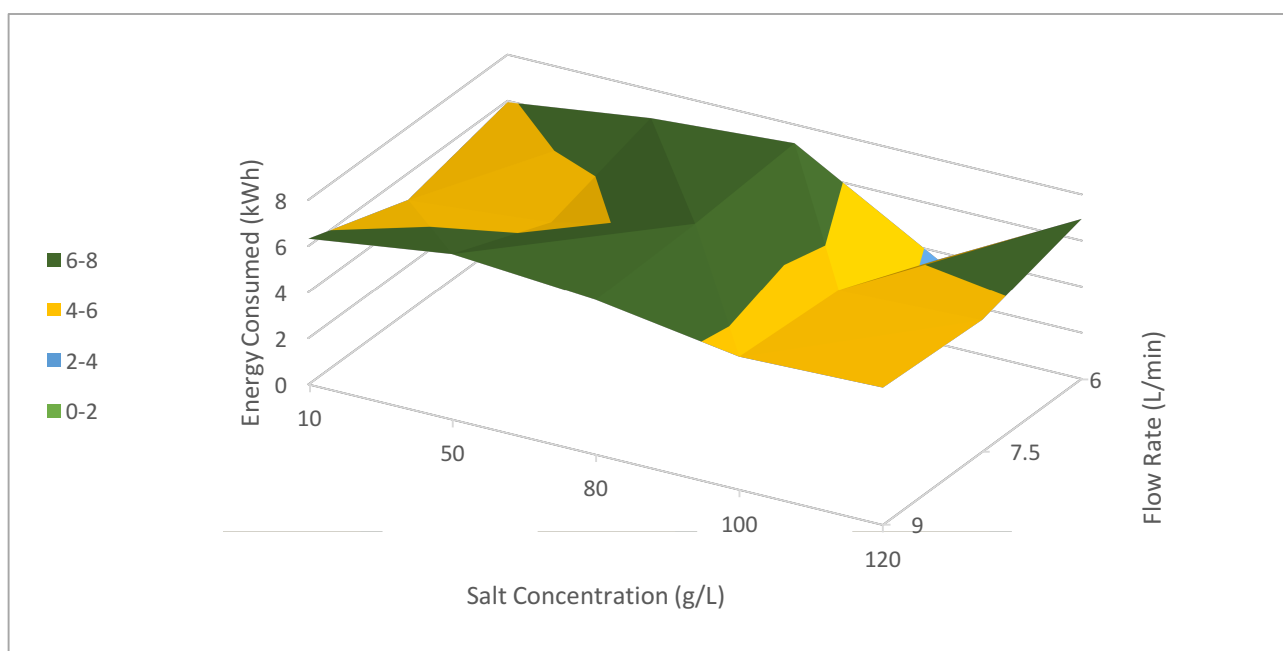


Figure 15 Power consumption as a function of salt concentration and flow rate

The lowest energy consumption of 4.85 kWh resulted from the 10 gNaCl/L operated at 7.5 L/min flow rate (initial temperature 36.8°C). It also had the shortest treatment time of 46 minutes. The same salt concentration consumed the least amount of energy at 6 L/min flow rate compared to other sets at this flow rate (initial temperature 21.4°C). Furthermore, this set resulted in the highest heating rate. It can be concluded that substances having low ionic concentration generate more heat when subjected to MW radiation.

A flow rate of 7.5 L/min on average resulted in the least amount of energy consumed for all salt concentrations tested, except 80 g/L. However, this salt concentration resulted in the lowest variance (6%) among the different flow rates tested.

A linear regression equation to predict power consumption rate within the range of factors studied obtained the following equation:

$$\text{Energy Consumed} = 5.38991 - 0.00051 * \text{Salt Concentration} + 0.092 * \text{Flow Rate} \quad (9)$$

A correlation coefficient (R) of 0.12 resulted in a poor fit, indicating that none of the factors were statistically significant.

3.3.5 Energy absorption

The results above are reflected in the amount of energy absorbed by the substrate as the temperature increases. The graphical presentation of results is provided in Appendix B5. The amount of absorbed energy was determined by subtracting the reflected energy from applied energy by the MW generator. Sudden changes in energy absorbed were due to tuning. Irrespective of flow, 10 gNaCl/L absorbed the most energy; at least 89% at any given point in treatment time. After reaching optimum energy absorption at approximately 17 minutes, a steady decrease was observed with the rise in temperature at all three flow rates. No clear trend with regards to energy being absorbed with change in temperature for all other sets was identified. The least amount of energy was absorbed by 120 gNaCl/L at flow rates of 7.5 and 9 L/min; at 6 L/min flow rate, a set with a concentration of 50 gNaCl/L performed the worst. Energy absorption did not fall below 78% for all the sets.

3.4 Conclusion

In summary, improved hydraulics resulted in greatly improved performance with approximately 50% reduction in heating time and energy consumption.

The highest heating rate and temperature rise per pass was achieved by 10 gNaCl/L at 6 L/min with moderate heating time and energy consumed; this was due to low initial temperature of the solution. The lowest energy consumption and shortest treatment time was produced by the set with the same salt concentration but at a flow rate of 7.5 L/min that had a 15°C higher initial temperature. No clear trend in energy consumption was observed among the factors studied.

Heating rate and temperature rise per pass increased with decrease in salt concentration and flow rate. The dominant heating mechanism was dipolar polarization and ionic conduction at high flow rate and high salt concentration, respectively. Furthermore, temperature rise per pass and flow rate exhibited a strong correlation; increase in flow rate decreased temperature rise per pass. In support to previous studies, it may be concluded that temperature rise per pass can be controlled by the flow rate. Similarly, salt concentration produced the same effect but to a lesser extent.

Chapter 4: Dairy manure experiments

4.1 Introduction

Dairy Manure (DM) has been a focus of this research group for over the decade due to its high phosphorus content, in particular ortho-P. Ortho-P is a constituent of inorganic P that makes up to 63% of total phosphorus in DM (Barnett, 1994). The concentration of ortho-P in DM is highly dependent on the diet of animals and the age of DM and as much as 97% of TP could be in the form of inorganic P.

Ortho-P is a constituent of struvite, a slow release fertilizer. Pan et al. (2006) successfully demonstrated the use of MW/H₂O₂-AOP in release of ortho-P; a treatment temperature of 120°C resulted in 85% of TP in the form of ortho-P. The tests were carried out with a 2450MHz MW unit that operated in a batch-mode. The effectiveness of the MW/H₂O₂-AOP pretreatment was further investigated for the potential of struvite recovery in terms of disintegration of organic matter and nutrient release (Qureshi et al., 2008). It was found that the MW/H₂O₂-AOP treated solution was ideal for anaerobic digestion followed by struvite recovery; approximately 90% of ortho-P was removed from the treated solution. The potential use of MW/H₂O₂-AOP treated solution in the anaerobic digestion process was further investigated by Chan et al. (2013). The results showed that the treated solution was not suitable for subsequent methane production, since methanogen activity was inhibited by sulphate-reducing bacteria (SBR) that compete for organic substrates in the solution.

Based on the highly positive findings on nutrient release, various operating conditions were investigated. Factors such as pH, hydrogen peroxide dosage, temperature and power intensity were examined as well as treatment effectiveness on liquid and solid fractions after liquid-solid separation of DM.

The effect of pH was found to play a significant role in ortho-P and ammonia release. Neutral and alkaline conditions were found to have a negative effect on nutrient solubilization (Kenge et al., 2009c). Acidic conditions were also favorable in disintegrating solids; treatment temperature of 90°C resulted in 90% SCOD as TCOD with a 1% acid dosage in a continuous-flow system (Yu et al. 2010d). The use of mineral acids in combination with organic acids were examined in terms of their potential to be combined in the single stage process (Srinivasan et al., 2014a). Oxalic acid combined with sulphuric acid was able to disintegrate solids, release phosphorus and remove calcium in the MW/H₂O₂-AOP, whilst simultaneously producing clear supernatant with the right molar ratios of calcium to magnesium for subsequent struvite crystal formation. Acid treatment alone was reported to decrease SCOD concentration (Lo and Liao, 2011; Chan et al., 2013; Srinivasan et al., 2016).

A high hydrogen peroxide dosage (1.2 g/gTS) resulted in decrease in SCOD at 160°C (Yawson et al., 2011). However, a high H₂O₂ dosage is required in breaking down the organic matter in acidified DM at low treatment temperature below (Yu et al., 2010d). In addition, when H₂O₂ is used in combination with sulphuric acid it caused TCOD and VFA to decrease, irrespective of treatment conditions (Qureshi et al., 2008; Kenge et al., 2009c; Yawson et al., 2011; Lo and Liao, 2011). Some researches reported that the effect of H₂O₂ is more pronounced at treatment temperatures below 120°C, where increased dosage favors solids solubilization (Srinivasan et al., 2014a; Zhang et al., 2014; Srinivasan et al., 2016).

MW heating alone is capable of solubilizing SCOD from DM without the use of chemicals (Lo and Liao, 2011). Temperature was the dominant factor in SCOD release with a low H₂O₂ dosage (Yu et al., 2010d; Lo and Liao, 2011; Lo et al., 2012). However,

treatment temperature below 70°C was ineffective in breaking down the organic matter in acidified DM at a low H₂O₂ dosage (Yu et al., 2010d). Ortho-P release was enhanced at elevated temperatures irrespective of H₂O₂ used (Qureshi et al., 2008; Yawson et al., 2011; Lo and Liao, 2011). Yawson et al. (2011) found that phosphorus was completely solubilized at a temperature of 160°C. VFA production was shown to be sensitive to high temperatures; temperatures above 80°C oxidized VFA to CO₂ (Qureshi et al., 2008).

The effect of preheating was also studied. Preheating alone was unable to solubilize organic material and release nutrients from acidified DM into solution, but CH in combination with the MW/H₂O₂-AOP treatment produced great results (Nkansah-Boadu et al., 2015a). The benefit of preheating is a reduced MW heating time resulting in lower energy consumption.

Performance of batch-mode and continuous-flow MW systems were evaluated (Yu et al., 2010d; Lo and Liao, 2011; Srinivasan et al., 2014a). Continuous-flow studies showed superiority with respect to breaking down the organic matter and nutrient solubilization. The ability to introduce H₂O₂ into the system at any treatment stage enhances the degree of effectiveness in combination with temperature. Heating promotes decomposition of H₂O₂ into hydroxyl radicals, enhancing the oxidation process when H₂O₂ is applied simultaneously with MW heating, thus increasing SCOD. Yu et al. (2010d) reported an increase from approximately 40 to 90% in SCOD/TCOD ratios after the MW/H₂O₂-AOP with 1% acid and a low hydrogen peroxide dosage at 90°C. Nearly 100% of TP was in the form of ortho-P at pH 3 and 96°C treatment temperature (Zhang et al., 2014). Zhang et al. (2014) also successfully recovered over 95% of phosphorus as struvite crystals with 91-97% purity.

The majority of work was undertaken with the 2450 MHz MW systems (batch-mode and continuous-flow). The depth of penetration of a 2450 MHz MW system is three times lower compared to an industrial scale 915 MHz MW, which is also more energy efficient (> 80%) than the 2450 MHz MW (Srinivasan et al., 2016). As a result, higher flow rates and substrate with a higher TS concentration could be utilized. The 2450 MHz pilot-scale continuous-flow system was only able to operate at flow rates of approximately 1 L/min or less at a maximum power capacity of 6 kW at which a boiling point of the substrate was reached (Zhang, 2013). The tubing inside the chamber was prone to getting plugged due to a low flow rate. In addition, the arrangement of tubing in a helical coil configuration had a potential to reduce the absorption of microwaves by the substrate resulting in cold and hot spots. The current system consists of two vertical silicone tubes that allows uniform distribution of MW irradiation which further enhanced the efficiency of the treatment.

Although the treatment of DM was extensively studied, the aim of this study was to establish the treatment effectiveness of the 915 MHz 5kW pilot-scale continuous-flow system after the modifications discussed in Chapter 3 were applied; this, in turn, will further advance scientific knowledge. Previous studies with the 915 MHz pilot-scale system were compared with the present study results in order to establish the trends with respect to H₂O dosage and treatment temperature. Bailey (2015) studied the effects of H₂O dosage on acidified DM to pH 3.5 at a low temperature regime (60-90°C); the unit was operated as an open system. For the system to operate above boiling temperatures, a pressurized tank was installed and consequently, further tests on acidified DM were performed by MacSween (2015) with temperatures reaching 110 and 130°C with a hydrogen peroxide dosage of 0.6 %H₂O₂/%TS.

4.2 Materials and methods

4.2.1 Microwave system

The 915 MHz pilot-scale microwave digestion system that operates in a continuous-flow mode was utilized. Details can be found in Section 2.2.1.

4.2.2 Substrate

The dairy manure liquid fraction with 2.8% TS was obtained from the Dairy Education and Research Centre, University of British Columbia in Agassiz, BC. Liquid fraction of DM mainly consists of nutrients and metal ions and solid fraction is primarily made up of total and volatile solids (Chan et al., 2013). Liquid-solid separation is performed on site at the research centre. Based on the previous studies, the resulting substrate was acidified with sulphuric acid (H_2SO_4) to achieve a pH of 4 (Kenge et al., 2009c; Zhang et al., 2014; Srinivasan et al., 2014a). The characteristics of raw DM are summarized in Table 6.

Table 6 The characteristics of raw dairy manure

Parameter	Value
TS (%)	2.8 ± 0.01
pH	7.34
TCOD (mg/L)	36964 ± 5157
SCOD (mg/L)	3828 ± 179
VFA (mg/L)	2735 ± 124
TP (mg/L)	245 ± 23
STP (mg/L)	32 ± 5
ortho-P (mg/L)	29 ± 3
TKN (mg/L)	1527 ± 37
NH_3 (mg/L)	462 ± 13
Mg (mg/L)	390 ± 3
Ca (mg/L)	1038 ± 4

4.2.3 Experiment design

Experimental design is provided in Table 7. Acidified DM was treated at two different temperatures 90 and 110°C, with hydrogen peroxide dosage of 0.6 %H₂O₂/%TS. H₂O₂ was introduced into the system after treatment temperature reached 35°C (MacSween, 2015).

Table 7 Operating conditions for 915 MHz pilot-scale MW/H₂O₂-AOP treatment of DM

pH	Sludge Volume (L)	%H ₂ O ₂ /% TS	Temperature (°C)
3.6	20	0.6	90
3.6	20	0.6	110

4.2.4 Chemical and physical sample analysis

Chemical and physical sample analysis performed was the same as for waste activated sludge summarized in Section 2.2.4. The PSD test was omitted in the case of DM sample analysis.

4.3 Results and discussion

Soluble fraction of treated DM was adjusted to include the dilution effect of hydrogen peroxide. Dilution factor was determined as the ratio of DM volume by total sample volume in the holding tank during the experiment.

4.3.1 Solids disintegration

Solids concentrations before and after each treatment including acid and the MW/H₂O₂-AOP are summarized in Table 8. The results are consistent with the previous studies, total solids (TS) content increased after acid addition due to the formation of salts in the solution (Srinivasan et al., 2014b; Srinivasan et al., 2016). Following the MW/H₂O₂-AOP treatment, the TS concentration dropped below its initial value at both treatment temperatures. Suspended solids (SS) concentration is of most significant importance, since concentration >1000 (mg/L) are known to interfere with struvite crystal formation (Schuiling & Andrade, 1999). The MW/H₂O₂-AOP in combination with acid reduced the TSS value in the treated solution by 51 and 53% at 90 and 110°C temperatures, respectively. The organic portion of solids had also decreased by more than half after the treatment at both operating temperatures.

Table 8 Solids concentrations before and after MW/H₂O₂-AOP treatment of DM

Sample	TS (%)	VS (%)	TSS (g/L)	VSS (g/L)
Raw DM	2.8 ± 0	1.9 ± 0	23.9 ± 0.4	17.9 ± 0.5
Raw Acidified DM	3.3 ± 0	2.1 ± 0	22.8 ± 0.8	17.5 ± 0.3
90°C MW treated	2.7 ± 0	1.6 ± 0	11.6 ± 0.4	8.6 ± 0.4
110°C MW treated	2.9 ± 0	1.7 ± 0	11.2 ± 0.2	7.8 ± 0.1

Chemical Oxygen Demand (COD)

Results of this study (0.6 %H₂O₂/%TS) show that SCOD/TCOD increased from 0.10 before treatment to 0.46 and 0.51 after the MW/H₂O₂-AOP treatment at 90 and 110°C temperatures, respectively. The ratio of SCOD/TCOD was not affected by the acid treatment (initial-10%, acid treated-11%). Srinivasan et al. (2016) observed an immediate drop in SCOD/TCOD ratio after acid addition. The acid treatment caused SCOD value to decrease slightly due to agglomeration of fine suspended particles; this increase in particle size caused precipitation and subsequent decrease in SCOD (Chan et al., 2013). However, the consequent MW treatment increased SCOD as it broke down the agglomerated particles. SCOD value also increased upon the injection of hydrogen peroxide (Srinivasan et al., 2016).

In comparison to the previous studies, results presented in Figure 16 illustrate the effectiveness of H₂O₂ dosage at low temperature; (a) is from Bailey (2015); (b) is from MacSween (2015).

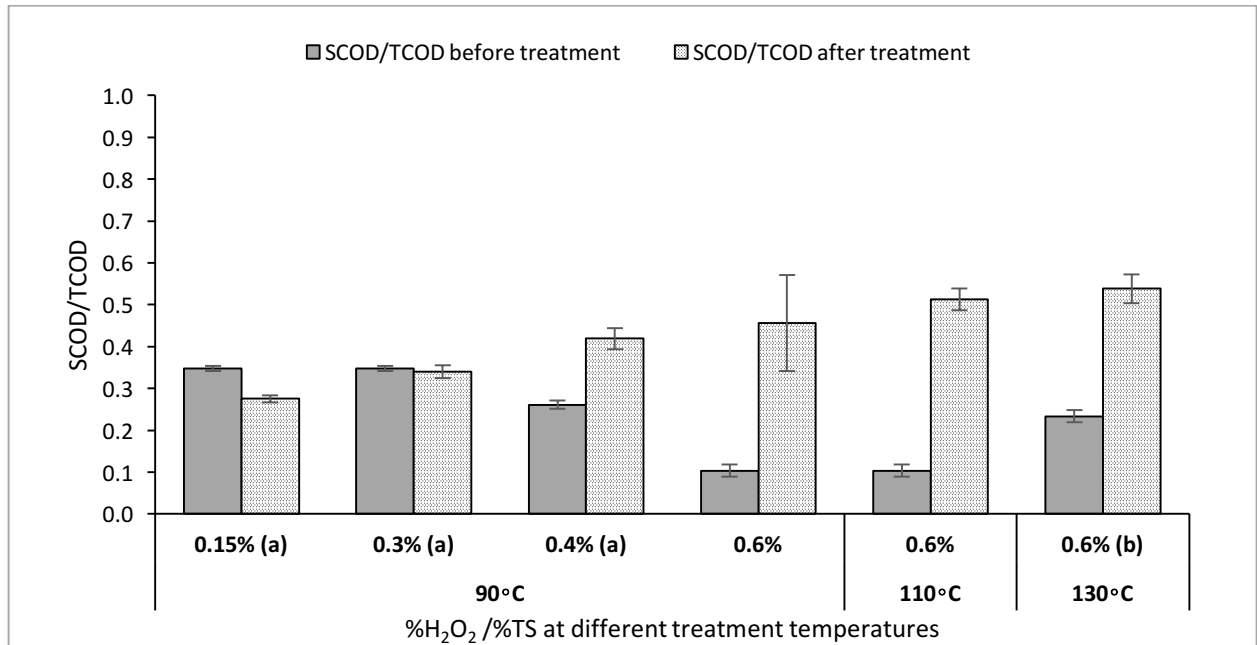


Figure 16 SCOD to TCOD ratio before and after MW/H₂O₂-AOP treatment of DM

The extent of solids solubilization solely depends on the H_2O_2 dosage in the treatment of acidified DM at 60-90°C treatment temperature (Srinivasan et al., 2016). The MW/ H_2O_2 -AOP treatment at 90°C with 0.15, 0.3, 0.4 and 0.6 % H_2O_2 /%TS resulted in SCOD/TCOD ratio of 28, 34, 42 and 46%, respectively. The MW/ H_2O_2 -AOP treatment with hydrogen peroxide lower than 0.3 % H_2O_2 /%TS did no increase SCOD/TCOD ratio from that of initial, it had an opposite effect, due to increase in TCOD after the treatment. As a result, a double amount of hydrogen peroxide dosage per percent TS (0.6% vs 0.3%) resulted in approximately 35 times higher SCOD solubilization at 90°C temperature.

The temperature effect was assessed with the sets that utilized the hydrogen peroxide dosage of 0.6 % H_2O_2 /%TS. The ratio of SCOD/TCOD increased by 35, 41 and 31% from that of initial at temperatures of 90, 110 and 130, respectively. The treatment temperature of 110°C resulted in the highest SCOD solubilization. High H_2O_2 dosage at high treatment temperatures converted soluble organics to CO_2 , thus reducing SCOD (Yawson et al., 2011).

In addition, all treated sets with 0.6 % H_2O_2 /%TS had a decrease in TCOD; the effect was more pronounced at a temperature of 110°C and above, where 55% decrease in TCOD was observed at 130°C. The results are consistent with the previous studies that used sulphuric acid in combination with hydrogen peroxide. Qureshi et al., (2008) reported that TCOD decreased at treatment temperatures above 80°C in the presence of H_2O_2 . Treatment temperatures of approximately 120°C resulted in 36% drop in TCOD. It appeared that solids destruction and solubilization occurred simultaneously and high temperatures resulted in higher oxidation reaction producing CO_2 as an end product.

The multiple linear regression analysis to predict SCOD/TCOD ratios for all treatment sets within the range of factors studied resulted in the following equation:

$$\text{SCOD/TCOD} = 0.06355 + 0.0012 * \text{Temperature} + 0.58385 * \text{Dosage (\%H}_2\text{O}_2/\text{\%TS)} \quad (10)$$

A correlation coefficient (R) of 0.98 was obtained, indicating a good fit. At 95% confidence level the null hypothesis was rejected for H₂O₂ dosage (p-level < 0.001). The results indicated SCOD release was statistically different with changes in hydrogen peroxide dosage level. Hydrogen peroxide was a significant factor in solids solubilization.

It can be concluded, that treatment at 110°C with 0.6 %H₂O₂/‰TS yielded the best results in terms of solids solubilization.

Volatile Fatty Acids (VFA)

Volatile fatty acids present in DM were mainly in the form of acetic acid before and after MW treatment. However, the concentration of acetic acid doubled after the MW/H₂O₂-AOP treatment irrespective of treatment temperature. Other forms, such as propionic, iso-butyric, iso-valeric and valeric were present in the treated solution. Treated solution to 110°C had no valeric acid left. The MW/H₂O₂-AOP treatment helped in breaking down longer chain VFAs into simpler fatty acids that are of importance in anaerobic digestion and methane production (Qureshi et al., 2008).

Lo et al. (2012) identified treatment temperature and hydrogen peroxide dosage as being the key parameters in VFA formation, heating time, however, caused VFAs to

decrease. Similarly, as previously reported by other researchers (MacSween, 2015; Bailey, 2015), acid treatment alone caused VFA concentration to decrease, which is in agreement with the present study results. Very high acid dosage was disadvantageous as it caused VFA to decrease in concentration (Yu et al., 2010d). Lo and Liao (2011) reported that MW/H₂O₂-AOP in combination with acid produced more VFA with increasing temperature, however, a 1% acid dosage resulted in a decrease in VFA at treatment temperature of 90°C. Kenge et al. (2009c) reported that the MW/H₂O₂-AOP treatment alone is able to produce VFAs irrespective of pH, however a pH of 3.5 yielded the best results. Results from this and other two studies are summarized in Table 9.

Table 9 VFA concentration before and after MW/H₂O₂-AOP treatment of DM

%H₂O₂/%TS	Temperature (°C)	VFA Before Treatment (mg/L)	VFA After Treatment (mg/L)	Increase/Decrease in VFA (%)
0.15(a)	90	3878 ± 15	3699 ± 81	-5%
0.3(a)	90	3878 ± 15	3572 ± 22	-8%
0.4(a)	90	3462 ± 51	3456 ± 61	0%
0.6	90	2735 ± 124	2678 ± 26	-2%
0.6	110	2735 ± 124	2817 ± 42	3%
0.6(b)	130	3218 ± 19	3136 ± 83	-3%

No trend was observed with respect to hydrogen peroxide dosage or temperature. A slight increase in VFA concentration was only observed at a treatment temperature of 110°C. All other MW treated sets yielded lower concentrations than that of initial DM. These results indicate that the concentration dropped after the DM was acidified and did not recover at 90°C treatment temperature, irrespective of H₂O₂ dosage used. However, a slight recovery

appeared at 110°C temperature, after which VFAs were vaporized or oxidized to CO₂ as an end product at 130°C treatment temperature.

The ratio of VFA from treated and initial DM statistically compared for all six treatment sets resulted in the correlation coefficient (R) of 0.74 indicating a poor fit. None of the two factors were found to be statistically significant.

4.3.2 Nutrient release

Phosphorus

The effect of acid treatment on phosphorus solubilization is illustrated in Figure 17. The results were consistent with the previous studies on the MW/H₂O₂-AOP process in batch and continuous-mode operation (Kenge et al., 2009c; Yu et al., 2010d; Lo and Liao, 2011; Chan et al., 2013; Srinivasan et al., 2014a; Zhang et al., 2014; Srinivasan et al., 2016).

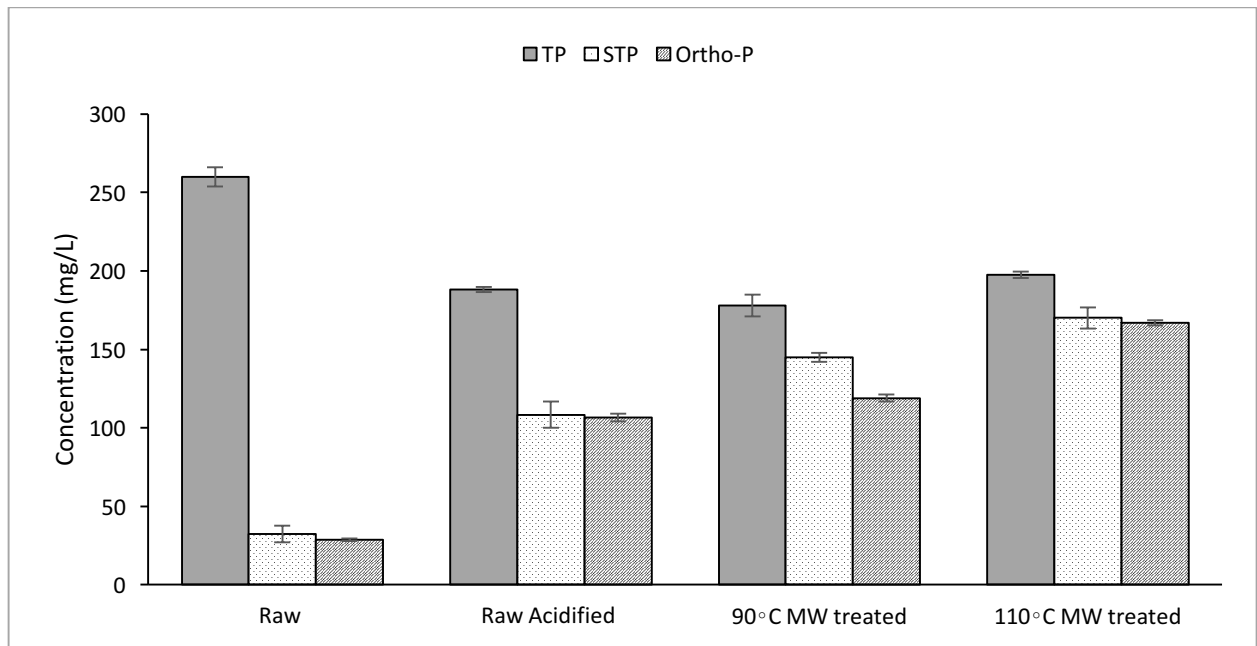


Figure 17 The effect of acid and/or MW/H₂O₂-AOP treatment on phosphorus release

The study by Kenge and colleagues proved that near neutral and alkaline conditions can be detrimental to phosphorus release into the solution in the treatment of DM, where phosphorus was converted to an insoluble form resulting in decrease of ortho-P below the untreated DM value. Furthermore, in the absence of acid addition, ortho-P decreased as treatment temperature increased (Yu et al., 2010d). The release of Ortho-P into solution was evident at pH 5; approximately 55-75% of TP was in the form of ortho-P after MW

treatment, regardless of the type of acid used (Srinivasan et al., 2014a). Ideal pH for ortho-P release was pH 3 where close to 100% of TP was in the form of ortho-P (Zhang et al., 2014).

The STP concentration increased from 32 mg/L to 108 mg/L after acid addition. Temperature in combination with hydrogen peroxide further increased the concentration by 33 and 57% at 90 and 110°C, respectively. Ortho-P release followed a similar trend, however, lower temperature (90°C) did not induce a great amount of ortho-P following acidification. Polyphosphates were the dominant phosphorus species in the solution treated at 90°C temperature (Pan et al. 2006).. However, the addition of acid in DM treatment is vital in solubilizing phosphorus (Kenge et al., 2009c; Lo and Liao, 2011).

Table 10 illustrates the combined effect of acid, hydrogen peroxide dosage and temperature after the MW/H₂O₂-AOP treatment. Regardless of hydrogen peroxide dosage and temperature, all treatment sets had a substantial increase in STP (> 60%) of which more than 80% were in the form of ortho-P. Hydrogen peroxide dosage at low temperature (90°C) had no effect on ortho-P release.

Table 10 Ortho-P release before and after MW/H₂O₂-AOP treatment of DM

Temperature (°C)	% H ₂ O ₂ / % TS	Ortho-P/TP Before Treatment	Ortho-P/TP After Treatment	Increase in Ortho-P (%)
90	0.15(a)	0.01	0.68	98
90	0.3(a)	0.01	0.63	98
90	0.4(a)	0.05	0.72	93
90	0.6	0.11	0.67	84
110	0.6	0.11	0.85	87
130	0.6(b)	0.01	0.92	99

The synergistic effect between hydrogen peroxide dosage and temperature is more pronounced at high temperatures (110°C and above), where at least 85% of TP is in the form of ortho-P compared to approximately 70% for the sets treated at 90°C, regardless of H₂O₂ used.

The multiple linear regression analysis to predict ortho-P/TP ratio for all treatment sets within the range of factors studied, resulted in the following equation:

$$\text{Ortho-P/TP} = 0.16605 + 0.00582 * \text{Temperature} - 0.14976 * \text{Dosage (\%H}_2\text{O}_2/\%\text{TS)} \quad (11)$$

A correlation coefficient (R) of 0.81 was obtained indicating a poor fit. None of the two factors were found to be statistically significant.

By setting initial STP and ortho-P value after the samples were subjected to the acid treatment, the pH effect on phosphorus solubilization was eliminated. As a result, a better understanding of the effect that temperature and hydrogen peroxide dosage has on the treatment can be gained.

Temperature alone after acid treatment had a profound effect on phosphorus solubilization and ortho-P release as illustrated in Figure 18 on the following page.

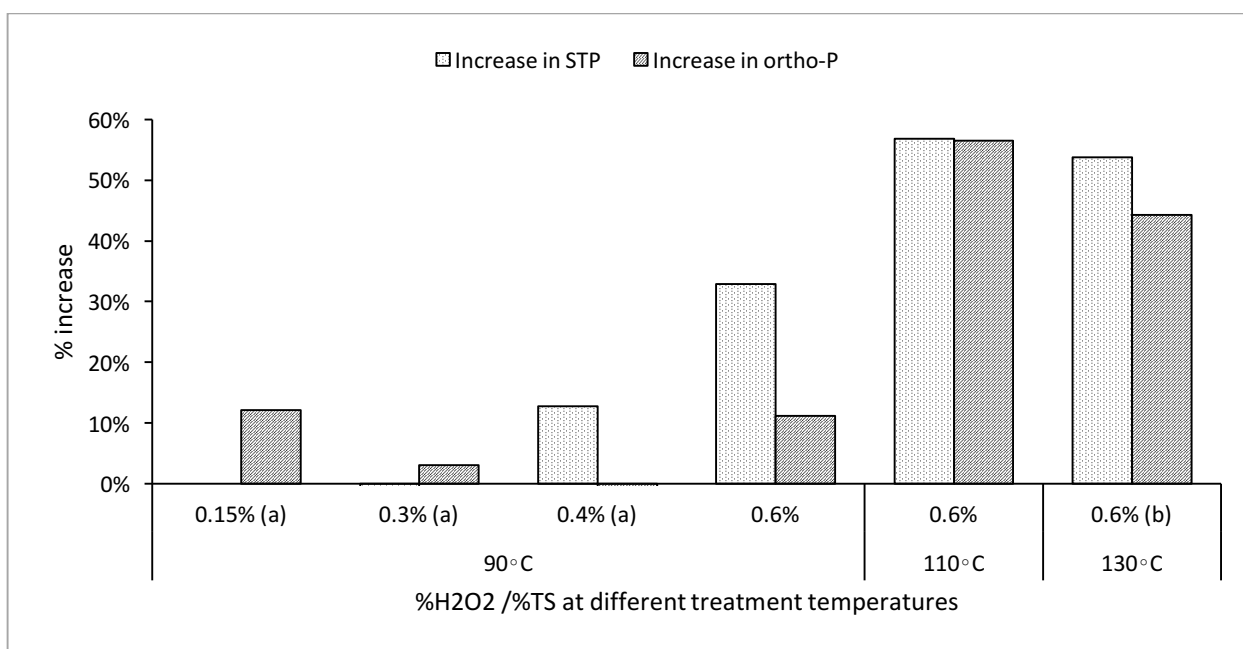


Figure 18 The effect of temperature and/or hydrogen peroxide on phosphorus release

Ortho-P concentration increased by 56% at 110°C treatment temperature compared to 11% increase at 90°C treatment temperature for the sets with the same H₂O₂ dosage (0.6 %H₂O₂/%TS). These results are in agreement with the observations made by this research group that treatment temperature is the key factor for ortho-P release (Pan et al., 2006; Qureshi et al., 2008; Lo and Liao, 2011; Lo et al., 2012; MacSween, 2015; Srinivasan et al., 2016).

The effect of hydrogen peroxide on phosphorus solubilization is more pronounced at lower temperatures (< 80°C) (Pan et al., 2006; Qureshi et al., 2008). This, to some extent, is evident at 90°C and the highest hydrogen peroxide dosage, where an increase in soluble phosphorus and ortho-P was 33 and 11%, respectively. High temperature is required for the formation of ortho-P (Lo and Liao, 2011; Srinivasan et al., 2015).

Nitrogen

The significant factors in ammonia release were temperature and hydrogen peroxide dosage (Qureshi et al., 2008; Yawson et al., 2011; Lo et al., 2012). Ammonia concentration did not change after acid addition. However, after the MWH_2O_2 -AOP treatment, ammonia concentration increased from 462 (initial) to 841 and 857 mg/L for 90 and 110°C temperatures, respectively. The significance of pH on release of ammonia is reported by Kenge et al. (2009c). The study found that acidified sample to pH 3.5 after the MW/ H_2O_2 -AOP treatment, increased in concentration by 125%. Acid addition was necessary for the release of ammonia in the treatment of DM by MW irradiation; ammonia concentration decreased without addition of acid at 90°C treatment temperature (Yin et al., 2009). Figure 19 presents the results on TKN, STKN and ammonia.

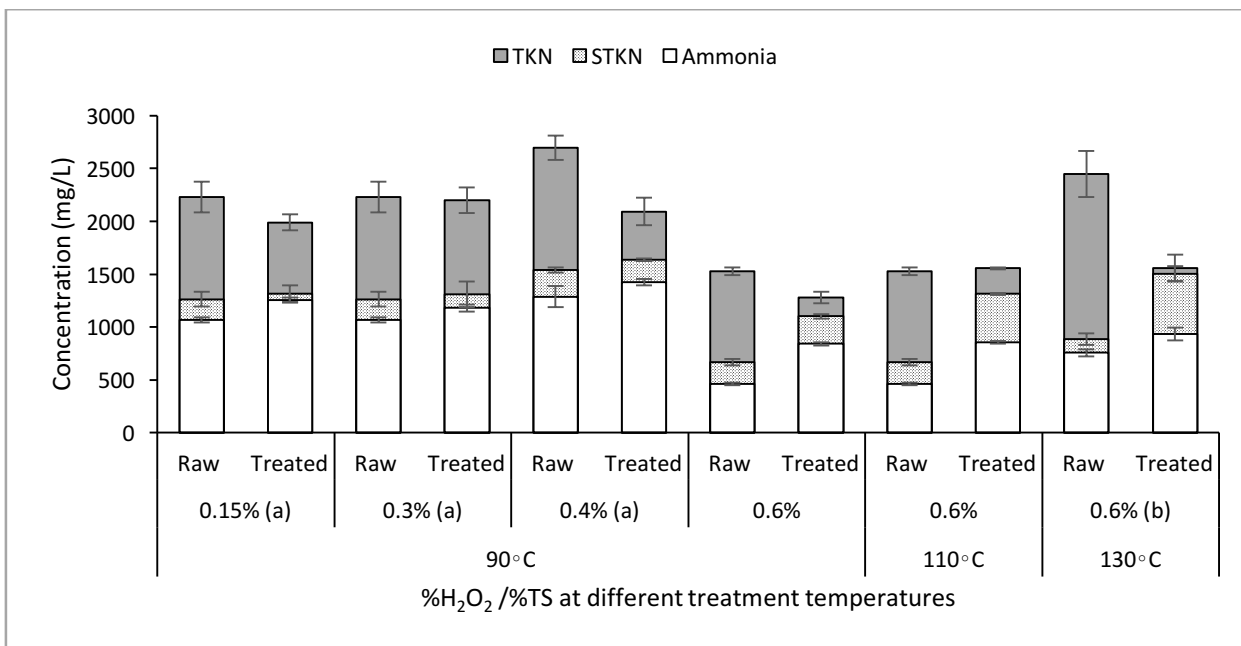


Figure 19 Ammonia release before and after MWH_2O_2 -AOP treatment of DM

Hydrogen peroxide dosage was superior in the release of ammonia into solution at 90°C treatment temperature. The STKN and ammonia concentrations increased by 40 and 45%, respectively, in the treatment set with 0.6 %H₂O₂/ %TS. Treatment sets with 0.15 %H₂O₂/ %TS (4% increase in STKN and 15% increase in ammonia) and 0.3 %H₂O₂/ %TS (4% increase in STKN and 9% increase in ammonia) barely increased from the initial values.

The ratio of ammonia to TKN were in the range of 54 to 68% for all the treated sets, with the highest and the lowest resulting from 0.6 %H₂O₂/ %TS/90°C and 0.3 %H₂O₂/ %TS/90°C, respectively.

Although treatment temperature aided in nitrogen solubilization, it did not increase ammonia concentration greatly. MW irradiation in combination with hydrogen peroxide and sulphuric acid was found to release protein and amino acids into solution, however, they were not converted to ammonia (Srinivasan et al., 2014a). This was evident at high treatment temperature where more than 84% of TKN was solubilized of which only 65% was in the form of ammonia.

These results are contradictory to the previous DM studies that reported temperature as being the most significant factor in ammonia release (Yu et al., 2010d) with hydrogen peroxide dosage being less effective (Zhang et al., 2014). However, differences in results could be attributed to the different treatment conditions.

In addition, all sets, except 0.6 %H₂O₂/ %TS/110°C, had a decrease in TKN value after the MWH₂O₂-AOP treatment.

More than 90% of Ca and Mg was released into solution after the addition of acid, whereas potassium concentration barely increased as shown in Figure 20. The results are consistent with the previous studies (Bailey 2015; MacSween, 2015). The addition of acid and the MW/H₂O₂-AOP treatment did not affect soluble K, but for Ca and Mg solubilization, acid addition was necessary (Chan et al., 2013). As well as ortho-P, Ca and Mg increased with decreased pH regardless of H₂O₂ dosage (Zhang et al., 2014).

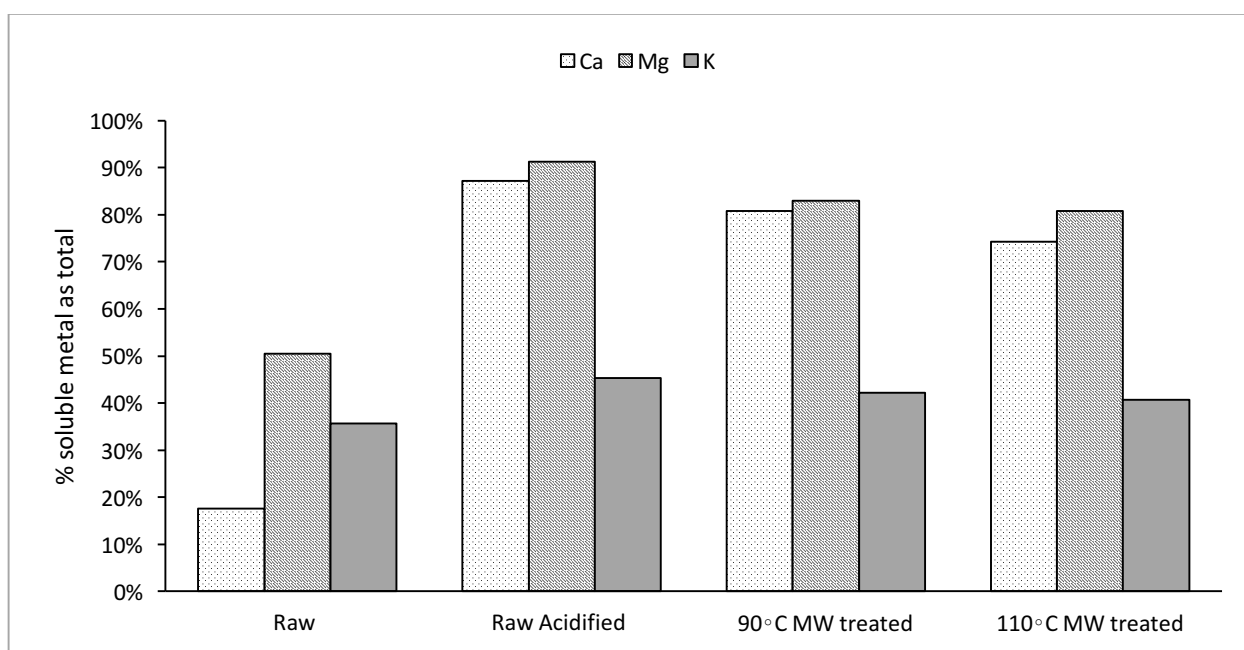


Figure 20 The effect of acid and/or MW/H₂O₂-AOP treatments of DM on metals solubilization

The release of metals into solution, in particular magnesium, is important for the slow release fertilizer in the form of struvite (magnesium ammonium phosphate) or K-struvite (magnesium potassium phosphate) (Qureshi et al., 2008). Some metals such as calcium are undesirable in high amounts, since Ca ions disrupt the process of struvite crystallization (Srinivasan et al., 2014a). However, this can be overcome by the addition of oxalic acid.

Excess calcium was successfully removed with oxalic acid without altering the ortho-P, ammonia and Mg concentration in the solution (Zhang et al., 2014).

4.3.3 Physical properties

Settling

Figure 21 illustrates the resulting substrate before and after the MW/H₂O₂-AOP treatment. The results are consistent with the previous studies. Acid treatment alone did not improve settling as is evident in Figure 21. The solids cannot settle out of solution without hydrogen peroxide or sulphuric acid (Srinivasan et al., 2014a). However, MW treatment in combination with H₂O₂ resulted in very little solids and clear supernatant at both treatment temperatures. Previous studies from the continuous-flow system showed that settling improved with increasing temperature and H₂O₂ dosage (Srinivasan et al., 2016). Hydrogen peroxide dosage of 0.3 to 0.5% (v/v) resulted in similar settling properties (Zhang et al., 2014), whereas an increased dosage from 0.5 to 1.5% (v/v) displayed substantial improvement (Srinivasan et al., 2016). Furthermore, low pH displayed a positive impact on settling; the least volume of sludge was obtained for MW treated DM at pH 3.5 (Zhang et al., 2014).

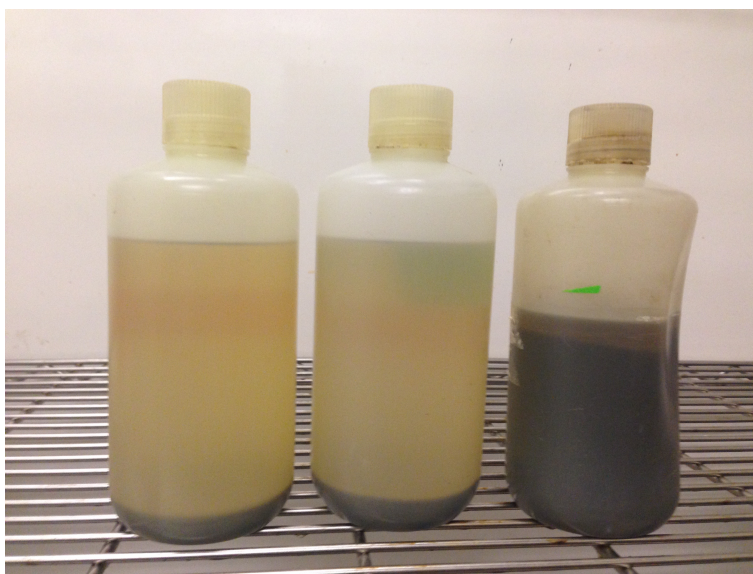


Figure 21 Settling of acidified and MW/H₂O₂-AOP treated DM (from left to right: MW/H₂O₂-AOP at 110°C, MW/H₂O₂-AOP at 90°C and acid treated DM)

TSS concentration after MW treatment was 11.02 ± 0.33 and 10.65 ± 0.24 at temperatures 90 and 110°C, respectively. However, TSS was not determined for a supernatant after gravity settling took place. TSS levels >1000 mg/L are undesirable since they interfere with the struvite formation. Based on the visual assessment (Figure 21) the MW/H₂O₂-AOP treatment in combination with sulphuric acid produced a supernatant similar to that of Zhang et al. (2014). The MW/H₂O₂-AOP with 0.25 %H₂O₂/%TS and DM adjusted to pH 3.5, produced a supernatant with SS levels less than 600 mg/L. The advantage of the MW/H₂O₂-AOP treatment is that the resulting supernatant could be directly used for struvite formation (Qureshi et al., 2008).

Capillary Suction Timer (CST)

Dewaterability measured in terms of CST in seconds, decreased dramatically after the MW/H₂O₂-AOP treatment (Table 11). After acid was introduced, CST decreased by 43% despite the high amount of SS; this could be due to agglomeration of particles. Further decrease in CST was induced by the MW/H₂O₂-AOP, resulting in a 99% reduction at both treatment temperatures. These results support a substantial reduction in TSS that resulted in a clear supernatant.

Table 11 CST results before and after MW/H₂O₂-AOP treatment of DM

Sets	CST (s)
Raw DM	2789.73 ± 904.87
Raw Acidified DM	1591.33 ± 237.97
90°C MW treated	22.6 ± 1.94
110°C MW treated	15.03 ± 1.36

4.3.4 Energy analysis

To correlate the energy consumption data with the performance of the 915 MHz continuous-flow microwave system was assessed in terms of nutrient and solids solubilization as described in Section 2.2.5. The results are summarized in Figure 22. No data was available for the 130°C treatment set.

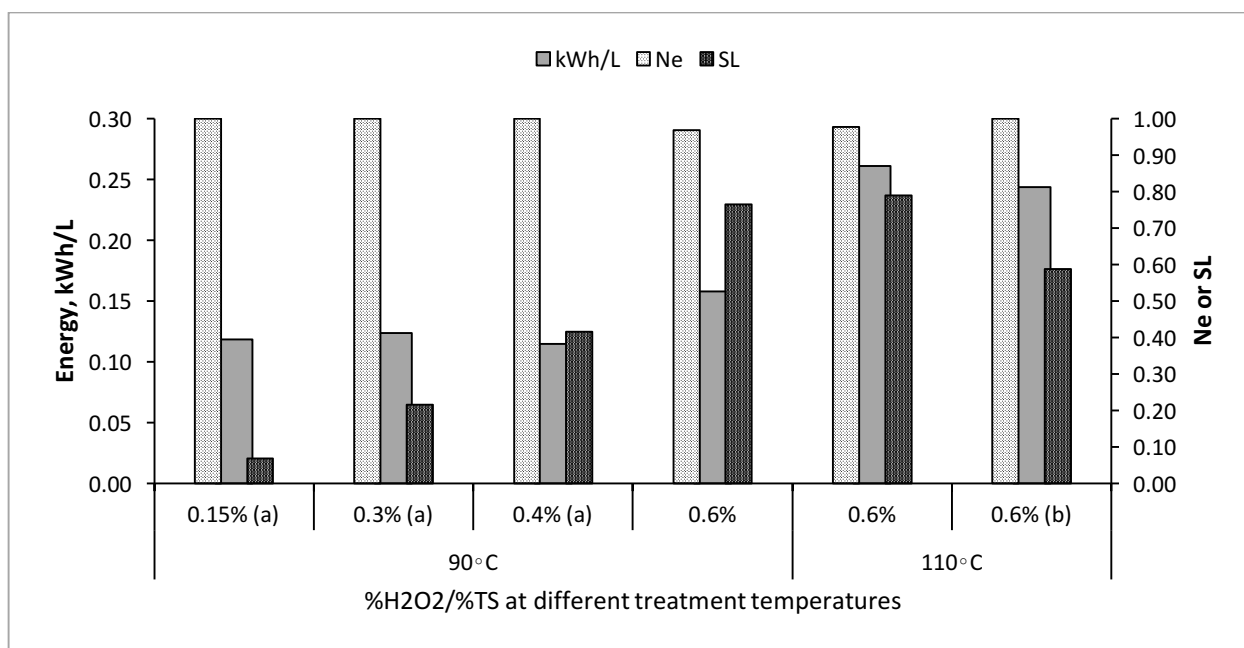


Figure 22 Energy consumed by the 915 MHz continuous-flow microwave system plotted against solids solubilization (SL) and nutrient release (Ne) indices for the MW/H₂O₂-AOP treatment of DM

With regards to nutrient solubilization, all sets produced a substantial amount of nutrients in the solution regardless of treatment temperature. However, treatment to a higher temperature resulted in higher energy consumption. The solids solubilization index varied greatly among different sets. At a lower operating temperature, the set with the highest

hydrogen peroxide dosage produced a substantial increase in solids solubilization. Although the sets at 110°C produced comparable results, the energy demand was 33% higher.

With respect to the systems upgrades detailed in Section 3, two MW runs with the same treatment conditions were compared. For approximately the same amount of energy consumed, the system resulted in a reduced treatment time and a higher solids solubilization index. The treatment time was reduced from 53 minutes to 48 minutes. Since the pump was operating at the predetermined flow rate of 9 L/min, the heating time was slightly lower (1.97°C/min) than that of 6 L/min (2.07°C/min).

4.4 Conclusion

The MW/H₂O₂-AOP, utilizing the 915 MHz pilot-scale system, proved to be an effective pretreatment method of DM. The resulting solution was free from suspended solids and high in soluble nutrients required for the formation of struvite crystals. Both treatment temperatures resulted in greatly improved settling and dewaterability properties.

The treated effluent had considerable amounts of ortho-P; treatment at a temperature of 110°C resulted in as high as 85% of TP being in the form of ortho-P. Hydrogen peroxide dosage was a significant factor in phosphorus solubilization at low temperature. However, for the formation of ortho-P, higher temperatures were required. A similar trend was observed in the release of ammonia, however, higher temperatures did not increase ammonia concentration despite yielding high concentrations of soluble TKN.

Treatment at a temperature of 110°C with hydrogen peroxide dosage of 0.6 %H₂O₂/%TS yielded the best results in terms of solids solubilization; SCOD/TCOD increased from 10% before treatment to 51% after treatment. MW/H₂O₂-AOP treatment was ineffective in the formation of VFA under the treatment conditions studied.

Modification of the system resulted in a better performance in terms of solids destruction and nutrient release with respect to energy consumption and treatment time.

Chapter 5: Conclusions

The results indicated that the MW/H₂O₂-AOP could reduce amounts of waste residuals for disposal and produce a high quality treated effluent for further resource and energy recovery. Depending on the needs of each WWTPs treatment priority, the experimental conditions applied in the process can be adjusted accordingly.

The 915 MHz pilot-scale continuous-flow system resulted in higher treatment efficiency in terms of solids solubilization and nutrient release than that of the 2450 MHz bench-scale MW unit. In the treatment of WAS, alkaline conditions produced an effluent with high SCOD and VFA concentrations, ideal for anaerobic digestion. Despite this, a high pH yielded poor dewaterability properties in the treated solution. Acidic conditions yielded a supernatant rich in nutrients with greatly improved dewaterability and settling properties of treated WAS. The struvite crystal formation process can directly utilize such effluent without further treatment. MW/H₂O₂-AOP treated WAS, without pH adjustment, yielded ideal conditions for a reduction in the amount of sludge to be disposed. Energy consumption was lower for the pH adjusted sets.

The 915 MHz pilot-scale continuous-flow system was superior in the treatment of acidified DM. The treatment at the optimum flow rate resulted in reduced process time and produced effluent low in suspended solids and high in nutrients such as ortho-P and ammonia, essential in the struvite recovery process.

Lower heating temperatures were produced by a high flow rate and high ionic concentration. Therefore, exit temperatures of the fluid can be controlled by the flow rate in the 915 MHz pilot-scale continuous-flow system.

Chapter 6: Recommendations

- The next stage in research on MW irradiation to treat organic slurries is the design of a full-scale system that operates in a continuous-flow mode and utilizes the high-power MW generator with a frequency of 915 MHz that will provide deeper penetration allowing higher flow rates and higher loadings to be used. As a result, optimum treatment conditions would have to be determined depending on the characteristics of the substrate to be treated. Higher power input was shown to be advantageous for solids solubilization and nutrient release; therefore, increased power intensity would increase overall treatment efficiency by increasing heating and reaction rates thus reducing energy consumption and operating time.
- To improve energy efficiency of the current 5 kW MW generator, automation of tuning rods would be necessary; currently the impedance of MW to that of the target liquid is correlated manually by adjusting tuning rod heights. Therefore, the reflected power varies throughout an experiment. In addition, a complete system automation in full-scale application would be necessary to facilitate a continuous, uninterrupted operation mode and prevent hazards associated with human error. In addition, preheating unit should be considered which would reduce MW heating time resulting in lower energy consumption.
- Given such a positive outcome in the treatment of WAS and DM, other wastes such as source separated organic (SSO), fat, oil and grease (FOG) or a combination of wastes need to be investigated as the potential to expand the application of MW technology.

Bibliography

- Abelleiraa, J., Perez-Elvirab, S.I., Sanchez-Onetoa, J., Portelaa, J.R., Nebotc, E. (2012). Advanced thermal hydrolysis of secondary sewage sludge: a novel process combining thermal hydrolysis and hydrogen peroxide addition. *Resources, Conservation and Recycling*, 59, 52-57.
- Acero, J. L., & Von Gunten, U. (2001). Characterization of oxidation processes: ozonation and the AOP O_3/H_2O_2 . *American Water Works Association*, 93(10), 90-100.
- Anwar, J., Shafique, U., Rehman, R., Salman, M., Dar, A., Anzano, J. M., ... & Ashraf, S. (2015). Microwave chemistry: Effect of ions on dielectric heating in microwave ovens. *Arabian Journal of Chemistry*, 8(1), 100-104.
- APHA (2012). Standard methods for the examination of water and wastewater. (2012). *Choice Reviews Online*, 49(12).
- Appels, L., DegrEve, J., Van der Bruggen, B., Van Impe, J., and Dewil, R. (2010). Influence of low temperature thermal pre-treatment on sludge solubilisation, heavy metal release and anaerobic digestion. *Bioresource Technology*, 101, 5743-5748.
- Ariunbaatar, J., Panico, A., Esposito, G., Pirozzi, F., & Lens, P. N. (2014). Pretreatment methods to enhance anaerobic digestion of organic solid waste. *Applied energy*, 123, 143-156.
- Bailey, S. W. (2015). *Pilot-scale microwave treatment of wastewater slurries: assessment of a 915 MHz microwave generator and custom applicator* (Master's thesis). Retrieved on 16th January 2017 from <https://open.library.ubc.ca/cIRcle/collections/ubctheses>
- Barber, W. P. F. (2016). Thermal hydrolysis for sewage treatment: A critical review. *Water Research*, 104, 53-71.
- Barnett, G. M. (1994). Phosphorus forms in animal manure. *Bioresource Technology*, 49(2), 139-147.
- Bolton, J. R., & Cater, S. R. (1994). Homogeneous photo-degradation of pollutants in contaminated water: an introduction. *Aquatic and surface photochemistry*, 33, 467-490.
- Bougrier, C., Delgenes, J. P., & Carrère, H. (2008). Effects of thermal treatments on five different waste activated sludge samples solubilisation, physical properties and anaerobic digestion. *Chemical Engineering Journal*, 139(2), 236-244.
- Boyle, J. D., & Gruenwald, D. D. (1975). Recycle of liquor from heat treatment of sludge. *Journal (Water Pollution Control Federation)*, 2482-2489.
- Brooks, R. B. (1970). Heat treatment of sewage sludge. *Water Pollution Control*, 69, 92-99.

- Carrère, H., Dumas, C., Battimelli, A., Batstone, D. J., Delgenès, J. P., Steyer, J. P., & Ferrer, I. (2010). Pretreatment methods to improve sludge anaerobic degradability: a review. *Journal of hazardous materials*, 183(1), 1-15.
- Chan, I., Srinivasan, A., Liao, P. H., Lo, K. V., Mavinic, D. S., Atwater, J., & Thompson, J. R. (2013). The Effects of Microwave Pretreatment of Dairy Manure on Methane Production. *Natural Resources*, 04(03), 246-256.
- Chan, W.I., Liao, P.H., and Lo, K.V. (2010). Effect of Irradiation Intensity and pH on Nutrient Release and Solids Destruction of Waste Activated Sludge using the Microwave-Enhanced Advanced Oxidation Process. *Water Environmental Research*, 82(11), 2229-2238.
- Chan, W.I., Wong, W.T., Liao, P.H., and Lo, K.W. (2007). Sewage sludge nutrient solubilisation using a single-stage microwave treatment. *Journal of Environmental Science and Health Part A*, 42(1), 59-63.
- Chang, C., Tyagi, V. K., & Lo, S. (2011). Effects of microwave and alkali induced pretreatment on sludge solubilization and subsequent aerobic digestion. *Bioresource Technology*, 102(17), 7633-7640.
- Chen, Y., Yang, H., & Gu, G. (2001). Effect of acid and surfactant treatment on activated sludge dewatering and settling. *Water Research*, 35(11), 2615-2620.
- Chi, Y., Li, Y., Fei, X., Wang, S., & Yuan, H. (2011). Enhancement of thermophilic anaerobic digestion of thickened waste activated sludge by combined microwave and alkaline pretreatment. *Journal of Environmental Sciences*, 23(8), 1257-1265.
- Chi, Y.Z., Li, Y.Y., Ji, M., Qiang, H., Deng, H.W., and Wu, Y.P. (2010). Use of combined NaOH-microwave pretreatment for enhancing mesophilic anaerobic digestibility of thickened waste activated sludge. *Advanced Materials Research*, (113), 459–68.
- Decareau, R. V., & Peterson, R. A. (1986). *Microwave processing and engineering*. Weinheim: VCH.
- Doğan, I., & Sanin, F. D. (2009). Alkaline solubilization and microwave irradiation as a combined sludge disintegration and minimization method. *Water Research*, 43(8), 2139-2148.
- EPA. (2012a). 5.9 Conductivity. In *Water: Monitoring and Assessment*. Retrieved on 5th April 2017 from <http://water.epa.gov/type/rs/monitoring/vms59.cfm>
- EPA. (2012b). 5.8 Total Dissolved Solids. In *Water: Monitoring and Assessment*. Retrieved on 5th April 2017 from <http://water.epa.gov/type/rs/monitoring/vms58.cfm>
- Erdinçler, A., and Vesilind, P.A. (2000). Effect of sludge cell disruption on compactibility of biological sludges. *Water Science and Technology*, 42(9), 119–126.

- Erickson, A. H., & Knopp, P. V. (1970). Biological treatment of thermally conditioned sludge liquors.
- Eskicioglu, C., Kennedy, K. J., & Droste, R. L. (2006). Characterization of soluble organic matter of waste activated sludge before and after thermal pretreatment. *Water research*, 40(20), 3725-3736.
- Eskicioglu, C., Prorot, A., Droste, R.L., Kennedy, K.J. (2008). Synergetic pretreatment of sewage sludge by microwave irradiation presence of H₂O₂ for enhanced anaerobic digestion. *Water Research*, 42(18), 4674-4682.
- Eskicioglu, C., Terzian, N., Kennedy, K.J., Droste, R.L., and Hamoda, M. (2007). Athermal microwave effects for enhancing digestibility of waste activated sludge. *Water Research*, 41(11), 3725-3736.
- Everett, J. G. (1972). Dewatering of wastewater sludge by heat treatment. *Water Pollution Control Federation*, 92-100.
- Fondriest Environmental, Inc. (2014) "Conductivity, Salinity and Total Dissolved Solids." Fundamentals of Environmental Measurements. <http://www.fondriest.com/environmental-measurements/parameters/water-quality/conductivity-salinity-tds>
- Frølund, B., Palmgren, R., Keiding, K., & Nielsen, P. H. (1996). Extraction of extracellular polymers from activated sludge using a cation exchange resin. *Water Research*, 30(8), 1749-1758.
- Gabbita, K. V., & Huang, J. Y. (1984). Catalase activity of activated sludge. *Toxicological & Environmental Chemistry*, 8(2-3), 133-150.
- Gadani, D. H., Rana, V. A., Bhatnagar, S. P., Prajapati, A. N., & Vyas, A. D. (2012). Effect of salinity on the dielectric properties of water.
- Griffini, O., & Iozzelli, P. (1996). The Influence of H₂O₂ in Ozonation Treatment: Experience of the Water Supply Service of Florence, Italy. *Ozone: Science & Engineering*, 18(2), 117-126.
- Guwy, A.J., Buckland, H., Hawkes, F.R., and Hawkes, D.L. (1998). Active biomass in activated sludge: comparison of respirometry with catalase activity measured using an on-line monitor. *Water Research*, 32(12), 3705-3709.
- Guwy, A.J., Martin, S.R., Hawkes, F.R., and Hawkes, D.L. (1999). Catalase activity measurements in suspended aerobic biomass and soil samples. *Enzyme and Microbial Technology*, 25(8), 669-676.
- Hales, A., Quarini, G., Hilton, G., Jones, L., Lucas, E., McBryde, D., & Yun, X. (2015). The effect of salinity and temperature on electromagnetic wave attenuation in brine. *International Journal of Refrigeration*, 51, 161-168.

- Harold, F. M. (1960). Accumulation of inorganic polyphosphate in mutants of *Neurospora crassa*. *Biochimica et biophysica acta*, 45, 172-188.
- Haug, R. T. (1977). Sludge processing to optimize digestibility and energy production. *Water Pollution Control Federation*, 1713-1721.
- Haug, R. T., Stuckey, D. C., Gossett, J. M., & McCarty, P. L. (1978). Effect of thermal pretreatment on digestibility and dewaterability of organic sludges. *Water Pollution Control Federation*, 73-85.
- Hiraoka, M., Takeda, N., Sakai, S., & Yasuda, A. (1985). Highly efficient anaerobic digestion with thermal pretreatment. *Water Science and Technology*, 17(4-5), 529-539.
- Hong, S. M., Park, J. K., and Lee, Y. O. (2004). Mechanisms of microwave irradiation involved in the destruction of fecal coliforms from biosolids. *Water Research*, 38(6), 1615–1625.
- Hong, S. M., Park, J. K., Teeradej, N., Lee, Y. O., Cho, Y. K., & Park, C. H. (2006). Pretreatment of sludge with microwaves for pathogen destruction and improved anaerobic digestion performance. *Water Environment Research*, 78(1), 76-83.
- Houghton, J.I., Quarmby, J., Stephenson, T. (2001). Municipal wastewater sludge dewaterability and the presence of microbial extracellular polymer. *Water Science and Technology*, 44(2-3), 373-379.
- Hsieh, C. H., Lo, S. L., Chiueh, P. T., Kuan, W. H., and Chen, C. L. (2007). Microwave-enhanced stabilization of heavy metal sludge. *Journal of Hazardous Materials*, B139, 160–166.
- Jin, Y., Hu, Z., & Wen, Z. (2009). Enhancing anaerobic digestibility and phosphorus recovery of dairy manure through microwave-based thermochemical pretreatment. *Water Research*, 43(14), 3493-3502.
- Karr, P. R., & Keinath, T. M. (1978). Influence of particle size on sludge dewaterability. *Water Pollution Control Federation*, 1911-1930.
- Kenge, A., Liao, P. H., & Lo, K. V. (2009a). Solubilization of municipal anaerobic sludge using microwave-enhanced advanced oxidation process. *Journal of Environmental Science and Health Part A*, 44(5), 502-506.
- Kenge, A., Liao, P.H., and Lo, K.V. (2009b) Factors affecting microwave-enhanced advanced oxidation process for sewage sludge treatment, *Journal of Environmental Science and Health Part A*, 44(11), 1069-1076.
- Kenge, A. A., Liao, P. H., & Lo, K. V. (2009c). Treating solid dairy manure using microwave-enhanced advanced oxidation process. *Journal of Environmental Science and Health, Part B*, 44(6), 606-612.

- Kuroda, A., Takiguchi, N., Gotanda, T., Nomura, K., Kato, J., Ikeda, T., and Ohtake, H. (2002). A simple method to release polyphosphate from activated sludge for phosphorus reuse and recycling. *Biotechnology and Bioengineering*, 78(3), 333-338.
- Lenihan, P., Orozco, A., O'Neill, E., Ahmad, M., Rooney, D., & Walker, G. (2010). Dilute acid hydrolysis of lignocellulosic biomass. *Chemical Engineering Journal*, 156(2), 395-403.
- Liao, P. H., Wong, W. T., & Lo, K. V. (2005a). Release of phosphorus from sewage sludge using microwave technology. *Journal of Environmental Engineering and Science*, 4(1), 77-81.
- Liao, P. H., Wong, W. T., & Lo, K. V. (2005b). Advanced oxidation process using hydrogen peroxide/microwave system for solubilization of phosphate. *Journal of Environmental Science and Health*, 40(9), 1753-1761.
- Liao, P.H., Lo, K.V., Chan, W.I., and Wong, W.T. (2007). Sludge Reduction and Volatile Fatty Acid Recovery using Microwave Advanced Oxidation Process. *Journal of Environmental Science and Health Part A*, 42(5), 633-639.
- Lin, J., Chang, C., & Chang, S. (1997). Enhancement of anaerobic digestion of waste activated sludge by alkaline solubilization. *Bioresource Technology*, 62(3), 85-90.
- Liu, Y. (2003). Chemically reduced excess sludge production in the activated sludge process. *Chemosphere*, 50(1), 1-7.
- Lo, K. V., Chan, W. I., Lo, I. W., & Liao, P. H. (2010). The effects of irradiation intensity on the microwave-enhanced advanced oxidation process. *Journal of Environmental Science and Health Part A*, 45(2), 257-262.
- Lo, K., & Liao, P. (2011). Microwave Enhanced Advanced Oxidation Process Application to Treatment of Dairy Manure. *Microwave Heating*.
- Lo, K. V., Chan, W. W., Yawson, S. K., & Liao, P. H. (2012). Microwave enhanced advanced oxidation process for treating dairy manure at low pH. *Journal of Environmental Science and Health, Part B*, 47(4), 362-367.
- Lo, K.V., Liao, P.H., Srinivasan, A., Bailey, S., and MacSween, J. (2014). Briefing: H₂O₂ Strategy on Microwave Treatment of Sewage Sludge. *Journal of Environmental Engineering and Science*, 9(3), 158-161.
- Lo, K.V., Srinivasan, A., Liao, P.H., and Bailey S. (2015). Microwave Oxidation Treatment of Sludge. *Journal of Environmental Science and Health Part A*, 50(8), 882-889.
- Lo, K.V., Liao, P.H., and Srinivasan, A. (2016). Continuous-flow microwave enhanced oxidation process for treating sewage sludge. *The Canadian Journal of Chemical Engineering*, 94(7), 1285-1294.

- Lo, K. V., Ning, R., de Oliveira, C. K. Y., De Zetter, M., Srinivasan, A., & Liao, P. H. (2017). Application of Microwave Oxidation Process for Sewage Sludge Treatment in a Continuous-Flow System. *Journal of Environmental Engineering*, 143(9), 04017050.
- Lu, H. W., Xiao, S., Le, T., Al-Omari, A., Higgins, M., Boardman, G., & Murthy, S. (2014). Evaluation of Solubilization Characteristics of Thermal Hydrolysis Process. *Proceedings of the Water Environment Federation*, 2014(15), 6312-6336.
- Lumb, C. (1940). Heat Treatment as an Aid to Sludge Dewatering-Ten Months' Full-Scale Operation. *Surveyor*, 98(2550), 287-91.
- Lumb, C. (1951). Heat treatment as an aid to sludge dewatering: ten years' full-scale operation. In *J. Proc. Inst. Sew. Purif*, 1(5).
- MacSween, J.V. (2015). Investigating the microwave-hydrogen peroxide treatment process for potential commercialization (Master's thesis). Retrieved on 16th January 2017 from <https://open.library.ubc.ca/cIRcle/collections/ubctheses>
- Mehdizadeh, S. N., Eskicioglu, C., Bobowski, J., & Johnson, T. (2013). Conductive heating and microwave hydrolysis under identical heating profiles for advanced anaerobic digestion of municipal sludge. *Water Research*, 47(14), 5040-5051.
- Menendez, J.A., Inguanzo, M., and Pis, J. J. (2002). Microwave induced pyrolysis of sewage sludge. *Water Research*, 36(13), 3261-3264.
- Neyens, E., Baeyens, J., Weemaes, M., and De heyder, B. (2002). Advanced biosolids treatment using H₂O₂-oxidation. *Environmental Engineering Science*, 19(1), 27-35.
- Neyens, E., Baeyens, J. (2003). A review of thermal sludge pre-treatment process to improve dewaterability. *Journal of Hazardous Materials* 98 (1-3), 51-67.
- Neyens, E., Baeyens, J., and Creamers, C. (2003a). Alkaline thermal sludge hydrolysis. *Journal of Hazardous Materials* 97(1), 295-314.
- Neyens, E., Baeyens, J., Weemaes, M., De heyder, B. (2003b). Hot acid hydrolysis as a potential treatment of thickened sewage sludge. *Journal of Hazardous Materials*, 98(1-3), 275-293.
- Neyens E, Baeyens J, Dewil R, De heyder B. (2004). Advanced sludge treatment affects extracellular polymeric substances to improve activated sludge dewatering, *Journal of Hazardous Materials*, 106 (2-3), 83-92.
- Ning, R. (2016). An effective microwave system to achieve solid disintegration and nutrient release of sewage sludge (Master's thesis). Retrieved on 23rd August 2016 from <https://open.library.ubc.ca/cIRcle/collections/ubctheses>

- Nkansah-Boadu, F., Srinivasan, A., Liao, P.H., and Lo, K.V. (2015a) Effect of pre-heating on microwave enhanced advanced oxidation process. *Journal of Environmental Engineering Science*, 10(1), 2-9.
- Nkansah-Boadu, F., Srinivasan, A., Liao, P. H., & Lo, K. V. (2015b). Radiofrequency oxidation treatment of separated dairy manure. *Process Biochemistry*, 50(9), 1429-1433.
- Noike, T. L. Y. Y. (1992). Upgrading of anaerobic digestion of waste activated sludge by thermal pretreatment. *Water Science and Technology*, 26(3-4), 857-866.
- Pan, S., Lo, K., Liao, P., & Schreier, H. (2006). Microwave Pretreatment for Enhancement of Phosphorus Release from Dairy Manure. *Journal of Environmental Science and Health, Part B: Pesticides, Food Contaminants, and Agricultural Wastes*, 41(4), 451-458.
- Paul, E., Camacho, P., Lefebvre, and Ginestet, P. (2006a). Organic matter release in low temperature thermal treatment of biological sludge for reduction of excess sludge. *Water Science Technology* 54(5), 59-68.
- Paul, E., Camacho, P., Sperandio, M., & Ginestet, P. (2006b). Technical and Economical Evaluation of a Thermal, and Two Oxidative Techniques for the Reduction of Excess Sludge Production. *Process Safety and Environmental Protection*, 84(4), 247-252.
- Pino-Jelcic, S. A., Hong, S. M., & Park, J. K. (2006). Enhanced Anaerobic Biodegradability and Inactivation of Fecal Coliforms and Salmonella spp. in Wastewater Sludge by Using Microwaves. *Water Environment Research*, 78(2), 209-216.
- Qiao, W, Wan, W, Xun, R, Lu, W, and Yin, K. (2008). Sewage sludge hydrothermal treatment by MW irradiation combined with alkali addition. *Journal of Material Science*, 43(7), 2431-6.
- Qureshi, A., Lo, K. V., & Liao, P. H. (2008). Microwave treatment and struvite recovery potential of dairy manure. *Journal of Environmental Science and Health, Part B*, 43(4), 350-357.
- Remya, N., & Lin, J. G. (2011). Current status of microwave application in wastewater treatment—a review. *Chemical Engineering Journal*, 166(3), 797-813.
- Rocher, M., Goma, G., Pilas Begue, A., Louvel, L., & Rols, J. L. (1999). Towards a reduction in excess sludge production in activated sludge processes: biomass physicochemical treatment and biodegradation. *Applied Microbiology and Biotechnology*, 51(6), 883-890.
- Romero, I., Ruiz, E., Castro, E., & Moya, M. (2010). Acid hydrolysis of olive tree biomass. *Chemical Engineering Research and Design*, 88(5-6), 633-640.
- Rosenfeldt, E. J., Linden, K. G., Canonica, S., & Gunten, U. V. (2006). Comparison of the efficiency of OH radical formation during ozonation and the advanced oxidation processes O₃/H₂O₂ and UV/H₂O₂. *Water Research*, 40(20), 3695-3704.

- Sakai, Y., Fukase, T., Yasui, H., Shibata, M. (1997). An activated sludge process without excess sludge production. *Water Science Technology*, 36(11), 163-170.
- Sanz, J., Lombrana, J. I., De Luis, A. M., Varona, F., & Ortueta, M. (2002). Study and comparison of advanced oxidation techniques in the treatment of contaminated effluents. *Afinidad*, 59(501), 542-552.
- Schuiling, R. D., & Andrade, A. (1999). Recovery of struvite from calf manure. *Environmental Technology*, 20(7), 765-768.
- Srinivasan, A., Nkansah-Boadu, F., Liao, P. H., & Lo, K. V. (2014a). Effects of acidifying reagents on microwave treatment of dairy manure. *Journal of Environmental Science and Health, Part B*, 49(7), 532-539.
- Srinivasan, A., Bailey, S., Macsween, J., Lo, K. V., Koch, F., & Liao, P. H. (2014b). Briefing: A continuous-flow 915-MHz microwave treatment of dairy manure. *Journal of Environmental Engineering and Science*, 9(3), 155-157.
- Srinivasan, A., Young, C., Liao, P. H., & Lo, K. V. (2015). Effect of hydrogen peroxide on radiofrequency-oxidation of dairy manure. *Journal of Environmental Engineering and Science*, 10(2), 40-45.
- Srinivasan, A., Liao, P. H., & Lo, K. V. (2016). Microwave treatment of dairy manure for resource recovery: Reaction kinetics and energy analysis. *Journal of Environmental Science and Health, Part B*, 51(12), 840-846.
- Stuckey, D. C., & McCARTY, P. L. (1978, January). Thermochemical pretreatment of nitrogenous materials to increase methane yield. In *Biotechnol. Bioeng. Symp.:(United States)* (Vol. 8). Stanford Univ., CA.
- Tanaka, S., Kobayashi, T., Kamiyama, K. I., & Bildan, M. L. N. S. (1997). Effects of thermochemical pretreatment on the anaerobic digestion of waste activated sludge. *Water Science and Technology*, 35(8), 209-215.
- The national sewage report card (Number three): Grading the Sewage Treatment of 22 Canadian cities (2004) (A Sierra Legal Defence Fund report) (Rep.). (n.d.). Retrieved on 19th May, 2017 from: http://www.bucksuzuki.org/images/uploads/docs/sewage_report_card_III.pdf
- Thostenson, E. T., & Chou, T. W. (1999). Microwave processing: fundamentals and applications. *Composites Part A: Applied Science and Manufacturing*, 30(9), 1055-1071.
- Tyagi, V.K., and Lo, S.L. (2012). Enhancement in mesophilic aerobic digestion of waste activated sludge by chemically assisted thermal pretreatment method. *Bioresource Technology*, 119, 105-113.
- Tyagi, V.K., and Lo, S.L. (2013). Microwave irradiation: A sustainable way for sludge treatment and resource recovery. *Renewable and Sustainable Energy Review*, 18, 288-305.

- United Nations Environment Programme (UNEP), *Practices In Europe and North America: Waste Disposal Versus Resource Utilisation* (Rep.). (n.d.). Retrieved on 16th May, 2017 from: <http://www.unep.or.jp/ietc/Publications/Freshwater/FMS1/3.asp>
- Vlyssides, A. (2004). Thermal-alkaline solubilization of waste activated sludge as a pre-treatment stage for anaerobic digestion. *Bioresource Technology*, 91(2), 201-206.
- Wang, N., and Wang, P. (2016). Study and application status of microwave in organic wastewater treatment – a review. *Chemical Engineering Journal*, 283, 193-214.
- Wang, Y., Gui, C., Ni, X., Chen, M., and Wei, Y. (2015). Multivariate analysis of sludge disintegration by microwave-hydrogen peroxide pretreatment process. *Journal of Hazardous Materials*, 283, 856-864.
- Wang, Y., Wei, Y., and Liu, J., (2009). Effect of H₂O₂ Dosing Strategy on sludge pretreatment by microwave- H₂O₂ advanced oxidation process. *Journal of Hazardous Materials*, 169(1), 680-684.
- Wilson, C. A., & Novak, J. T. (2009). Hydrolysis of macromolecular components of primary and secondary wastewater sludge by thermal hydrolytic pretreatment. *Water research*, 43(18), 4489-4498.
- Wingren, A., Galbe, M., & Zacchi, G. (2008). Techno-Economic Evaluation of Producing Ethanol from Softwood: Comparison of SSF and SHF and Identification of Bottlenecks. *Biotechnology Progress*, 19(4), 1109-1117.
- Wojciechowska, E. (2005). Application of microwaves for sewage sludge conditioning. *Water Research*, 39(19), 4749-4754.
- Wong, W. T., Chan, W. I., Liao, P. H., & Lo, K. V. (2006a). A hydrogen peroxide/microwave advanced oxidation process for sewage sludge treatment. *Journal of Environmental Science and Health Part A*, 41(11), 2623-2633.
- Wong, W. T., Chan, W. I., Liao, P. H., Lo, K. V., & Mavinic, D. S. (2006b). Exploring the role of hydrogen peroxide in the microwave advanced oxidation process: solubilization of ammonia and phosphates. *Journal of Environmental Engineering and Science*, 5(6), 459-465.
- Wong, W. T., Lo, K. V., & Liao, P. H. (2007). Factors affecting nutrient solubilization from sewage sludge using microwave-enhanced advanced oxidation process. *Journal of Environmental Science and Health Part A*, 42(6), 825-829.
- Wyman, C. E. (1994). Ethanol from lignocellulosic biomass: Technology, economics, and opportunities. *Bioresource Technology*, 50(1), 3-15.
- Xiao, B. Y., & Liu, J. X. (2006). Study on treatment of excess sludge under alkaline condition. *Huan jing ke xue= Huanjing kexue/[bian ji, Zhongguo ke xue yuan huan jing ke xue wei yuan hui" Huan jing ke xue" bian ji wei yuan hui.]*, 27(2), 319-323

- Xiao, Q., Yan, H., Wei, Y., Wang, Y., Zeng, F. and Zeng, X. (2012). Optimization of H₂O₂ dosage in microwave- H₂O₂ process for sludge pretreatment with uniform design method. *Journal of Environmental Sciences*, 24(2), 2060-2067.
- Yawson, S. K., Liao, P., & Lo, K. (2011). Two-Stage Dilute Acid Hydrolysis of Dairy Manure for Nutrient Release, Solids Reduction and Reducing Sugar Production. *Natural Resources*, 2(4), 224-233.
- Yi, W., Lo, K.V. and Mavinic, D.S. (2014) Effects of microwave, ultrasonic and enzymatic treatment on chemical and physical properties of waste-activated sludge, *Journal of Environmental Science and Health Part A*, 49(2), 203-209.
- Yin, G. Q., Liao, P. H., & Lo, K. V. (2008). Sewage sludge treatment using microwave-enhanced advanced oxidation process. *Journal of Environmental Science and Health Part A*, 43(2), 191-201.
- Yin, G., Liao, P. H., & Lo, K. V. (2007). An ozone/hydrogen peroxide/microwave-enhanced advanced oxidation process for sewage sludge treatment. *Journal of Environmental Science and Health Part A*, 42(8), 1177-1181.
- Yu, Y., Chan, W. I., Liao, P. H., & Lo, K. V. (2010a). Disinfection and solubilization of sewage sludge using the microwave enhanced advanced oxidation process. *Journal of hazardous materials*, 181(1), 1143-1147.
- Yu, Y., Lo, I. W., Chan, W. W., Liao, P. H., & Lo, K. V. (2010b). Nutrient release from extracted activated sludge cells using the microwave enhanced advanced oxidation process. *Journal of Environmental Science and Health Part A*, 45(9), 1071-1075.
- Yu, Y., Chan, W.I., Lo, I.W., Liao, P.H., and Lo, K.V. (2010c). Sewage sludge treatment by a continuous microwave enhanced advanced oxidation process. *Journal of Environmental Engineering and Science*, 8(5), 534-540.
- Yu, Y., Lo, I. W., Liao, P. H., & Lo, K. V. (2010d). Treatment of dairy manure using the microwave enhanced advanced oxidation process under a continuous mode operation. *Journal of Environmental Science and Health, Part B*, 45(8), 804-809.
- Zhang, H., Lo, V. K., Thompson, J. R., Koch, F. A., Liao, P. H., Lobanov, S., Atwater, J. W. (2014). Recovery of phosphorus from dairy manure: a pilot-scale study. *Environmental Technology*, 36(11), 1398-1404.
- Zhang, H. (2013). Pilot scale application of microwave technology for dairy manure treatment and nutrient recovery through struvite crystallization (Master's thesis). Retrieved on 26th June 2017 from <https://open.library.ubc.ca/cIRcle/collections/ubctheses>

Appendix A

Waste activated sludge experiments

A.1 Complete data set for 2450 MHz batch-mode MW/H₂O₂-AOP treatment of WAS

Table 12 Solids disintegrated from 2450 MHz batch-mode MW/H₂O₂-AOP treatment of WAS

Sets	Acid/alkali concentration (g/g TS)	pH	TS (%)	TSS (g/L)	SCOD (mg/L)	TCOD (mg/L)	VFA (mg/L)	CST (s)
Set 1 - 110°C, MW/H ₂ O ₂ /pH 4								
Initial	0	6.4	0.9±0	8.6±0.2	265±11	9348±428	21±2.6	131±18
Acid	0.03	4.0	1.0±0	8.3±0.3	346±10	8954±205	24±0.7	188±22
Treated	0.03	3.8	1.0±0	7.3±0.2	2104±15	11493±1178	127±9.3	78±4.9
Set 2 - 110°C, MW/H ₂ O ₂ /pH 9								
Initial	0	6.4	0.9±0	8.6±0.2	265±11	9348±428	20.9±2.6	131±18
Alkaline	0.01	9.1	0.9±0	8.4±0.1	188±37	9015±303	15.2±1.1	126±7.5
Treated	0.01	6.8	0.9±0	6.3±0.4	1865±62	7270±786	99±12.7	756±38
Set 3 - 110°C, MW/H ₂ O ₂								
Initial	0	6.2	1.0±0	9.8±0.1	139±8.9	9791±186	8.8±1.4	88±7.5
Treated	0	6.2	1.0±0	8.0±0.5	1803±156	9097±253	111±13	661±11
Set 4 - 110°C, MW alone								
Initial	0	6.2	1.0±0	9.8±0.1	139±8.9	9791±186	8.8±1.4	88±7.5
Treated	0	6.6	1.1±0	8.8±0.1	1810±51	9584±958	102±25	1162±54
Set 5 - 90°C, MW/H ₂ O ₂ /pH 4								
Initial	0	6.7	0.9±0	9.0±0.2	0±0	8572±140	3.7±0.3	117±6.5
Acid	0.03	4.0	1.0±0	8.7±0.2	3.6±14	8654±348	2.8±0.5	99±4.8
Treated	0.03	4.9	1.0±0	8.5±0.2	1309±30	9031±246	25±5.3	188±39
Set 6 - 90°C, MW/H ₂ O ₂ /pH 9								
Initial	0	6.7	0.9±0	9.0±0.2	0±0	8572±140	3.7±0.3	117±6.5
Alkaline	0.01	9.0	1.0±0	9.1±0.0	140±73	8851±69	4.8±0.7	94±8.1
Treated	0.01	7.1	0.9±0	7.0±0.4	1858±218	9086±259	11±1.9	575±31
Set 7 - 90°C, MW/H ₂ O ₂								
Initial	0	6.7	0.9±0	9.0±0.2	0±0	8572±140	3.7±0.3	117±6.5
Treated	0	6.7	1.0±0	7.4±0.4	1759±457	9874±194	11.1±2.8	534±18
Set 8 - 90°C MW alone								
Initial	0	6.7	0.9±0	9.0±0.2	0±0	8572±140	3.7±0.3	117±6.5
Treated	0	6.6	1.0±0	8.2±0.2	1580±43	9398±529	14±1.4	492±17

Table 13 Nutrients released from 2450 MHz batch-mode MW/H₂O₂-AOP treatment of WAS

Sets	ortho-P (mg/L)	STP (mg/L)	TP (mg/L)	Ammonia (mg/L)	STKN (mg/L)	TKN (mg/L)	Sol Mg (mg/L)	Sol Ca (mg/L)
Set 1 - 110°C, MW/H ₂ O ₂ /pH 4								
Initial	5.7±0.4	6.2±1.6	382±2.9	0.3±0.0	6.3±1.2	701±9.6	1.3±0.4	1.8±1.4
Acid	202±2	231±24	382±5.7	3.1±0.2	28±2.1	706±19	71±8	65±6
Treated	71±3.6	223±80	392±14	12±1.1	145±12	760±10	84±14	47±1.3
Set 2 - 110°C, MW/H ₂ O ₂ /pH 9								
Initial	5.7±0.4	6.2±1.6	382±2.9	0.3±0.01	6.3±1.2	701±9.6	1.3±0.4	1.8±1.4
Alkaline	102±2	85±0.5	398±43	18±0.3	29±3.0	673±26	20±0.1	12±0.8
Treated	59±5.3	269±16	349±5.8	3.8±0.2	200±4.1	675±8.1	69±2.7	28±0.5
Set 3 - 110°C, MW/H ₂ O ₂								
Initial	3.2±0.3	0.3±0	406±5.4	0.1±0	3.9±1.0	641±42	1.4±0.0	5.8±0.1
Treated	79±3.2	295±13	397±6.6	1.9±0.1	170±1.0	597±52	80±2.5	45±8.4
Set 4 - 110°C, MW alone								
Initial	3.2±0.3	0.28±0	406±5.4	0.1±0	3.9±1.0	641±42	1.4±0.0	5.8±0.1
Treated	19±1.4	310±15	420±1.1	0.7±0.1	191±8.7	651±59	83±4.5	57±4.7
Set 5 - 90°C, MW/H ₂ O ₂ /pH 4								
Initial	0.2±0.2	0.8±0.9	375±18	0.4±0.0	2.8±0.4	585±126	1.4±0.1	2.2±1.5
Acid	37±0.8	36±0.7	405±12	1.6±0.1	8.5±0.9	671±15	8.7±0.2	29±0.9
Treated	42±4.8	227±59	404±6.9	5.5±0.1	78±1.8	617±14	88±15	57±19
Set 6 - 90°C, MW/H ₂ O ₂ /pH 9								
Initial	0.2±0.2	0.8±0.9	375±18	0.4±0.0	2.8±0.4	585±126	1.4±0.1	2.2±1.5
Alkaline	10±1.2	15.6±2.6	414±18	1.4±0.1	9.2±0.7	525±56	2.0±0.3	0.9±0.0
Treated	38±1	250±26	413±15	5.2±0.1	166±1.1	640±42	61±6.7	38±8.4
Set 7 - 90°C, MW/H ₂ O ₂								
Initial	0.2±0.2	0.8±0.9	375±18	0.4±0.0	2.8±0.4	585±126	1.4±0.1	2.2±1.5
Treated	35±4.2	217±12	424±13	4.1±0.8	143±5.9	610±17	54±3.5	27±3.5
Set 8 - 90°C MW alone								
Initial	0.2±0.2	0.8±0.9	375±18	0.4±0.0	2.8±0.4	585±126	1.4±0.1	2.2±1.5
Treated	32±5.7	208±25	449±2.3	3.6±0.3	204±80	591±46	50±6.1	24±4.4

Table 14 Particle size distribution of WAS from 2450 MHz batch-mode MW/H₂O₂-AOP treatment

Sets	D10 (μ, vol%)	D50 (μ, vol%)	D90 (μ, vol%)
Set 1 - 110°C, MW/H ₂ O ₂ /pH 4			
Raw Set 1	9.02±0.12	27.88±0.24	65.03±1.25
Acidified Set 1	8.01±0.13	24.59±0.54	63.28±1.47
Treated Set 1	9.99±0.24	35.15±0.58	95.2±2.5
Set 2 -110°C, MW/H ₂ O ₂ /pH 9			
Raw Set 2	9.02±0.12	27.88±0.24	65.03±1.25
Alkaline Set 2	9±0.04	28.11±0.14	64.71±0.29
Treated Set 2	8.94±0.37	35.92±1.85	152.17±10.87
Set 3 - 110°C, MW/H ₂ O ₂			
Raw Set 3	8.76±0.1	25.41±0.15	62.05±0.58
Treated Set 3	8.31±0.11	29.43±0.6	110.86±7.03
Set 4 - 110°C, MW alone			
Raw Set 4	8.76±0.1	25.41±0.15	62.05±0.58
Treated Set 4	7.51±0.06	25.6±0.18	69.79±1.85
Set 5 - 90°C, MW/H ₂ O ₂ /pH 4			
Raw Set 5	9.66±0.08	26.79±0.18	68.2±1.41
Acidified Set 5	9.66±0.1	26.82±0.16	69.67±0.65
Treated Set 5	8.46±0.28	24.86±0.4	65.9±0.91
Set 6 - 90°C, MW/H ₂ O ₂ /pH 9			
Raw Set 6	9.66±0.08	26.79±0.18	68.2±1.41
Alkaline Set 6	9.61±0.03	27.14±0.08	68.19±0.31
Treated Set 6	8.53±0.06	25.62±0.13	70.66±0.55
Set 7 - 90°C, MW/H ₂ O ₂			
Raw Set 7	9.66±0.08	26.79±0.18	68.2±1.41
Treated Set 7	8.5±0.03	25.61±0.08	72.07±0.97
Set 8 - 90°C MW alone			
Raw Set 8	9.66±0.08	26.79±0.18	68.2±1.41
Treated Set 8	8.81±0.04	25.71±0.04	69.3±0.26

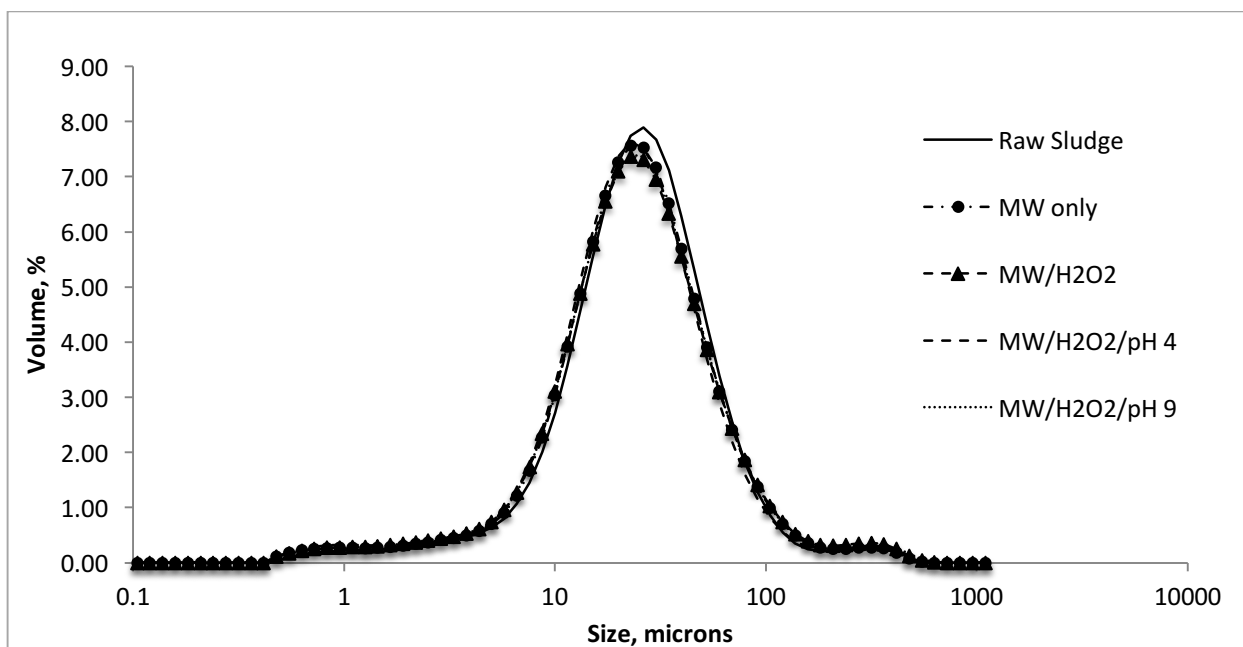


Figure 23 Particle size distribution of WAS from 2450 MHz batch-mode MW/H₂O₂-AOP treatment at 90°C

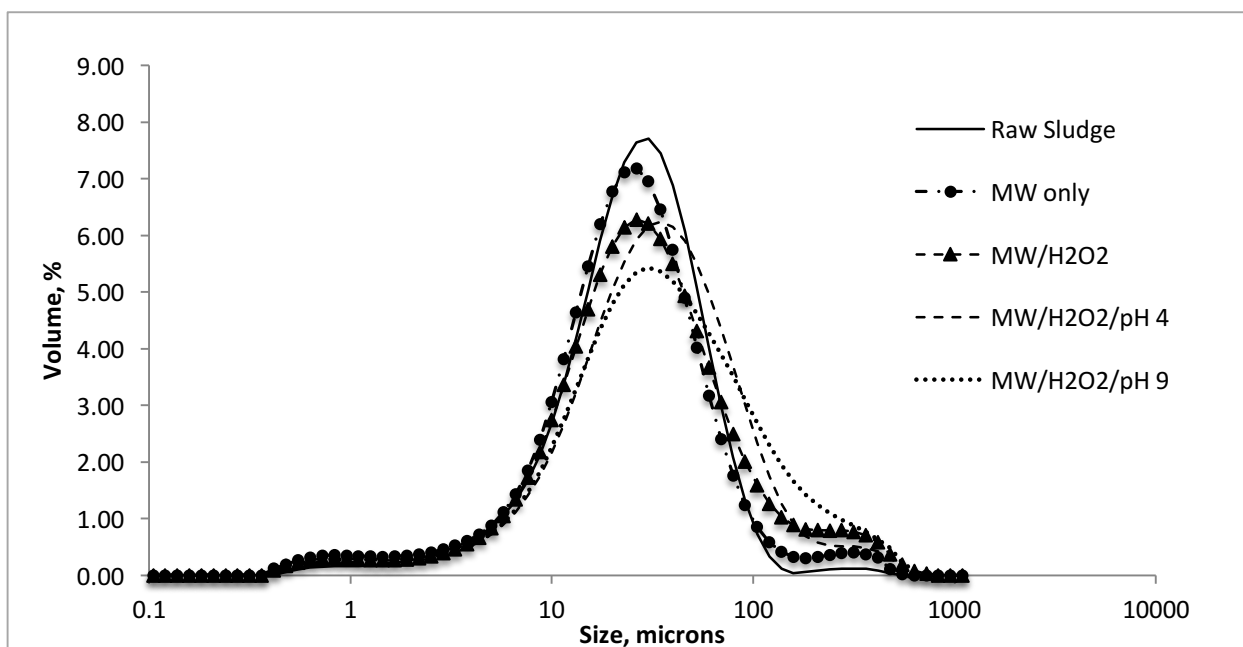


Figure 24 Particle size distribution of WAS from 2450 MHz batch-mode MW/H₂O₂-AOP treatment at 110°C

A.2 Complete data set for 915 MHz pilot-scale MW/H₂O₂-AOP treatment of WAS

Table 15 Solids disintegrated from 915 MHz pilot-scale MW/H₂O₂-AOP treatment of WAS

Sets	pH	TS (%)	TSS (g/L)	SCOD (mg/L)	TCOD (mg/L)	VFA (mg/L)
110°C, MW/H ₂ O ₂ /pH 4 (0.8%H ₂ O ₂ / %TS)						
Raw	6.4	1.0±0.2	8.9±0.0	140±139	9789±2787	7.1±0.2
Acidified	4.0	1.0±0	8.3±0.7	135±17	10277±965	7.8±0.9
Treated	3.0	0.6±0	1.9±0.1	5867±417	9654±3147	482±29
110°C, MW/H ₂ O ₂ /pH 9 (0.6%H ₂ O ₂ / %TS)						
Raw	6.1	0.9±0.1	9.6±0.1	82±18	9744±1452	8±1.2
Alkaline	9.1	1.0±0.1	9.1±0.0	174±17	11517±105	12±4.4
Treated	3.8	0.7±0	1.8±0.1	6030±143	7909±251	415±10
90°C, MW/H ₂ O ₂ /pH 4 (0.6%H ₂ O ₂ / %TS)						
Raw	6.4	1.1±0	10±0.1	67±36	8852±361	3.6±0.7
Acidified	4.3	1.1±0	9.7±0.2	200±129	9323±201	4.2±2.7
Treated	3.2	0.6±0.1	1.9±0.2	5152±22	10042±850	231±8.5
90°C, MW/H ₂ O ₂ /pH 9 (0.6%H ₂ O ₂ / %TS)						
Raw	6.2	0.9±0	8.7±0.1	67±21	9093±1223	5.4±0.2
Alkaline	9.0	0.9±0	8.1±0.4	162±28	9536±84	9.9±1.6
Treated	4.2	0.6±0.1	2.4±0.1	5423±353	8622±410	239±10
110°C, MW/H ₂ O ₂ (0.8%H ₂ O ₂ / %TS) ^a						
Initial	6.1	1.0±0	10.5±0.2	29±14	10745±134	4.7±1.2
Treated	3.9	0.7±0	2.3±0.1	4330±387	7070±272	509±4.2
110°C, MW alone ^b						
Initial	-	1.5±0	8.6±0.03	108±3	9880±70	3±1
Treated	-	1.2±0	5.8±0	2982±8	9900±200	21±2
90°C, MW/H ₂ O ₂ (0.6%H ₂ O ₂ / %TS) ^a						
Raw	6.1	1.3±0	13±0.1	65±38	11911±59	5.3± 0.9
Treated	4.0	0.9±0	3±0.2	6803±566	9575±533	333±13
90°C, MW alone ^c						
Raw	6.9	0.8±0	7.7±0.2	53±7	8493±216	1.1±0.1
Treated	7.1	0.7±0	5.8±0	1591±101	8394±149	25±0.8

Note: - data is not available; ^a is from Lo et al. (2017); ^b is from MacSween (2015); and ^c is from Lo et al. (2016).

Table 16 Nutrients released from 915 MHz pilot-scale MW/H₂O₂-AOP treatment of WAS

Sets	ortho-P (mg/L)	STP (mg/L)	TP (mg/L)	Ammonia (mg/L)	STKN (mg/L)	TKN (mg/L)	Sol Mg (mg/L)	Sol Ca (mg/L)
110°C, MW/H ₂ O ₂ /pH 4 (0.8%H ₂ O ₂ /‰TS)								
Raw	23±0.4	19±1.5	455±6.8	16±1.1	4.9±0.7	683±14	2.4±0.3	8.7±0.9
Acidified	74±0.6	95±3.8	459±2.0	23±0.7	13±0.5	683±51	17±0.6	43±1.8
Treated	239±8	353±4.3	426±18	406±10	515±15	584±62	77±0.9	69±0.8
110°C, MW/H ₂ O ₂ /pH 9 (0.6%H ₂ O ₂ /‰TS)								
Raw	39±0.4	37±1.2	451±3.2	30±0.4	6.3±1.3	758±21	3.6±0.2	12±0.9
Alkaline	84±0.9	90±2.9	484±43	44±0.6	31±1.5	745±19	7.5±0.3	16±1.5
Treated	183±2.6	402±51	430±9.1	395±9.4	596±22	702±14	81±3.9	59±1.1
90°C, MW/H ₂ O ₂ /pH 4 (0.6%H ₂ O ₂ /‰TS)								
Raw	31±0.6	31±0.4	490±36	21±2.2	6.1±1	685±39	3.2±0.2	12±0.5
Acidified	78±1.4	98±1.5	484±14	31±1.4	12±2.8	789±53	16±0.9	49±1.4
Treated	114±1.3	241±6.3	343±16	169±3.2	237±15	389±28	70±6.6	52±3.2
90°C, MW/H ₂ O ₂ /pH 9 (0.6%H ₂ O ₂ /‰TS)								
Raw	36±1.1	30±7.9	381±22	24±1.1	4.9±0.1	662±38	3.5±0.1	14±0.8
Alkaline	118±1.2	121±4.4	414±25	79±4.7	35±0.7	673±20	15±0.8	20±0.6
Treated	122±2.9	271±5	341±17	192±4.1	384±11	572±10	59±1.5	46±1.1
110°C, MW/H ₂ O ₂ (0.8%H ₂ O ₂ /‰TS) ^a								
Raw	4.1±0.1	21±1.3	415±71	2.5±0.1	11±0.4	762±29	2.9±0.1	7.1± 0.2
Treated	237±3.6	341±23	405±70	128±1.8	413±71	733±50	87±5.2	95± 7.3
110°C, MW alone ^b								
Raw	0.04±0.0	2.1±0.1	230±30	0.2±0.0	0±0	410±60	1.6±0.1	25±6
Treated	103±1	120±10	230±40	7.2±0.0	140±40	430±70	26±0.1	22±2
90°C, MW/H ₂ O ₂ (0.6%H ₂ O ₂ /‰TS) ^a								
Raw	5.8±0.1	26±1.0	538±44	4.6 ± 0.1	12±0.8	752±68	3.2±0.1	8±0.5
Treated	164±2.9	322±15	433±20	41.2 ± 1.1	459±50	666±50	79±0.2	73± 0.6
90°C, MW alone ^c								
Raw	5±0.2	7±0.2	371±18	0.5±0	12±0.9	675±46	-	-
Treated	47±1	188±0.7	345±17	4.6±0.1	134±11	755±23	44±0.6	32±0.2

Note: - data is not available; ^a is from Lo et al. (2017); ^b is from MacSween (2015); and ^c is from Lo et al. (2016).

Table 17 Particle size distribution of WAS from 915 MHz pilot-scale MW/H₂O₂-AOP treatment sets

Sets	D10 (μ, vol%)	D50 (μ, vol%)	D90 (μ, vol%)	CST (s)
110°C, MW/H ₂ O ₂ /pH 4 (0.8%H ₂ O ₂ /‰TS)				
Raw	8.12±0.2	23.13±0.44	50.81±1.57	69±3.4
Acidified	8.62±0.14	24.01±0.3	54.25±0.96	54±7.4
Treated	6.57±0.14	20.61±0.39	53.49±1.68	11±0.4
110°C, MW/H ₂ O ₂ /pH 9 (0.6%H ₂ O ₂ /‰TS)				
Raw	8.96±0.04	25.14±0.18	55.48±0.98	59±1.6
Alkaline	9.05±0.04	25.28±0.15	55.43±0.66	105±5.0
Treated	6.74±0.31	19.92±1.01	60.77±6.13	13±0.6
90°C, MW/H ₂ O ₂ /pH 4 (0.6%H ₂ O ₂ /‰TS)				
Raw	8.32±0.16	23.55±0.39	53.37±1.02	75±0.2
Acidified	8.36±0.15	23.52±0.37	53.35±0.8	58±1.6
Treated	9.89±0.17	30.55±0.32	79.99±0.67	16±0.6
90°C, MW/H ₂ O ₂ /pH 9 (0.6%H ₂ O ₂ /‰TS)				
Raw	8.97±0.1	25.15±0.25	55.22±2.03	51±2.7
Alkaline	9.34±0.06	25.68±0.04	54.53±0.09	79±6.9
Treated	4.71±0.08	20.37±0.45	55.8±1.26	68±14
110°C, MW/H ₂ O ₂ (0.8%H ₂ O ₂ /‰TS) ^a				
Raw	-	-	-	82±8.5
Treated	-	-	-	10±0.2
90°C, MW/H ₂ O ₂ (0.6%H ₂ O ₂ /‰TS) ^a				
Raw	-	-	-	96±7.5
Treated	-	-	-	28±1.5
90°C, MW alone ^c				
Raw	-	-	-	42±1.3
Treated	-	-	-	350±36

Note: - data is not available; ^a is from Lo et al. (2017) and ^c is from Lo et al. (2016).

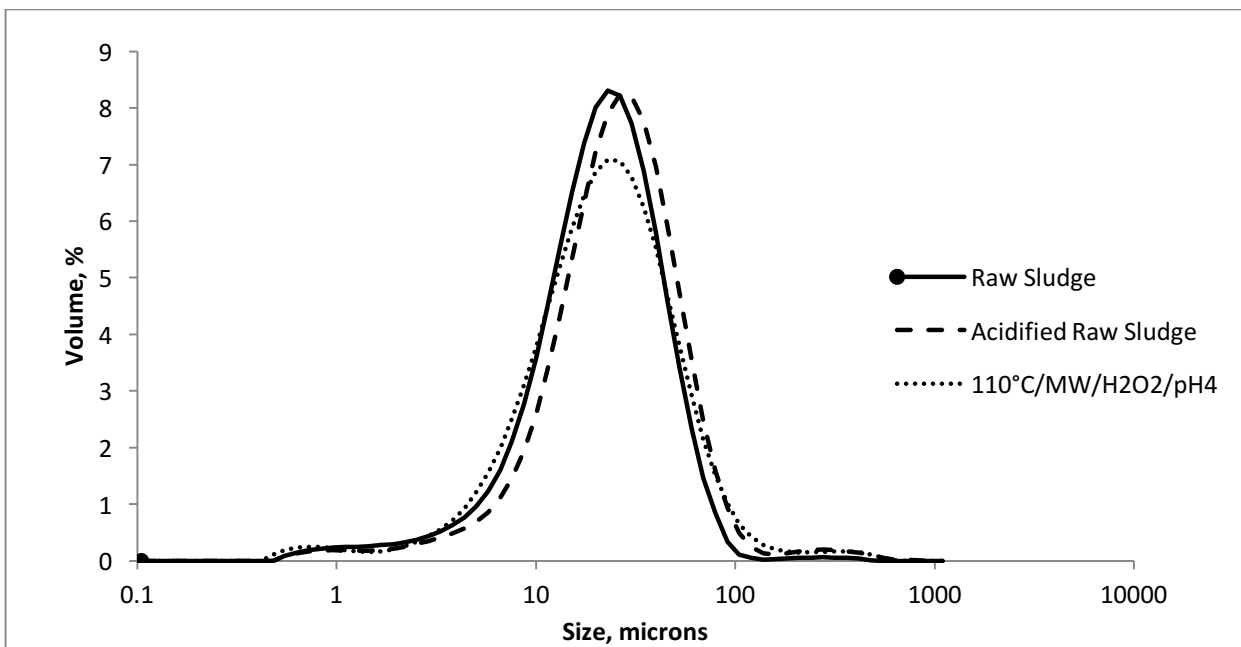


Figure 25 Particle size distribution of WAS from 915 MHz pilot-scale MW/H₂O₂-AOP treatment at 110°C/pH4

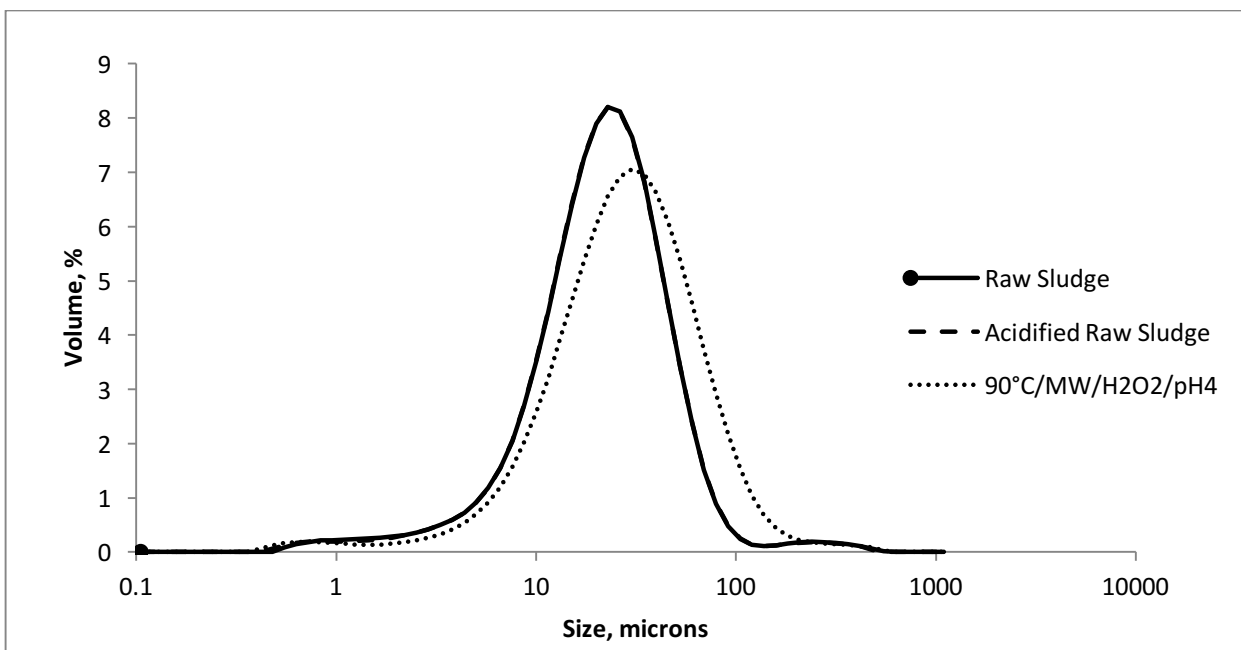


Figure 26 Particle size distribution of WAS from 915 MHz pilot-scale MW/H₂O₂-AOP treatment at 90°C/pH4

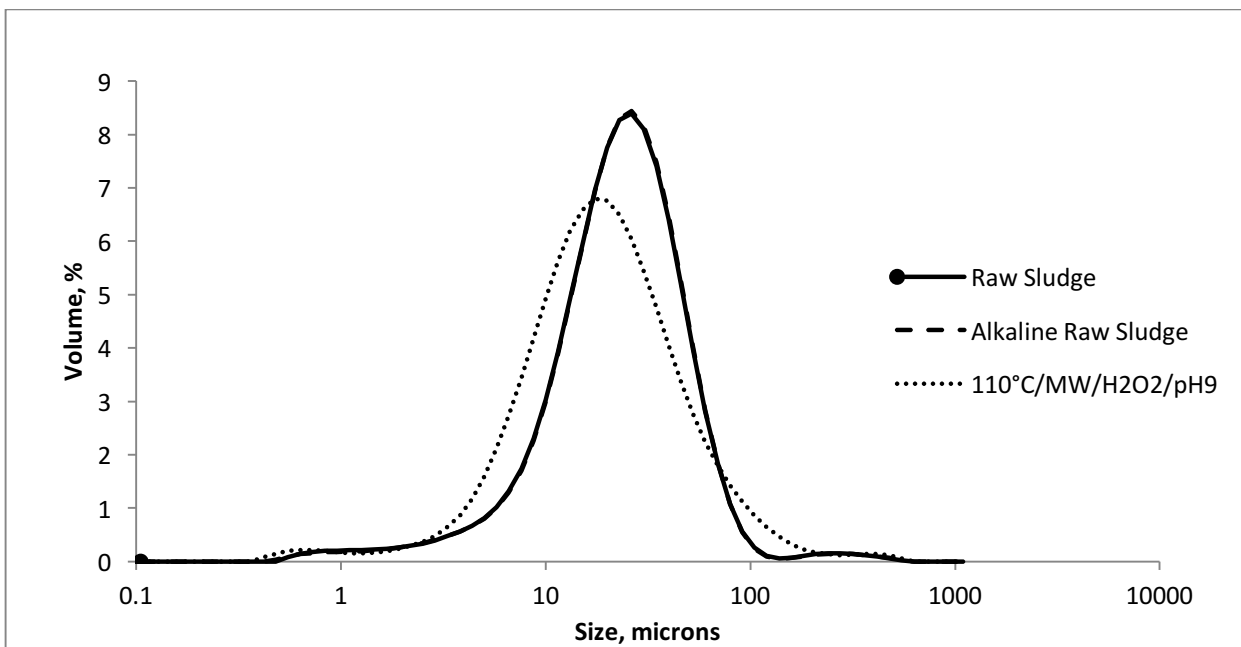


Figure 27 Particle size distribution of WAS from 915 MHz pilot-scale MW/H₂O₂-AOP treatment at 110°C/pH9

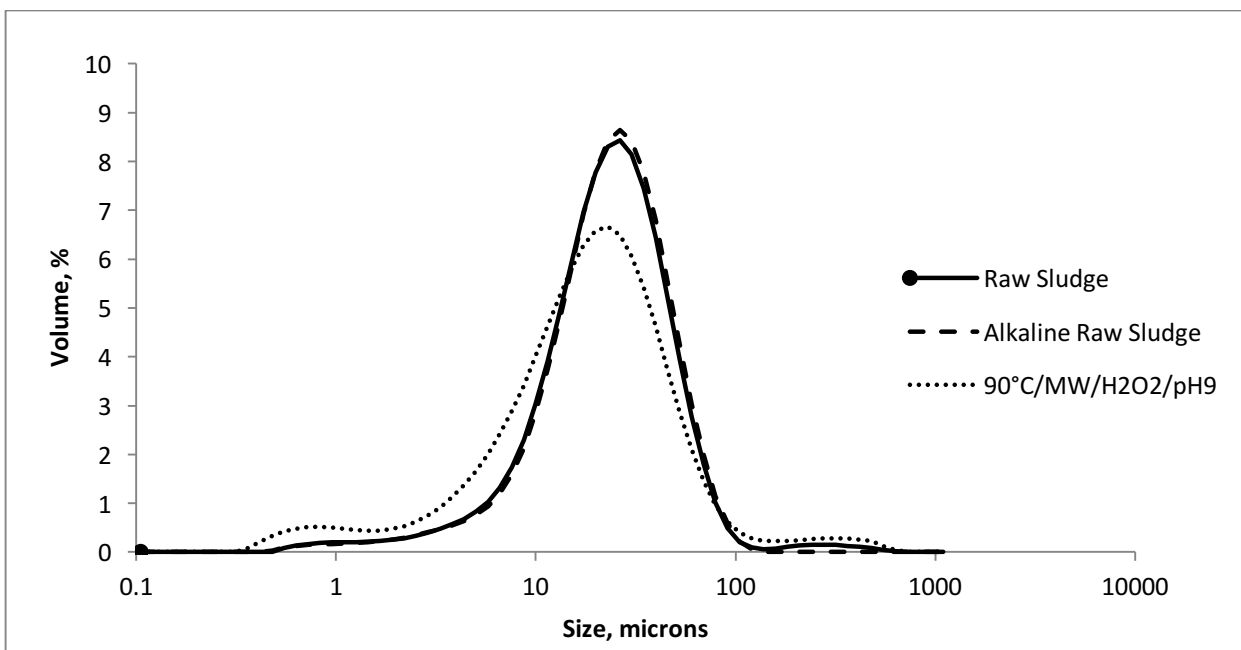


Figure 28 Particle size distribution of WAS from 915 MHz pilot-scale MW/H₂O₂-AOP treatment at 90°C/pH9

Appendix B
Salt water experiments

B.1 10 g/L salt concentration comparison graphs

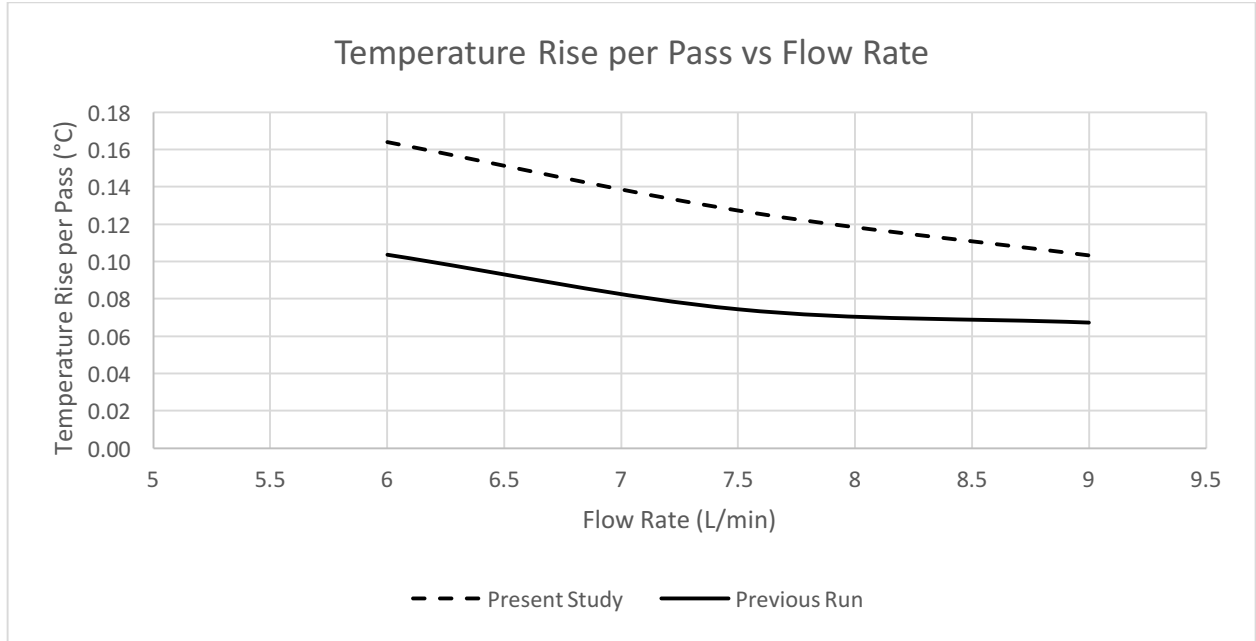


Figure 29 Temperature rise per pass vs flow rate for 10 gNaCl/L

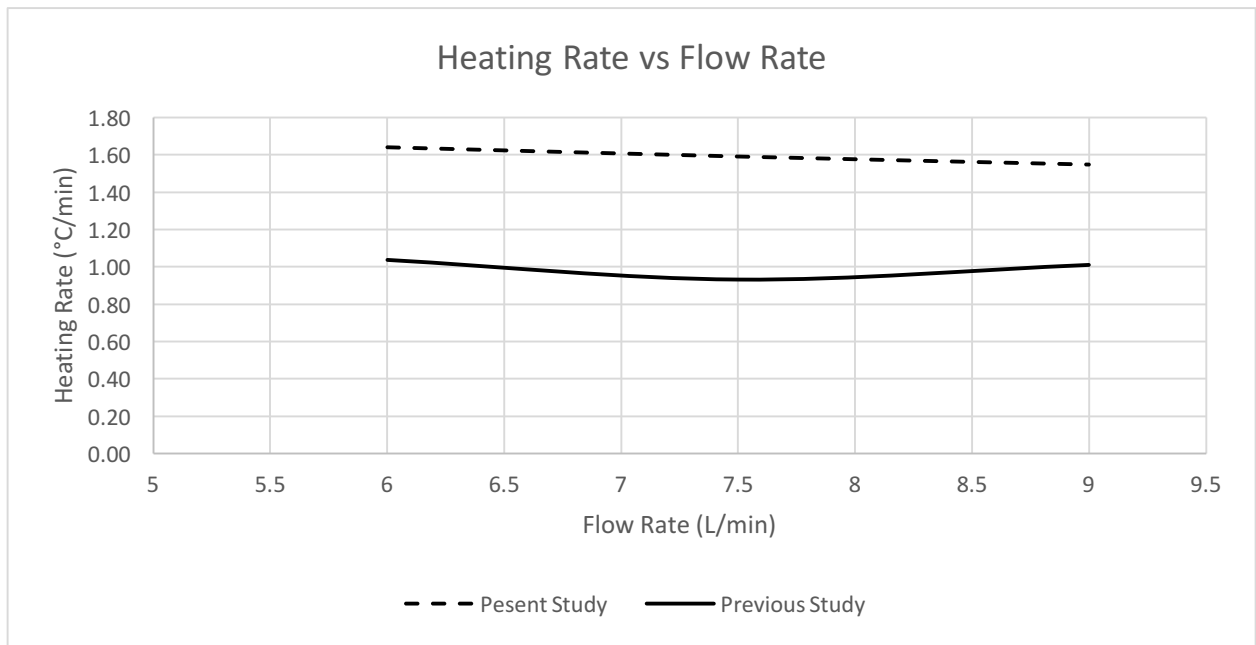


Figure 30 Heating rate vs flow rate for 10 gNaCl/L

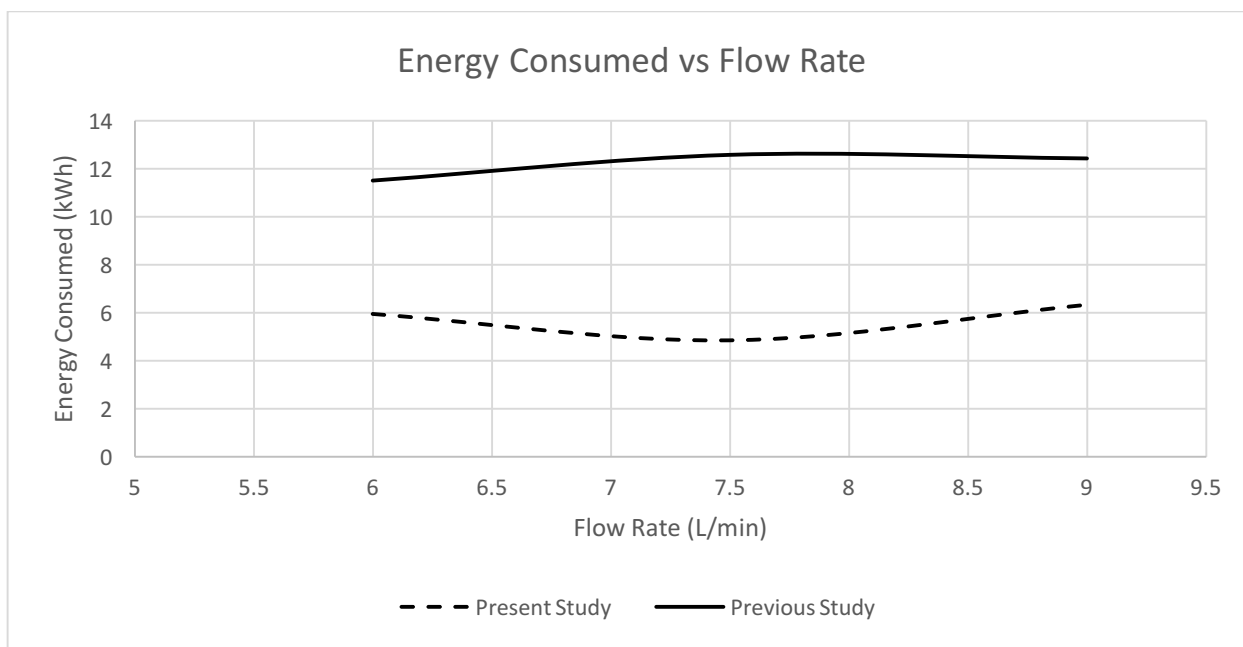


Figure 31 Energy consumed vs flow rate for 10 gNaCl/L

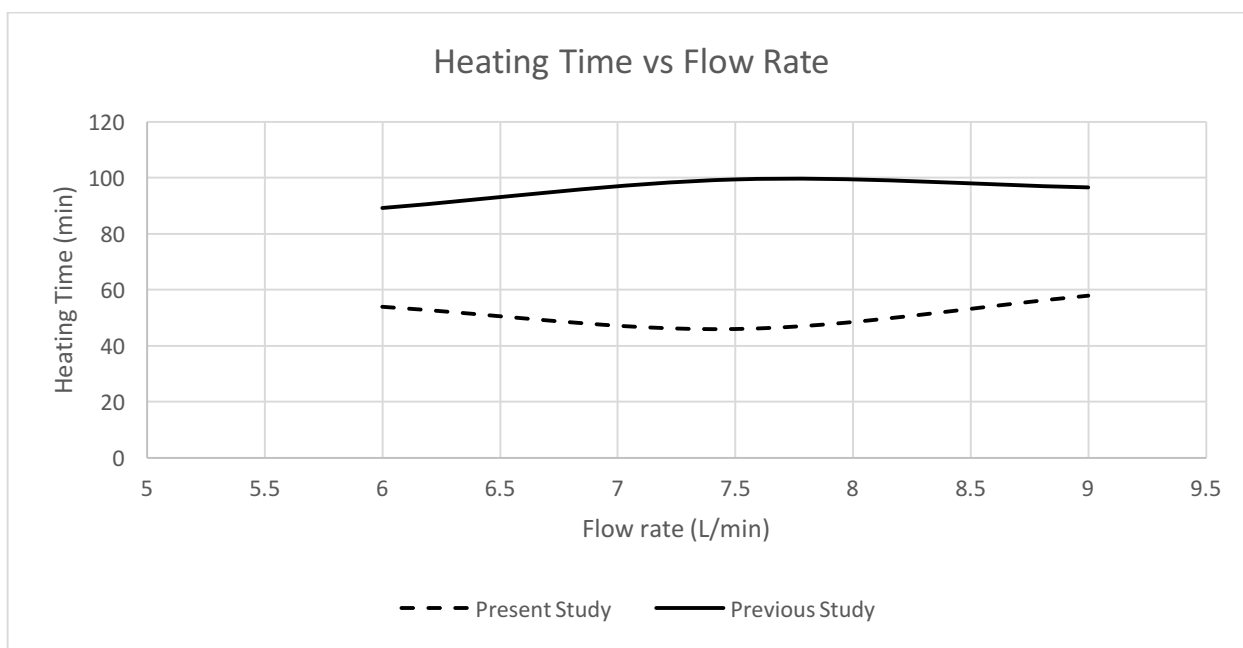


Figure 32 Heating time vs flow rate for 10 gNaCl/L

B.2 Graphical presentation of temperature rise per pass in response to flow rate/salt concentration

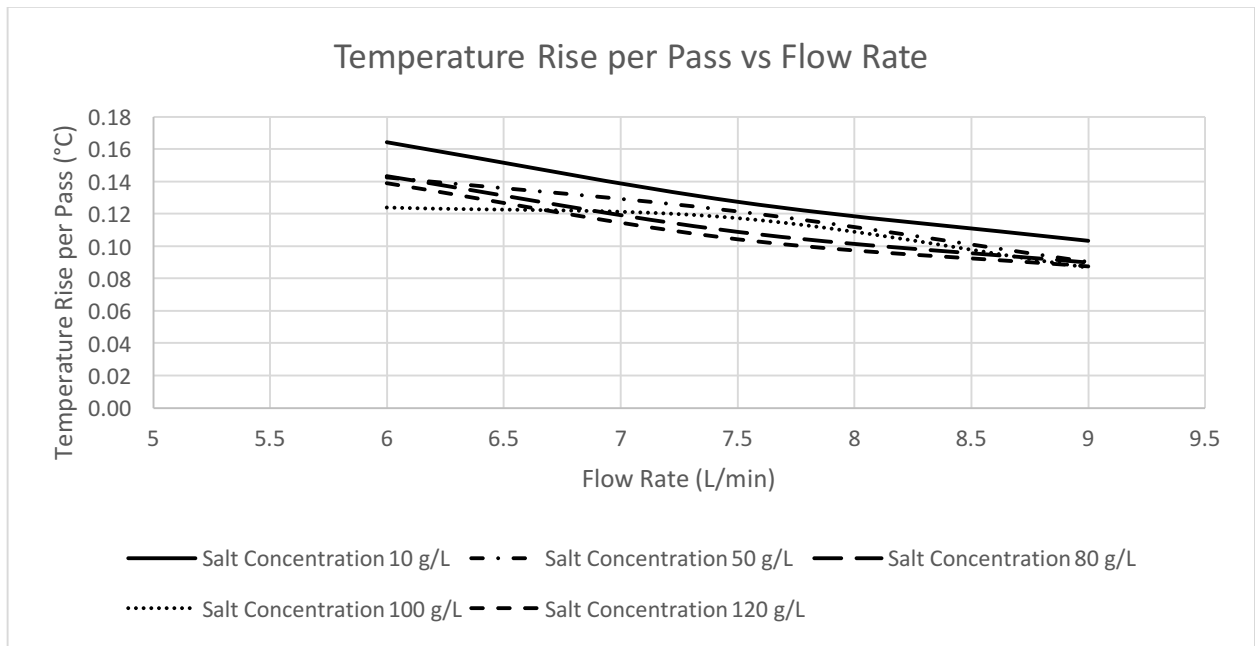


Figure 33 Temperature rise per pass vs flow rate for different salt concentrations

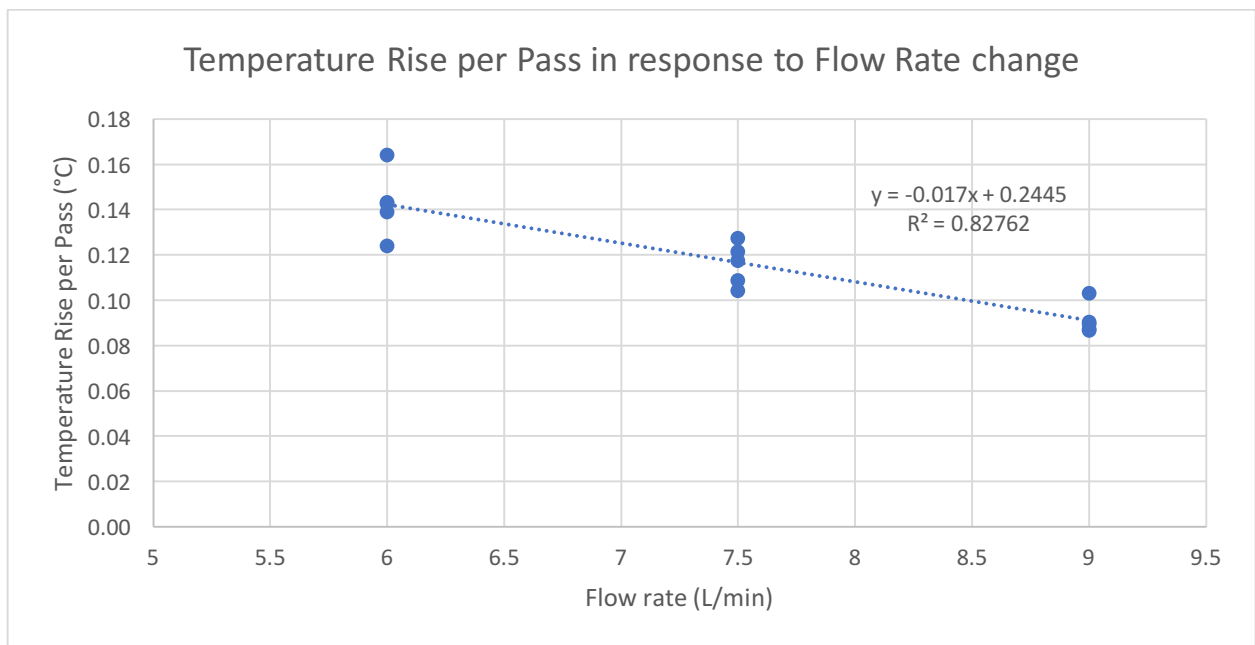


Figure 34 Temperature rise per pass in response to flow rate

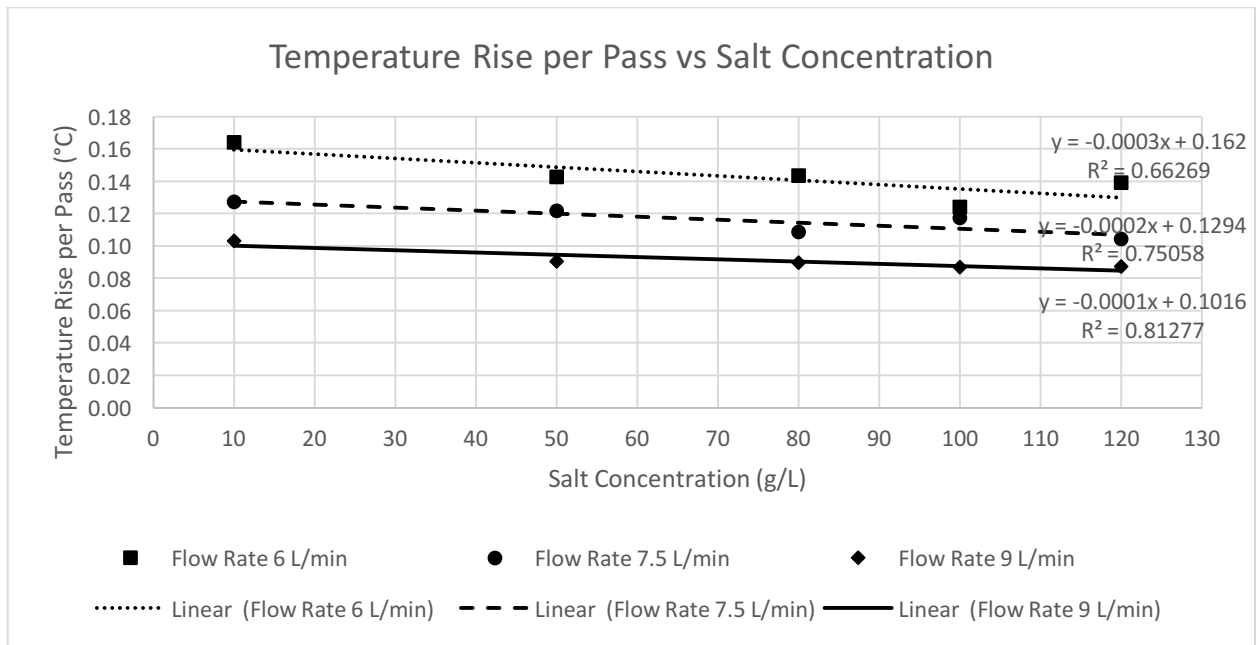


Figure 35 Temperature rise per pass vs salt concentration for different flow rates

B.3 Graphical presentation of heating rate in response to flow rate/salt concentration

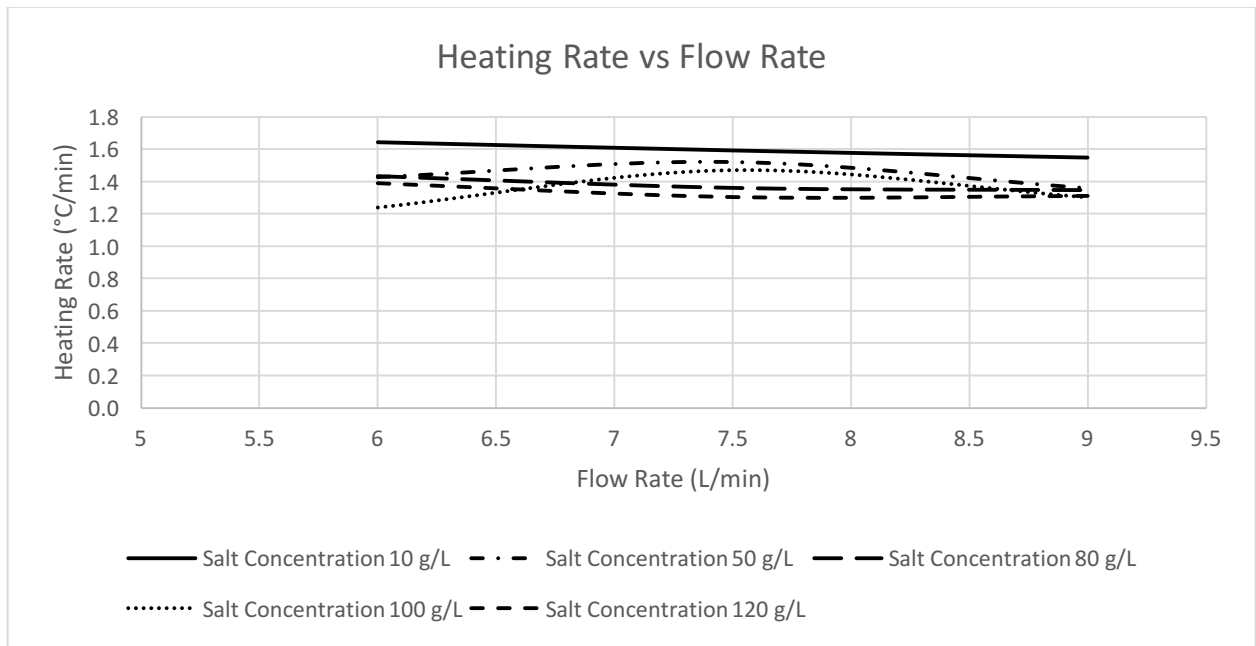


Figure 36 Heating rate vs flow rate for different salt concentrations

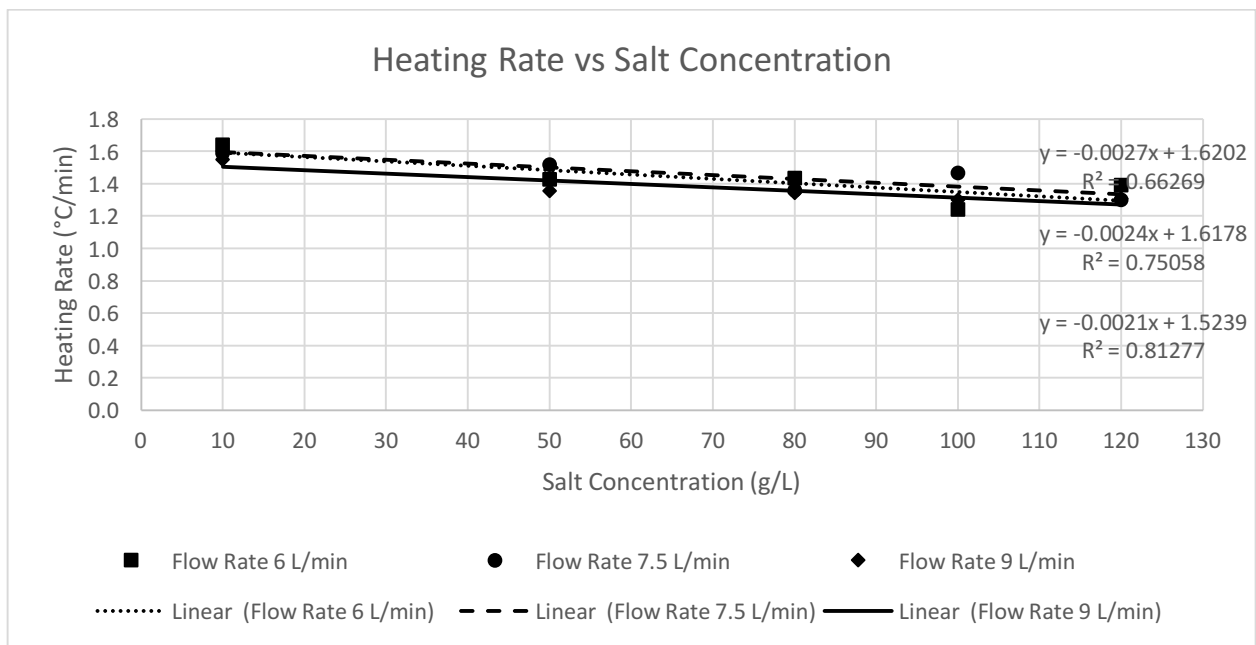


Figure 37 Heating rate vs salt concentration for different flow rates

B.4 Graphical presentation of power consumption in response to flow rate/salt concentration

concentration

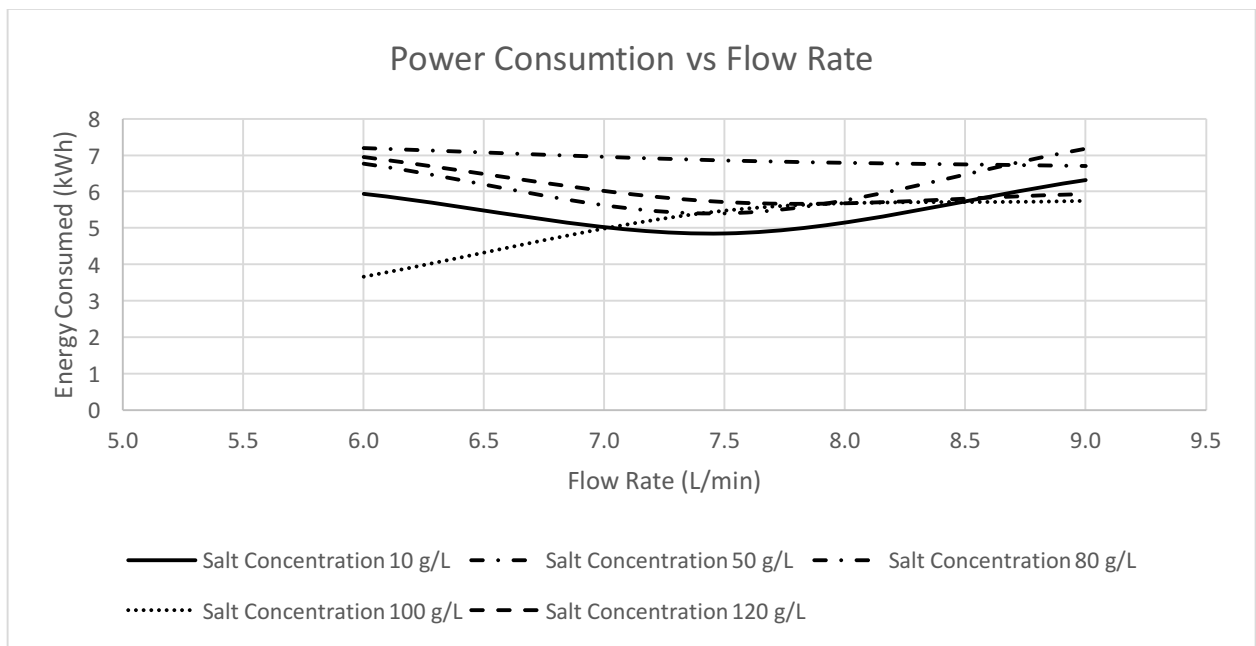


Figure 38 Energy consumed vs flow rate for different salt concentrations

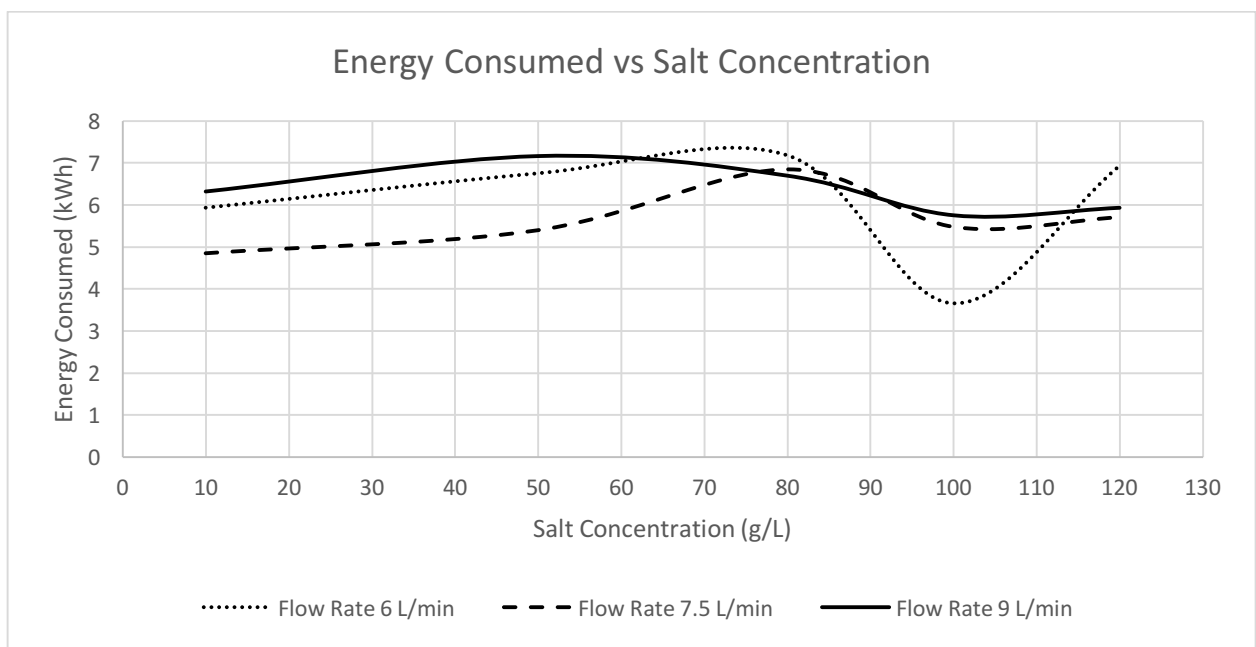


Figure 39 Energy consumed vs salt concentration for different flow rates

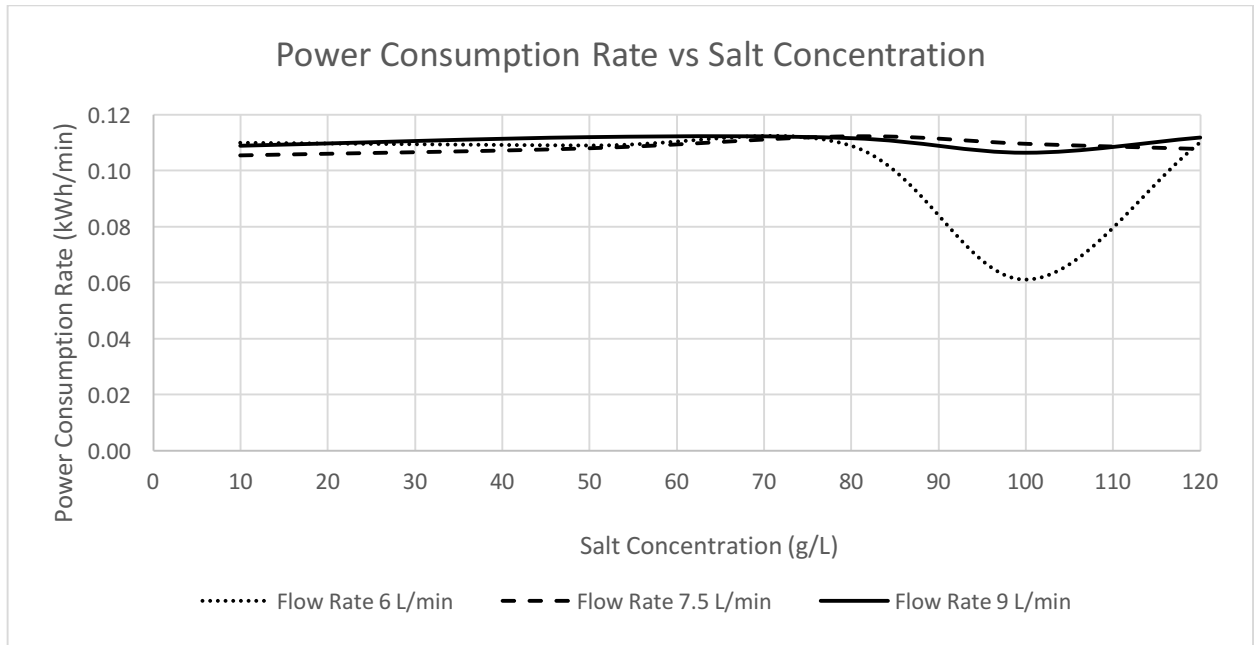


Figure 40 Power consumption rate vs salt concentration for different flow rates

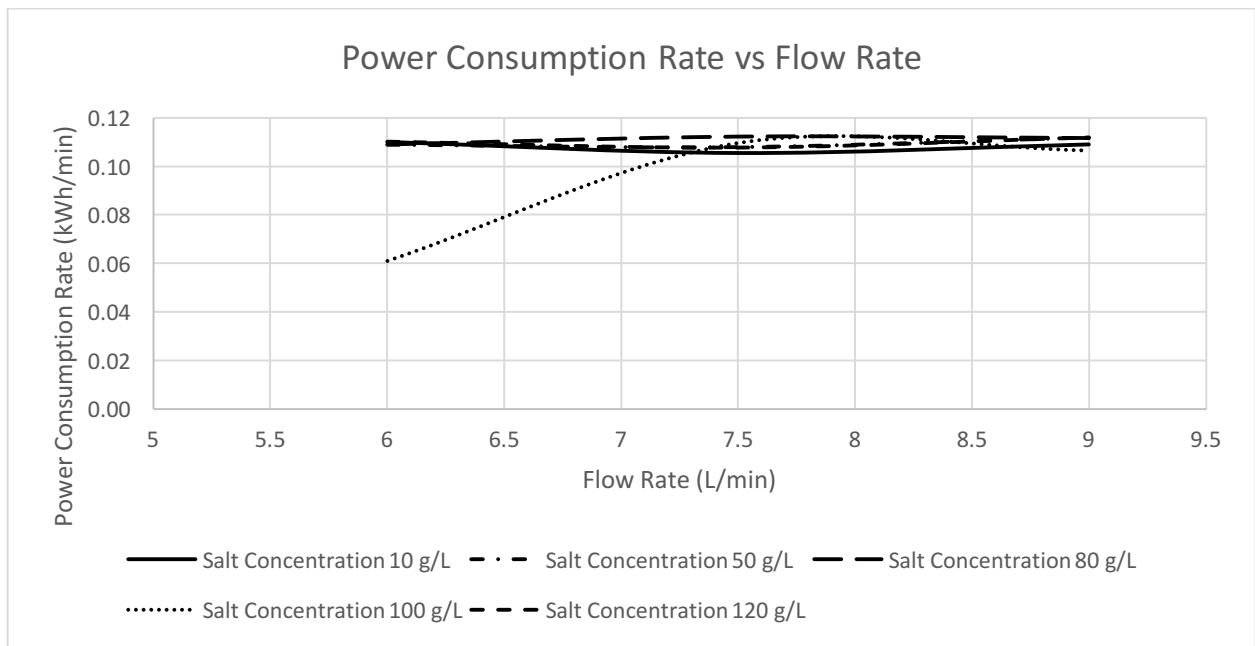


Figure 41 Power consumption rate vs flow rate for different salt concentrations

B.5 Energy absorption in response to flow rate/salt concentration

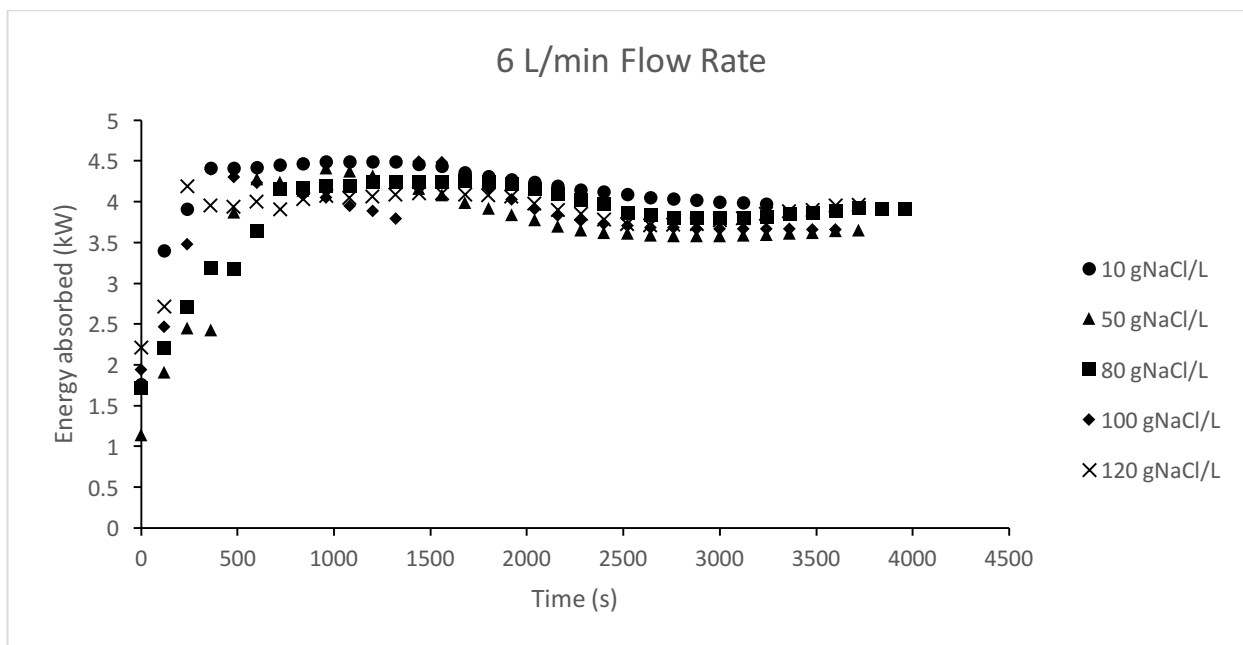


Figure 42 Energy absorbed vs treatment time for 6 L/min flow rate at different salt concentrations

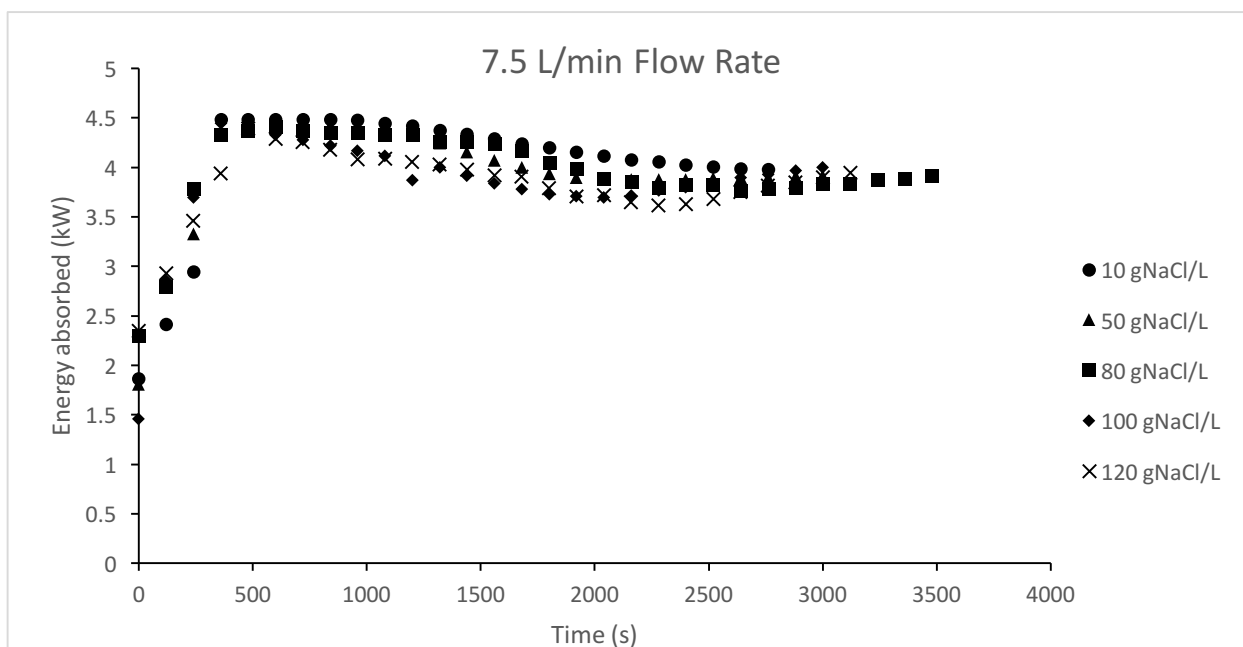


Figure 43 Energy absorbed vs treatment time for 7.5 L/min flow rate at different salt concentrations

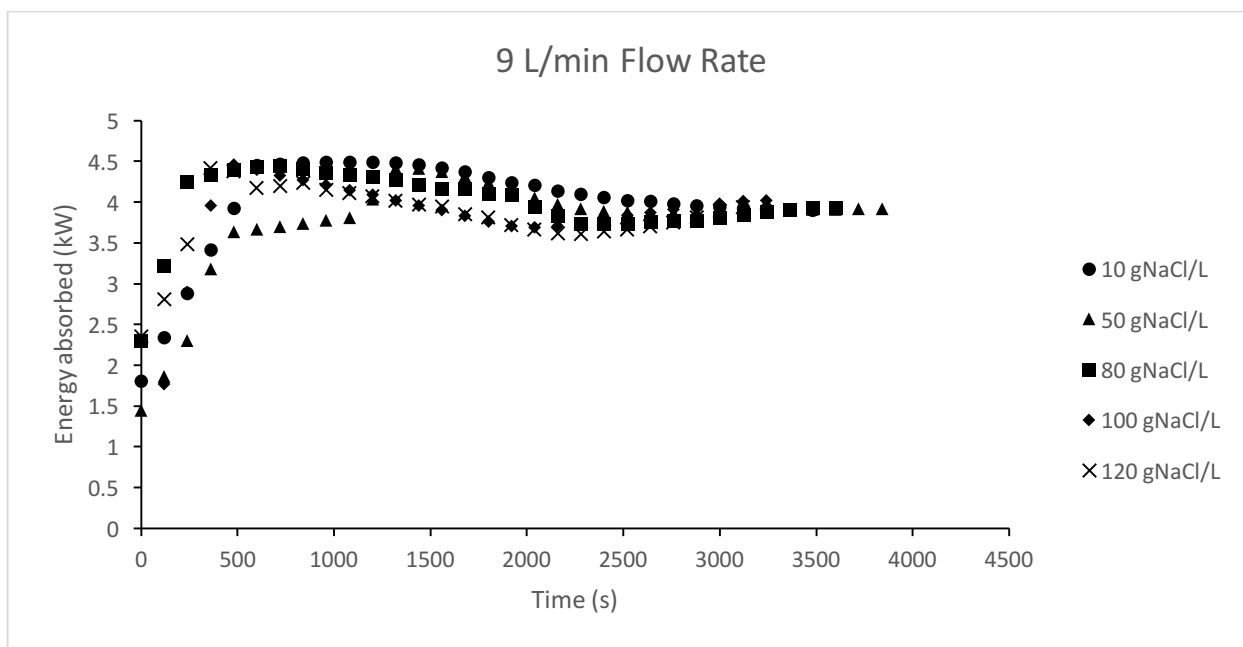


Figure 44 Energy absorbed vs treatment time for 9 L/min flow rate at different salt concentrations

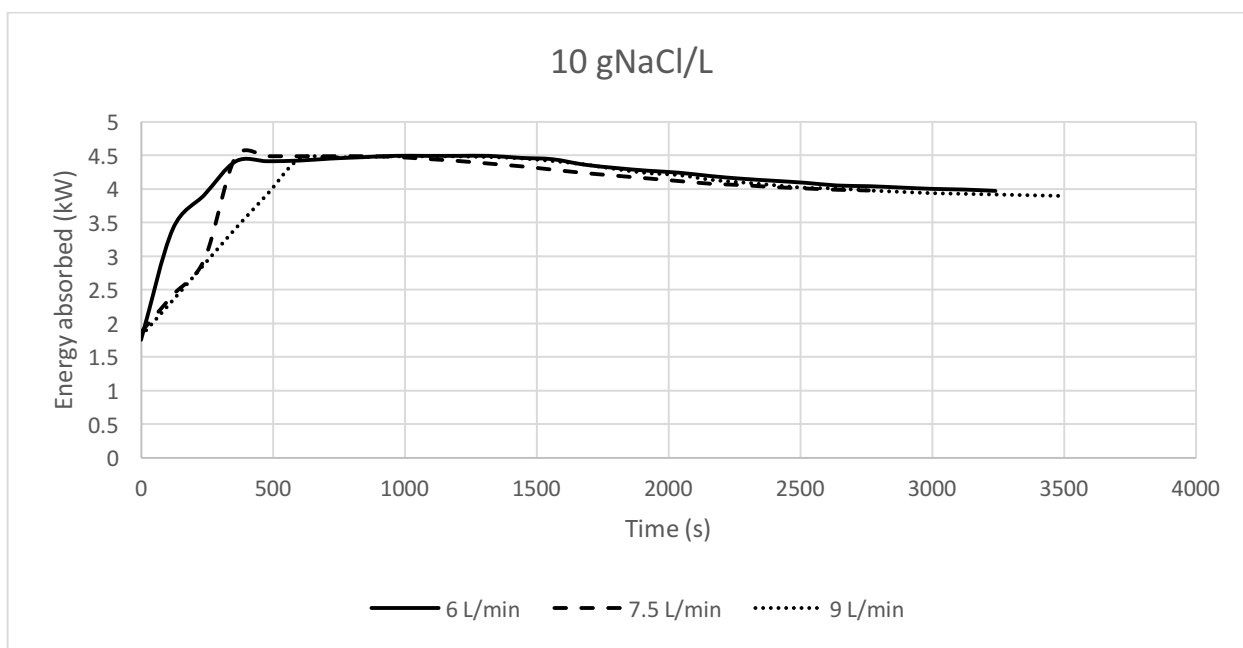


Figure 45 Energy absorbed vs treatment time for 10 gNaCl/L at different flow rates

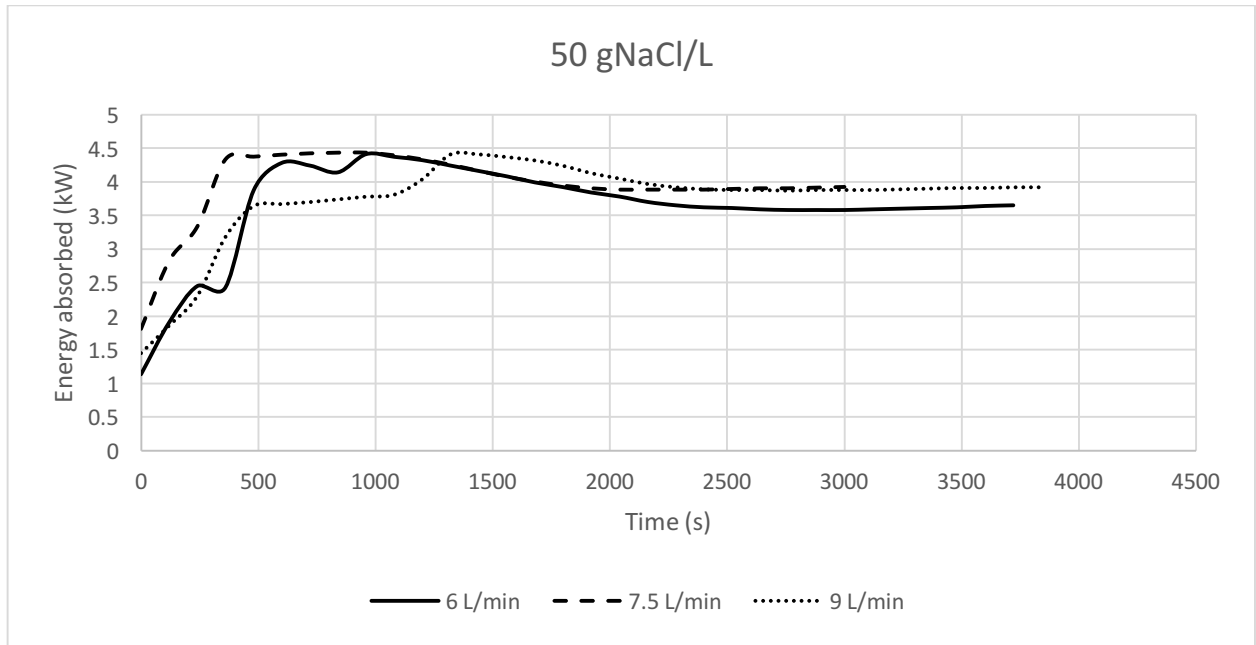


Figure 46 Energy absorbed vs treatment time for 50 gNaCl/L at different flow rates

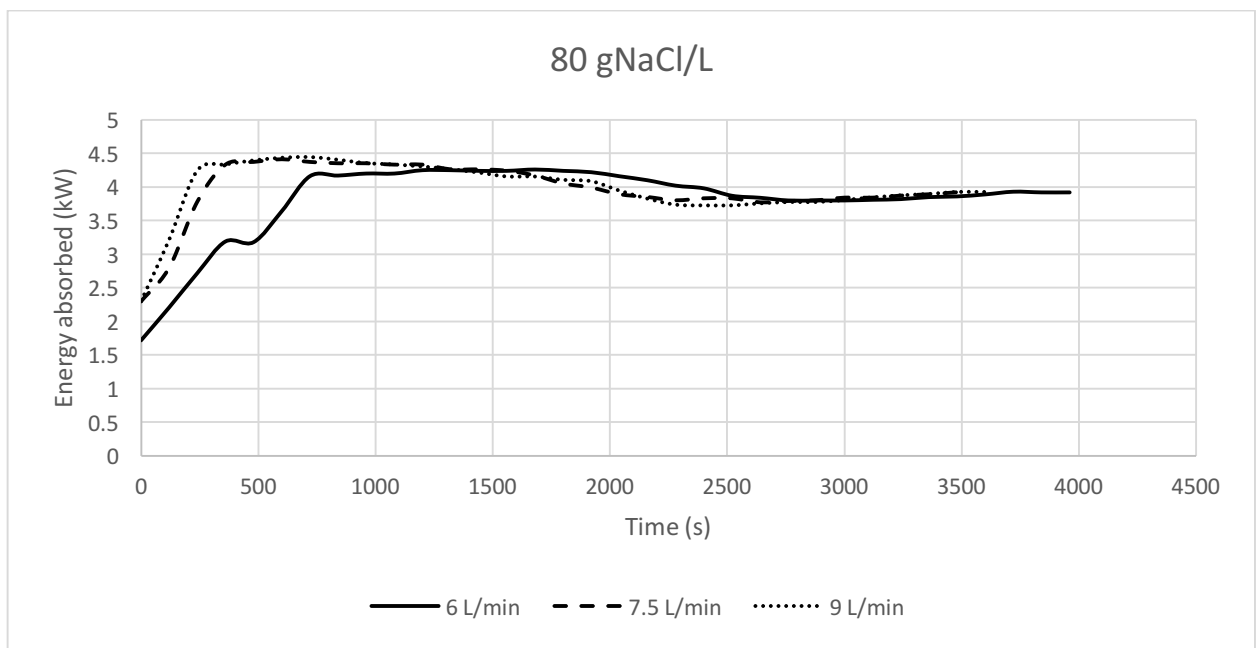


Figure 47 Energy absorbed vs treatment time for 80 gNaCl/L at different flow rates

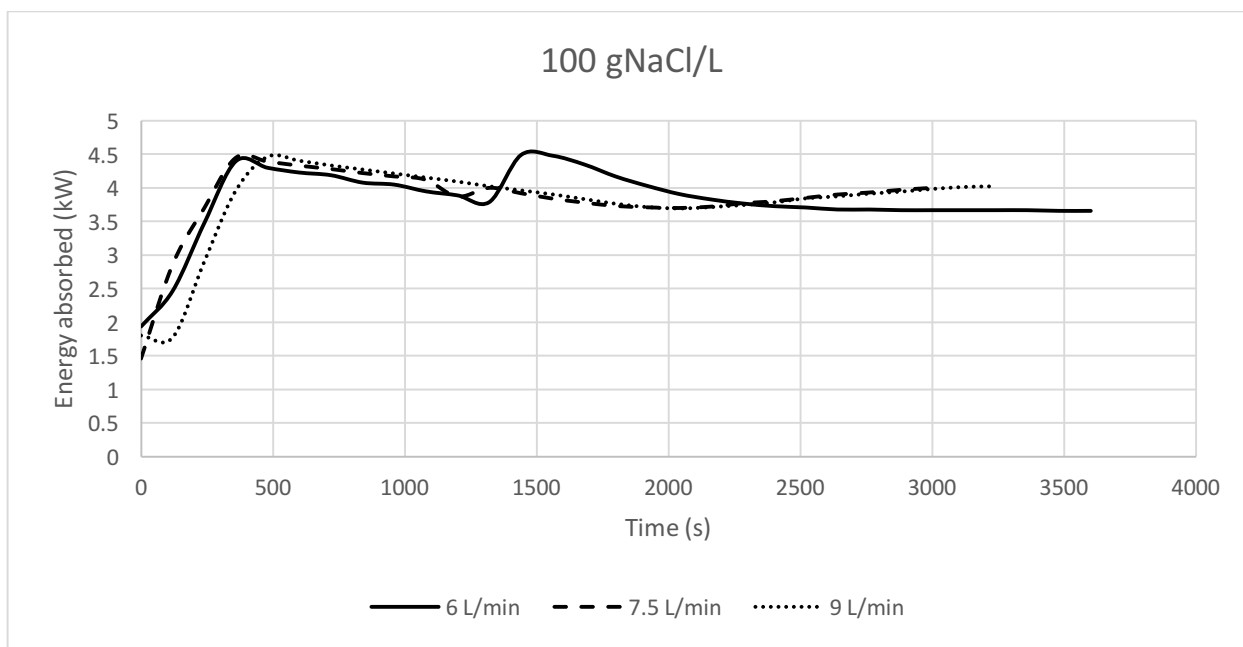


Figure 48 Energy absorbed vs treatment time for 100 gNaCl/L at different flow rates

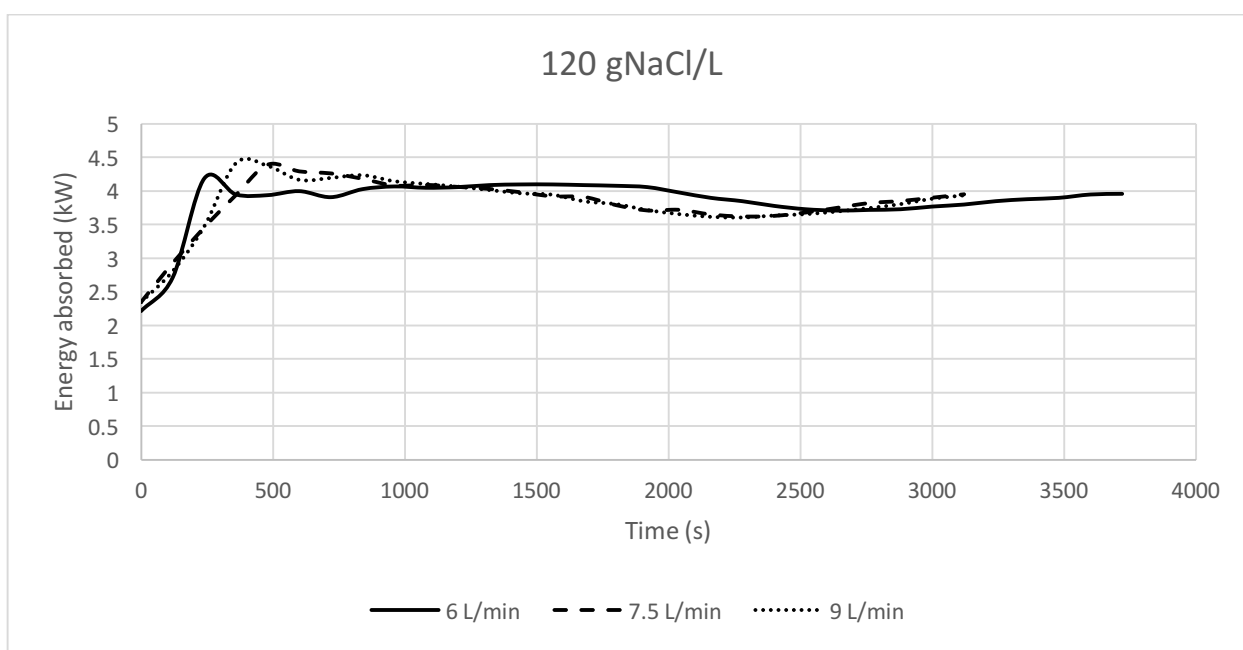


Figure 49 Energy absorbed vs treatment time for 120 gNaCl/L at different flow rates

B.6 Tuning rod heights

Table 18 Tuning rod heights in cm for salt water runs

Salt Concentration (g/L)	Flow Rate (L/min)	Position*			
		1	2	3	4
50	9	19.1	15.2	15	15.2
100	6	15.5	14.8	14.4	14.6
100	7.5	15.5	14.8	14	14.6

*No 1 is the closest to the MW generator and No 4 is the closest to the applicator

Table 19 Tuning rod heights in cm for WAS and DM

Substrate	Flow Rate (L/min)	Position*			
		1	2	3	4
WAS (1%TS)	9	18.9	14.2	15.1	14.6
DM (2.8%TS)	9	20	15.7	15.1	18

*No 1 is the closest to the MW generator and No 4 is the closest to the applicator

Appendix C

Dairy manure experiments

C.1 Complete data set for dairy manure experiments

Table 20 Solids disintegration before and after acid and/or MW/H₂O₂-AOP treatments of DM

Sets	TS (%)	TCOD (mg/L)	SCOD (mg/L)	VFA (mg/L)
Present Study				
Raw	2.8 ± 0	36964 ± 5157	3828 ± 179	2597 ± 117
Acidified	3.3 ± 0	32314 ± 2091	3483 ± 211	2275 ± 33
90°C (0.6%H ₂ O ₂ / %TS)	2.7 ± 0	34782 ± 8722	15897 ± 174	2678 ± 26
110°C (0.6%H ₂ O ₂ / %TS)	2.9 ± 0	25292 ± 1304	12965 ± 424	2817 ± 42
Bailey (2015)				
Raw	3.3 ± 0	32310 ± 513	11242 ± 57	3878 ± 15
Acidified	4.0 ± 0	33624 ± 2703	8630 ± 253	3269 ± 176
90°C (0.15%H ₂ O ₂ / %TS)	4.3 ± 0	40965 ± 1261	11276 ± 180	3699 ± 81
90°C (0.3%H ₂ O ₂ / %TS)	4.2 ± 0	39135 ± 1725	13316 ± 290	3572 ± 22
Raw	3.7 ± 0	46282 ± 1809	12088 ± 282	3462 ± 51
Acidified	4.3 ± 0	37965 ± 905	9308 ± 774	3459 ± 19
90°C (0.15%H ₂ O ₂ / %TS)	3.8 ± 0	41151 ± 1975	17239 ± 1059	3456 ± 61
MacSween (2015)				
Raw	3.8 ± 0	44220 ± 2796	10319 ± 125	3218 ± 19
Acidified	4.2 ± 0	40758 ± 154	9277 ± 645	2931 ± 17
110°C (0.6%H ₂ O ₂ / %TS)	3.5 ± 0.6	30535 ± 513	16833 ± 1368	3269 ± 97
Acidified	3.4 ± 0	33510 ± 1160	8063 ± 227	2673 ± 31
130°C (0.6%H ₂ O ₂ / %TS)	2.4 ± 0	20119 ± 1280	10837 ± 470	3136 ± 83

Table 21 Nutrient release before and after acid and/or MW/H₂O₂-AOP treatments of DM

Sets	ortho-P (mg/L)	TP (mg/L)	STP (mg/L)	Ammonia (mg/L)	TKN (mg/L)	STKN (mg/L)
Present Study						
Raw	29 ± 0.8	260 ± 6.1	32 ± 5.2	462 ± 13	1527 ± 37	666 ± 30
Acidified	107 ± 2.6	188 ± 1.7	108 ± 8.5	464 ± 65	1607 ± 31	756 ± 38
90°C (0.6%H ₂ O ₂ / %TS)	119 ± 2.2	178 ± 7.1	145 ± 2.9	841 ± 15	1281 ± 54	1102 ± 20
110°C (0.6%H ₂ O ₂ / %TS)	167 ± 1.5	197 ± 2.1	170 ± 6.7	857 ± 11	1557 ± 10	1313 ± 9.0
Bailey (2015)						
Raw	3.9 ± 1.9	287 ± 24	18 ± 1.9	1068 ± 25	2227 ± 145	1241 ± 68
Acidified	165 ± 4.0	267 ± 38	191 ± 2.2	1263 ± 3	1893 ± 67	1323 ± 27
90°C (0.15%H ₂ O ₂ / %TS)	185 ± 5.7	271 ± 51	191 ± 11	1258 ± 22	1990 ± 75	1315 ± 82
90°C (0.3%H ₂ O ₂ / %TS)	170 ± 10	271 ± 23	183 ± 12	1180 ± 32	2198 ± 121	1308 ± 121
Raw	15 ± 0.6	290 ± 24	22 ± 1.9	1287 ± 100	2697 ± 116	1539 ± 23
Acidified	167 ± 4.7	251 ± 38	165 ± 2.2	1453 ± 102	2545 ± 223	1600 ± 99
90°C (0.15%H ₂ O ₂ / %TS)	157 ± 4.2	219 ± 16	186 ± 1.3	1425 ± 30	2091 ± 131	1637 ± 14
MacSween (2015)						
Raw	4.0 ± 0.1	336 ± 7.8	77 ± 0.9	758 ± 34	2447 ± 217	885 ± 53
Acidified	204 ± 4.2	-	198 ± 7.5	842 ± 12	1931 ± 226	937 ± 87
110°C (0.6%H ₂ O ₂ / %TS)	245 ± 4.9	-	207 ± 9.1	926 ± 9.3	1947 ± 268	1467 ± 36
Acidified	179 ± 4.0	278 ± 8.6	147 ± 1.6	745 ± 61	2483 ± 451	1080 ± 26
130°C (0.6%H ₂ O ₂ / %TS)	257 ± 4.7	-	226 ± 5.5	934 ± 59	1559 ± 124	1505 ± 72

Table 22 Total and soluble portions of metals before and after acid and/or MW/H₂O₂-AOP treatments of DM

Set	Total Ca (mg/L)	Sol Ca (mg/L)	Total K (mg/L)	Sol K (mg/L)	Total Mg (mg/L)	Sol Mg (mg/L)
Present Study						
Raw	1038 ± 3.7	182 ± 1.6	178 ± 2.7	139 ± 3.4	390 ± 3.2	198 ± 4.5
Acidified	936 ± 7.6	816 ± 14	157 ± 1.8	156 ± 3.6	344 ± 2.1	314 ± 6.3
90°C (0.6%H ₂ O ₂ / %TS)	1004 ± 37	811 ± 3.7	175 ± 6.1	156 ± 2.2	370 ± 11	307 ± 2.2
110°C (0.6%H ₂ O ₂ / %TS)	961 ± 8.0	713 ± 27	162 ± 2.8	144 ± 4.3	354 ± 6.9	286 ± 10